Cell Therapy for the Treatment of Malignant Pleural Mesothelioma

Beth Sage

University College London

UCL Respiratory

Lungs for Living Research Centre

A thesis submitted for the degree of Doctor of Philosophy

2013

Declaration

I, Beth Sage confirm that the work presented in this thesis is my own. Where information has been derived from other sources I confirm that this has been indicated and acknowledged.

Abstract

Malignant pleural mesothelioma (MPM) is a rare but devastating malignancy of the pleural lining caused largely by exposure to asbestos. It presents insidiously with symptoms of chest pain and breathlessness and at the time of presentation the disease is often diffusely spread throughout the chest cavity. There are few effective therapies available with the mainstay of treatment being chemotherapy. The role of surgery is controversial with the only large scale randomised controlled trial showing a trend to worse outcome in patients undergoing surgery. The average survival is 9-12 months from diagnosis and 5-year survival rates are only 2%. New therapies are desperately needed.

There is increasing interest in combined gene and cell therapy approaches and for a malignant disease this is particularly appealing. Mesenchymal stem cells (MSCs) are known to home to tumours and are readily transduced with viral vectors making them ideal cells for delivering targeted therapy. TNF-related apoptosis inducing ligand (TRAIL) is an exciting anti-cancer therapy as it selectively causes apoptosis in cancer cells without affecting healthy cells. This makes the combination of MSCs carrying TRAIL (MSCTRAIL) a viable prospect for the targeted treatment of MPM.

Here I show that lentiviral vectors expressing TRAIL were used to transduce human bone marrow-derived MSCs (MSCTRAIL) which induced apoptosis and cell death in multiple human MPM cell lines. I produced a luciferase-expressing lentiviral vector and MPM cells were transduced successfully to express luciferase (MPMLuc). These cells were used to establish a murine model of MPM and enabled me to track tumour growth *in vivo* using bioluminescent imaging. I demonstrated that systemic delivery of MSCTRAIL to MPM tumours resulted in a significant reduction in tumour growth but topical delivery was not effective. Using dual bioluminescent and fluorescent imaging I showed that MSCs home to tumours when delivered both systemically and topically but that they engraft in greater numbers following systemic delivery. Combining chemotherapy with MSCTRAIL showed promising effects *in vitro* but was not effective in reducing tumour burden *in vivo* although this may be due to using a sub-therapeutic dose of chemotherapy. In summary, human bone marrow derived MSCs were shown to localise to areas of MPM and when modified to express TRAIL and delivered systemically they significantly reduced tumour burden.

Acknowledgements

Firstly I would like to thank my primary supervisor Dr Sam Janes for his unending support and faith in both myself and this project. He was always available for advice and encouragement and his ability to see the wood from the trees was always appreciated and is a lesson I take with me in life. Despite numerous stumbling blocks both within the project and outside, his calmness and understanding has helped me continue and given me a renewed enthusiasm for the world of science. I would also like to thank my secondary supervisor Professor Jerry Brown whose advice was always timely and supportive, Professor Rachel Chambers for her support and kindness during the more challenging moments of my project and to Dr Adam Giangreco for encouraging me to carry on when my project was stalling.

Within the Lungs for Living research centre I am extremely grateful to Dr Katrina McNulty for sharing her expansive knowledge of lentivirus production and her assistance with all of my animal studies and to Krishna Kolluri for all of his hard work and significant contribution to all of the work on combination chemotherapy and with the animal studies. I would also like to thank Katy Ordidge, Sofia Lourenco and Tammy Kalber for their help with animal studies and cell harvesting.

Finally I am very grateful to my funders, the Medical Research Council, the British Lung Foundation and the Mick Knighton Mesothelioma Research Fund for funding my PhD through a Clinical Research Training Fellowship.

Table of Contents

Table of Figures

LIST OF ABBREVIATIONS

AAV	adeno-associated virus
αMEM	minimum essential media alpha modification
ANOVA	analysis of variance
APAF	apoptotic protease-activating factor
ASC	active symptom control
ATP	adenosine triphosphate
BCA	bicinchoninic acid
BMSC	bone marrow-derived stem cell
BrdU	5-bromo 2-deoxyuridine
BSA	bovine serum albumin
CALGB	Cancer and Leukaemia Group B
cFLIP	cellular FLICE-like inhibitory protein
COPD	chronic obstructive pulmonary disease
DAB	3,3-diaminobenzidine
DAPI	4,6-diamidino-2-phenylindole
DcR	decoy receptor
ddH_2O	distilled and deionised water
DED	death effector domain
DIABLO	direct IAP binding protein with low PI
DiI	1,1-dioctadecyl-3,3,3,3-tetramethylindocarbocyanine perchlorate
DiR	3,3,3',3' tetramethylindotricarbocyanine iodide
DISC	death inducing signalling complex
DMEM	Dulbecco's modified Eagle's medium
DMSO	dimethyl sulfoxide
DNA	deoxyribonucleic acid
DNase	deoxyribonucleic acid endonuclease
dox	doxycycline
DR	death receptor

ECM	extracellular matrix
EDTA	ethyldiaminotetraacetic acid
EGF	epidermal growth factor
EIAV	equine infectious anaemia virus
ELISA	enzyme-linked immunosorbent assay
eNOS	endothelial nitric oxide synthase
EPP	extrapleural pneumonectomy
EGFR	epidermal growth factor receptor
EORTC	European Organisation for Research and Treatment of Cancer
ERK	extracellular signal-regulated kinase
FACS	fluorescence activated cell sorting
FADD	fas-activated death domain
Fas-L	fas-ligand
FBS	fetal bovine serum
FIV	feline immunodeficiency virus
flTRAIL	full length TRAIL
g	G-force
GFP	green fluorescent protein
GvHD	graft versus host disease
GM-CSF	granulocyte macrophage colony-stimulating factor
H&E	haematoxylin and eosin
HCl	hydrochloric acid
HDACi	histone deacetylase inhibitor
HIV-1	human immunodeficiency virus-1
HLA	human leukocyte antigen
HRP	horseradish peroxidase
HSC	haematopoietic stem cell
IAP	inhibitor of apoptosis
ICAM	intercellular adhesion molecule
ICG	indiocyanine green
IC_{50}	inhibitory concentration 50

IFN	interferon
IGF	insulin-like growth factor
IκB	inhibitor of NFκB
IKK	IκB kinase
IL	interleukin
IMIG	International Mesothelioma Interest Group
IP_3	inositol 1-, 4-, 5-, triphosphate
IRES	internal ribosome entry site
JNK	Jun N-terminal kinase
kDa	kilo Dalton
LB	Luria-Bertani
LTR	long terminal repeat
mAB	monoclonal antibody
MAPK	mitogen-activated protein kinase
MARS	Mesothelioma and Radical Surgery Trial
MCA	methylcholanthrene
MCP-1	monocyte chemotactic protein-1
MHC	major histocompatibility complex
MMMP	matrix metalloproteinase
MOI	multiplicity of infection
MPM	malignant pleural mesothelioma
MSC	mesenchymal stem cell
MSCFLT	mesenchymal stem cell transduced with the flTRAIL transgene
mRNA	messenger RNA
nd	no doxycycline
NFkB	nuclear factor kB
NHL	non-Hodgkin's lymphoma
NK	natural killer
NOD/SCID	non-obese diabetic/severe combined immunodeficiency
OPG	osteoprotegerin
PBS	phosphate-buffered saline

PCR	polymerase chain reaction
PDGF	platelet-derived growth factor
PDGFR	platelet-derived growth factor receptor
PEI	polyethylenimine
PFA	paraformaldehyde
PI	propidium iodide
PIT	Prophylactic Irradiation of Tracts in Patients with Malignant Pleural Mesothelioma Trial
PI3K	phosphatidylinositol 3-kinase
ROI	region of interest
RNA	ribonucleic acid
RNase	ribonucleic acid endonuclease
rRNA	ribosomal RNA
RPMI	Roswell Park Memorial Institute
SAHA	suberoylanilide hydroxamic acid
SDF1α	stromal derived factor 1α (aka CXCL12)
siRNA	small interfering ribonucleic acid
SMAC	second mitochondrial activator of caspases
SMART	Surgical and large bore pleural procedures in Malignant Pleural Mesothelioma and Radiotherapy Trial
SV40	simian virus 40
TBS	Tris-buffered saline
TBST	TBS/Tween
TdT	terminal deoxynucleotidyl transferase
TE	Tris-EDTA buffer
TGF	transforming growth factor
TIMP	tissue inhibitor of MMPs
TK	tyrosine kinase
TNF	tumour necrosis factor
TNM	tumour-node-metastasis
TRADD	FADD/TNF receptor associated death domain

TRAF	FADD/TNF receptor associated factor
TRAIL	TNF-related apoptosis-inducing ligand
TUNEL	TdT-mediated dUTP-X nick end labelling
UICC	Union International Contre le Cancer
VCAM	vascular cell adhesion molecule
VEGF	vascular endothelial growth factor
VEGFR	vascular endothelial growth factor receptor
VSV-G	vesicular stomatitis G protein
WT-1	Wilm's tumour-1 antigen
XTT	2,3-bis-(2-methoxy-4-nitro-5-sulfophenyl)-2H-tetrazolium-5-carboxanilide
YFP	yellow fluorescent protein

1 Introduction

1.1 Malignant Pleural Mesothelioma

1.1.1 Epidemiology and Aetiology

Malignant mesothelioma is a rare but devastating malignancy that is found most commonly within the pleura of the lung. It also develops in the peritoneum, pericardium and tunica vaginalis although at much lower frequencies. The majority of cases of mesothelioma are caused by exposure to asbestos – a link that was clearly established in the 1960's [1]. Although asbestos mining was banned in most developed countries during the 1980's and 1990's it is still mined today in Russia, China, Brazil and Canada and is widely used both in these countries and other emerging countries such as India.

Asbestos is the main aetiological agent of malignant mesothelioma and describes a group of six silicate minerals that are able to form very thin fibres. These minerals are amosite (brown), crysotile (white), crocidolite (blue), anthophyllite, tremolite and actinolite. Those most commonly used in industry are amosite, crysotile and crocidolite. Crysotile asbestos belongs to the serpentine group of asbestos fibres and is less biopersistant in the lungs than the other amphibole fibres giving it less carcinogenic potency. As most asbestos exposure is work-related, mesothelioma is largely considered to be an occupational disease and because past exposure was more common in occupations with a predominantly male workforce the current incidence of mesothelioma is higher in males than females.

Other potential causes of mesothelioma have been identified including radiotherapy for other malignancies such as lung and breast cancer [2], and a link between simian virus 40 (SV40) has been proposed but is controversial [3, 4]. Although tobacco smoking itself is not carcinogenic to the pleura it is known that patients who smoke and have been exposed to asbestos have a higher risk of developing lung cancer [5].

The lag time from asbestos exposure to development of mesothelioma is on average 30-40 years and consequently deaths from this cancer are continuing to increase. The UK mortality rate has increased from <160 in 1968 to >2000 in 2005 [6] and in Europe is predicted to peak between 2015 and 2020 [7]. For countries still mining and using asbestos in large quantities rates of mesothelioma are likely to continue increasing until long after its use is banned.

1.1.2 Clinical Presentation, diagnosis and staging

Although mesothelioma can present in a number of tissues >90% of cases are within the pleura and therefore called malignant pleural mesothelioma (MPM). These patients present with symptoms of breathlessness and chest pain that are often insidious in onset and at time of diagnosis they often have advanced disease. Chest x-ray and CT scanning usually show evidence of pleural effusions and once removed there is often irregular pleural thickening within the chest cavity. A definitive diagnosis is often challenging and almost always requires a pleural biopsy most commonly obtained by thoracoscopy. Even when good tissue samples are obtained diagnosis can be challenging. Firstly it requires detection of characteristic morphological abnormalities consistent with a malignant process of the pleural lining, which in itself can be difficult as mesothelioma is a very heterogeneous cancer and may resemble both benign pleural lesions and metastatic lesions both of which are more common than mesothelioma in the general population. In addition to H&E examination a definitive diagnosis of mesothelioma requires immunohistochemical confirmation using a panel of both positive and negative markers. These markers are somewhat dependent on what the mesothelioma subtype is and what the differential diagnosis is [8]. There are three distinct subtypes: epithelioid (50-60%), sarcomatoid (10%) and biphasic (30-40%) [9] and of these the sarcomatoid subtype is associated with the poorest prognosis.

A staging system is often used to describe the anatomical extent of a tumour and in the case of MPM there are at least five different staging systems. They are based on the TNM (tumour-node-metastasis) system which is used for the majority of cancer subtypes but its

main drawback when used in MPM is the inaccuracy in describing the T and N-extent using existing imaging techniques. The most recent classification proposed by the International Mesothelioma Interest Group (IMIG) is the most widely used and recommended by the Union International Contre le Cancer (UICC) [10].

All staging systems are surgically based and only correlate survival with stage in terms of early (stage I and II) or late stage (stage III and IV) disease [11]. A number of prognostic factors have been described in large multicentre series and independently validated [12]. Factors such as performance status (see appendix 1), stage and weight loss are common to other tumours and non-epithelioid subtype is consistently associated with a poorer prognosis. Other biological factors such as low haemoglobin, high lactate dehydrogenase, high white blood cell count and high thrombocyte count have been associated with a poor prognosis. Based on these factors, three prognostic scoring methods have been developed by the European Organisation for Research and Treatment of Cancer (EORTC) and the Cancer and Leukaemia Group B (CALGB) [13, 14]. Currently the only prognostic factors of clinical importance are the performance status of the patient and Histopathological subtype.

1.1.3 Treatment

Current treatment options are poor and first line chemotherapy with cisplatin and pemetrexed offers an average survival of 12 months [15]. The role of surgery is controversial with the only large scale clinical trial showing a trend to worse outcomes in patients undergoing surgery [16].

1.1.3.1 Surgery

There are two main surgical procedures offered: extrapleural pneumonectomy (EPP) which is performed with curative intent and partial pleurectomy/decortication which is done for symptom control and palliation. EPP is a radical surgical procedure with limited evidence of efficacy but has been shown to improve survival in a specific sub-group of patients, those with epithelioid histology, negative surgical resection margins and no evidence of extra-pleural nodal involvement [17]. However it is associated with a high morbidity and mortality of 50% and 4% respectively [18] and current guidelines are that EPP should only be

performed in the context of a clinical trial, in specialised centres as part of multi-modality treatment. The MARS (Mesothelioma and Radical Surgery) trial was set up to define the role of EPP in context of trimodal therapy and patients were assigned to EPP followed by post-operative hemithorax irradiation or to no EPP. The primary endpoint of the study was the feasibility of randomising 50 patients in 1 year and it was not powered to analyse the effectiveness of surgery. The study results were published in 2011 and despite meeting the primary end point of feasibility it was determined that due to the high morbidity associated with EPP both in this trial and other non-randomised studies radical surgery in the form of EPP within trimodal therapy offers no benefit and causes potential harm to the patient [19].

Partial pleurectomy/decortication can be defined as significant but incomplete resection of pleural tumour and is of particular utility to relieve an entrapped lung which may in turn relieve a restrictive ventilatory defect and reduce chest wall pain. This form of surgery should not be performed with curative intent but does have a role in a sub-group of patients who may obtain symptom control.

1.1.3.2 Chemotherapy and Radiotherapy

For the vast majority of patients with mesothelioma first line treatment is a combination chemotherapy regimen of pemetrexed (an anti-folate drug) and a platinum based drug (either cisplatin or carboplatin). Although this combination has been shown in randomised controlled trials to improve response rate compared to cisplatin alone (41% compared to 17% with single agent cisplatin) [20, 21] its benefit over active symptom control (ASC) has not yet been established.

Other combination regimens including gemcitabine/platinum and vinorelbine/cisplatin which demonstrated response rates of 12-40% but again none have been shown to have any benefit over active symptom control [22]. The MSO1 trial run by the Medical Research Council and British Thoracic Society randomised 409 patients to either ASC, ASC and vinorelbine or ACS plus MVP (mitomycin, vinorelbine and cisplatin) and the combination of ASC plus vinorelbine resulted in a non-significantly increased median survival compared to either ASC alone and ASC plus MVP (9.4 months vs 7.6 or 7.8 months; HR 0.81, p=0.11) [23].

However as the gold standard for first line treatment is cisplatin/pemetrexed in combination the results of this study are difficult to interpret.

For the majority of patients who have failed first line chemotherapy the disease has often progressed making them unfit for further treatment. For those that are suitable for further treatment there is no clearly agreed gold standard for second line therapy. Selected patients who received pemetrexed-based chemotherapy first line have been given repeated treatment with a pemetrexed containing regimen for disease progression ≥2 years after initial treatment which appears to be feasible [24]. For the same group of patients both oxaliplatin with or without gemcitabine and gemcitabine with vinorelbine have also been evaluated [25, 26] and shown some activity. For those patients who have not received pemetrexed first line a number of studies looked at the use of pemetrexed both as a single agent and in combination but benefits are limited [27] [28].

Radiotherapy plays only a limited role in the treatment of MPM and this is largely due to the extensive nature of the disease and the high risk of toxicity to the underlying lung [29]. Data from a phase II study in which high-dose hemi-thoracic radiation was administered following EPP showed low loco-regional recurrence [30] and a study looking at the role of intensity-modulated radiotherapy after EPP has also shown good local control but with severe pulmonary toxicity [31]. In view of the limited data, the general recommendation is that post-operative radiotherapy following EPP should only be performed within the setting of a clinical trial and at specialist centres.

Despite there being no proven role for radiotherapy in radical treatment of MPM there is a much clearer role for palliative radiotherapy for pain relief. Many patients with MPM will suffer from significant chest pain secondary to malignant infiltration of the chest wall and symptomatic benefit can be provided by radiotherapy to the affected area. Port site radiotherapy has been traditionally used to reduce the risk of tumour seeding along thoracoscopy and thoracentesis site but recent data suggests that this too may be ineffective [32] and there are currently two clinical trials on-going to assess this; SMART (Surgical and large bore pleural procedures in malignant pleural Mesothelioma And

Radiotherapy Trial) and PIT (Prophylactic Irradiation of Tracts in Patients with Malignant Pleural Mesothelioma).

1.1.3.3 Novel Agents

The resistance of MPM to conventional treatments has generated significant interest in identifying new therapeutic strategies. These include anti-angiogenic drugs, immunotherapies and molecules to target both the growth factor and apoptotic pathways.

Mesothelioma cells are known to overexpress angiogenic factors such as vascular endothelial growth factor (VEGF) and its receptor VEGFR, platelet derived growth factor (PDGF) and its receptor (PDGFR) and epidermal growth factor receptor (EGFR). Drugs against all of these targets have been tested in clinical trials with limited effect. The VEGF-blocking monoclonal antibody, bevacizumab, in combination with cisplatin/gemcitabine showed no improvement in overall survival or progression free survival in a phase II randomized trial [33]. When combined with cisplatin and pemetrexed a phase II/III trial showed a response rate of 14% and a 6 month disease control rate of 73.5% in the bevacizumab arm compared with 43.2% in the control arm [34]. Other VEGF targeting strategies have looked at blocking the tyrosine kinase (TK) domain of the VEGFR and cedarinib has shown some activity in MPM patients following first line treatment with platinum based chemotherapy [35] and a phase I/II trial to assess it in combination with cisplatin and pemetrexed in chemotherapy naïve patients is currently recruiting (NCT01064648).

Human tumour necrosis factor α (TNF-α) has shown promising pre-clinical activity against tumour endothelial cells but with high toxicity. A modified TNF-α molecule fused to a cyclic tumour-homing peptide (NGF0hTNF) which selectively binds to CD13 on tumour cells has been assessed as a single agent in a phase II clinical trial and shown promising results [36]. A phase III randomised trial comparing best investigator choice vs NGR-hTNF is currently being planned (NCT01098266).

Mesothelin is a 40kDa protein present on normal mesothelial cells. As it is overexpressed in malignant mesothelioma and is immunogenic, it is a potential antigenic target for a therapeutic cancer vaccine. Mesothelin has been targeted both with a monoclonal antibody

(amatuximab) and with an immunotoxin-linked antibody (SS1P) and studies using both of these agents have shown some efficacy [37, 38].

Growth factor pathways are a potential target for mesothelioma therapies and it is known that the PDGF-α receptor is overexpressed in mesothelioma cells [39]. There are currently two phase II trials assessing the use of a TK inhibitor of PDGFR, imatinib, in combination with other agents as both first and second line therapy (NCT00402766, NCT00551252).

1.2 Apoptosis

Apoptosis is the tightly regulated multi-step pathway of programmed cell death. This pathway is inherent to every cell and the balance of pro-apoptotic and anti-apoptotic signalling ensures that homeostasis is maintained. In the formation of cancer the balance of these signals is altered, the apoptotic pathway is disrupted resulting in reduced cell death, unlimited cell proliferation and ultimately tumour formation.

Apoptosis is activated via two main pathways; the intrinsic or the extrinsic pathway (Figure 1.1). Although the pathways have different mechanisms of activation they both trigger the same downstream pathway.

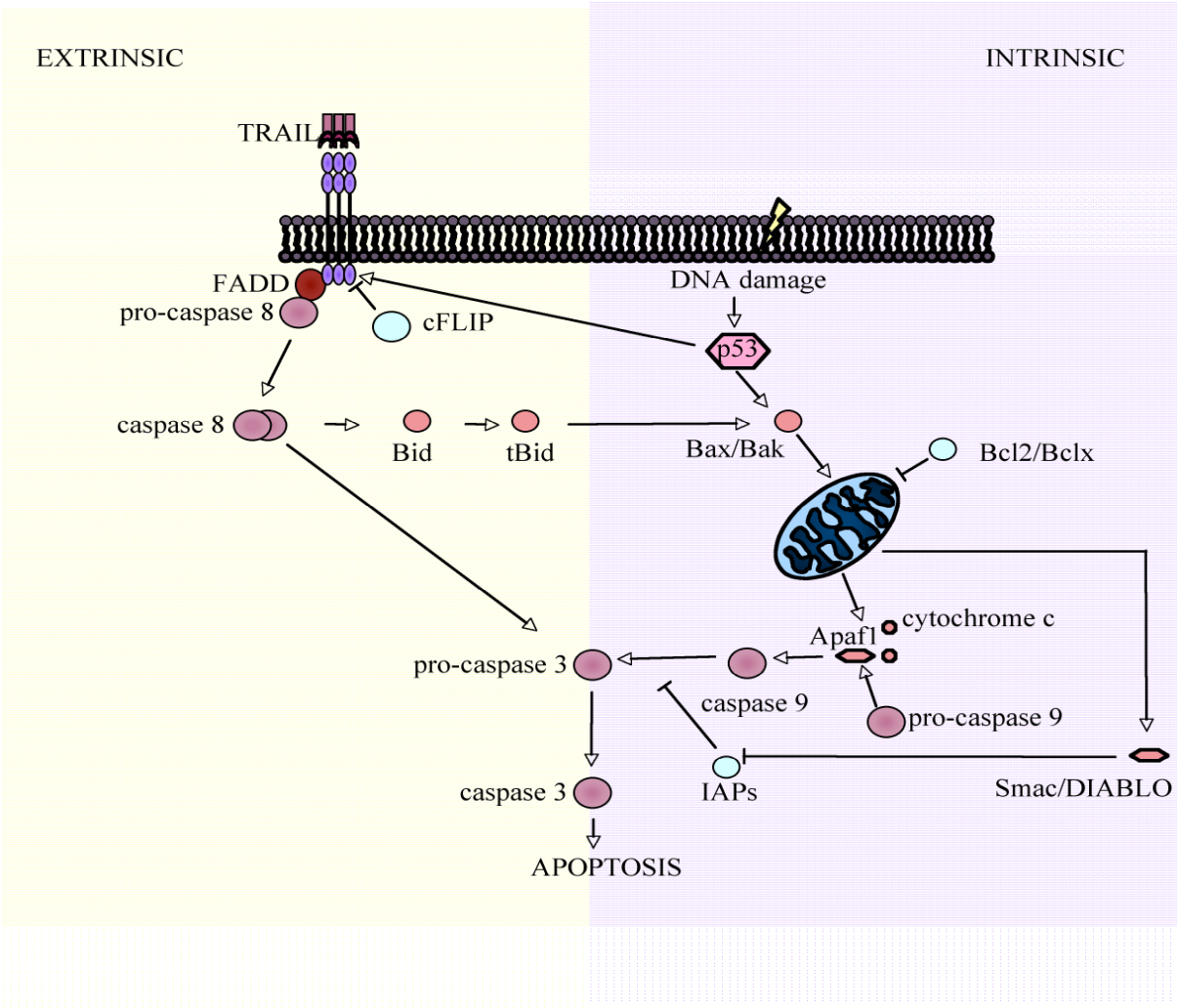

Figure 1.1 Schematic representation of the apoptotic pathways

The extrinsic apoptosis pathway is initiated by the binding of a death ligand to a specific receptor. This leads to recruitment of Fas associated death domain (FADD) and caspase 8, termed the death inducing signalling complex (DISC), and a resulting caspase cascade. Traditional cancer therapeutics work via the intrinsic apoptosis pathway, which centres on DNA damage, the activation of the proapoptotic members of the Bcl-2 family, Bax and Bak, and the release of cytochrome c from the mitochodria. Cytochrome c forms an apoptosome with caspase 9 and apoptotic protease-activating factor 1 (Apaf 1), leading to activation of the effector caspases and apoptosis. The pathways are interlinked as demonstrated and are heavily regulated with multiple activators (represented by arrows) including Smac/DIABLO and inhibitors (represented by headless arrows) such as inhibitors of apoptosis (IAPs), and cellular FLICE-like inhibitory protein (cFLIP).

Mitochondria are essential to living organisms and it is these organelles that are pivotal for apoptosis via the intrinsic pathway. Apoptotic proteins trigger the pathway by inducing changes of the mitochondrial membrane such as increased permeability or the formation of mitochondrial pores resulting in the leakage of apoptotic effectors. Mitochondrial proteins called SMACs (small mitochondria-derived activator of caspases) leak through the pores in the mitochondrial membranes and bind to inhibitors of apoptosis (IAPs) deactivating them. When functioning normally, IAPs inhibit the activity of a number of caspases. Caspases are cysteine-aspartate-proteases that are synthesised as precursors, and the initiator caspases (2, 8 and 9) cleave the inactive pre-cursor forms of the effector caspases (3, 6 &7) to activate them. Once activated the effector caspases cleave DNA and other intracellular structures resulting in apoptosis [40].

In addition to releasing SMACs to trigger apoptosis, the damaged mitochondria also release cytochrome c. Once released, this protein binds with apoptotic protease activating factor-1 (Apaf-1) and adenosine triphosphate (ATP), which then bind to pro-caspase 9 forming a protein complex called an apoptosome. This apoptosome cleaves the pro-caspase 9 to caspase 9 which in turn triggers the effector caspase 3 and apoptosis. The release of cytochrome c is dependent on activation of Bax, a member of the Bcl-2 family, which is ultimately regulated by the tumour suppressor gene p53 [41]. p53 has a critical role in the control of the cell cycle by preventing cell replication if there is DNA damage. If DNA is damaged the levels of p53 accumulate and when levels are high enough they arrest the cells at G1 or interphase to allow time for DNA repair to occur. If the damage is extensive and repair is not successful then p53 will induce cell apoptosis. Any disruption to the production or regulation of p53 will result in impaired apoptosis and possible tumour formation. Existing chemotherapy and radiotherapy agents work by inducing apoptosis via the intrinsic pathway, however, one of the main problems with relying on the activation of this pathway to initiate cancer cell death is that the majority of human tumours acquire p53 mutations [42]. With these mutations, p53 dependent apoptosis is not triggered and cancer cells will continue to grow.

Because of this inherent chemoresistance, there has been considerable interest in stimulating apoptosis via the extrinsic pathway as a new target for inducing cancer cell death. The extrinsic pathway is p53 independent and is activated by death inducing ligands which are members of the tumour necrosis factor (TNF) superfamily and include TNF, Fas-ligand (Fas-L) and TNF related apoptosis inducing ligand (TRAIL). TNF is a monocyte-derived cytotoxin which is thought to have a role in tumour regression, septic shock and cachexia [43, 44]. The expression of both TNF and Fas-L is tightly controlled but the main concern with using these molecules as a clinically useful therapy is that they induce apoptosis of healthy cells as well as cancer cells. In addition to the induction of apoptosis, TNF triggers a significant inflammatory response and subsequent hypotension if used clinically whilst Fas-L causes hepatocyte apoptosis and subsequent hepatic injury. TRAIL, however, is able to selectively trigger apoptosis of malignant cells whilst having no effects on healthy cells making it an exciting candidate for cancer therapy.

1.3 TRAIL

1.3.1 Cellular and physiological effects of TRAIL

TRAIL is a type 2 transmembrane protein first identified in 1995 as sharing sequence homology to the extracellular domain of Fas-L [45]. TRAIL can bind to any of five receptors that are found on the surface of all human cells. There are two active receptors; death receptor 4 (DR4) and death receptor 5 (DR5) which both have active cytoplasmic death domains (Figure 2). TRAIL binds as a homotrimer to either of these receptors causing receptor trimerisation and the recruitment of Fas-activated death domain (FADD) along with procaspases 8 and 10 resulting in the formation of a death inducing signalling complex (DISC). Procaspases 8 and 10 are then proteolytically cleaved to form the active caspases 8 and 10 which in turn induce downstream activation of caspases 3, 6 and 7 (also termed the effector caspases) resulting in apoptosis.

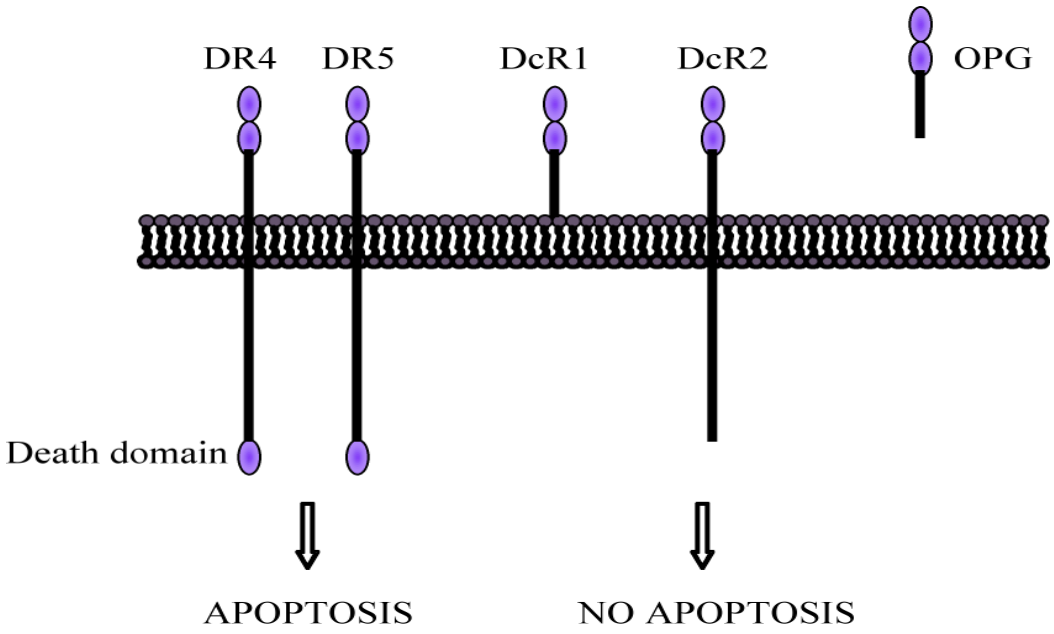

Figure 1.2 Schematic representation of TRAIL receptors

TRAIL has 5 receptors. DR4 and DR5 contain active cytoplasmic death domains, leading to apoptosis. The decoy receptors DcR1 and DcR2 lack active death domains; DcR1 lacks an intracellular region and is attached to the cell membrane by a glycophospholipid, DcR2 has a shortened and inactive cytosolic portion. Osteoprotegerin (OPG) is a soluble receptor, its role as a decoy receptor in TRAIL has not been fully established.

In addition to the active receptors three decoy receptors have also been identified; decoy receptor 1 (DcR1), decoy receptor 2 (DcR2) and osteoprotegerin (OPG). These differ from the active receptors by having either truncated or absent cytoplasmic portions meaning they are unable to bind to FADD or form the DISC so apoptosis cannot occur. The precise function of the decoy receptors is not clear although *in vitro* data suggests that over expression of decoy receptors can inhibit TRAIL-induced apoptosis [46]. The importance of OPG has not been established as TRAIL binds with lower affinity than to DR4 or DR5 and its main role seems to be in the regulation of bone turnover and osteoclast remodelling [47].

One of the key factors regarding TRAIL is its ability to induce apoptosis selectively in tumour cells, whilst sparing normal cells. The mechanism underlying this selectivity is not fully understood, but multiple hypotheses have been investigated. Initial thoughts regarding the control of TRAIL induced apoptosis were the balance between the active TRAIL receptors and decoy receptors, which could explain the difference in sensitivity between tumour cells and normal cells to TRAIL-induced apoptosis. The decoy receptors have been shown to provide some protection to cells against the activities of TRAIL. Transient transfection experiments using DcR1 and DcR2 have demonstrated its ability to inhibit TRAIL-induced apoptosis [48, 49]. Although the mechanism of this effect has yet to be fully clarified it is proposed to be due to competitive inhibition and the formation of ineffective mixed receptor complexes [50]. Interestingly, DcR2 receptors lacking their intracellular domain do not protect cells from apoptosis suggesting that some intracellular mechanism is necessary for the decoy effect [51]. Despite this initial hypothesis, most studies have failed to show a correlation between the expression of these receptors and susceptibility to TRAIL-induced apoptosis [50] and experiments with receptor specific monoclonal antibodies have also suggested that decoy receptor expression does not explain the relative sensitivity of a cell [52]. Even the relative importance of DR4 and DR5 to the apoptosis of individual cells appears to differ between cell types and cannot be determined by the receptor expression. B chronic lymphocytic leukaemia cells rely predominantly on DR4 to transmit the apoptotic signal, however have DR5 more abundantly expressed [53].

Another suggested mechanism is post-translational modification of DR4 and DR5 receptors. Tumours may over-express O-glycosyltransferase which leads to O-glycosylation of TRAIL receptors, enhancing ligand-mediated receptor clustering, DISC formation and caspase 8 activation [54]. Cells sensitive to TRAIL-mediated apoptosis have O-glycosylation of DR4 and DR5, whereas inhibition of this post-translational modification suppressed apoptosis [54]. The association of TRAIL receptors with lipid rafts may also be important. Lipid rafts are cholesterol and sphingolipid rich areas in the cell membranes that concentrate signalling molecules and provide specific and distinct signalling, which may be different to the actions of the same proteins in different subcellular locations. It has recently been demonstrated that TRAIL receptors not associated with lipid rafts may preferentially activate the non-apoptotic signalling pathways in response to TRAIL, such as NFκB and ERK [55].

Whatever the mechanism responsible for the selectivity of tumour cells to TRAIL, it is clear that cancer cells contain multiple molecular abnormalities, which normally lead to their death by apoptosis. Even malignant cells that have developed the ability to evade these normal safety mechanisms are primed for apoptosis and hence may be more sensitive to death ligand targeting.

TRAIL induces apoptosis via the extrinsic pathway as described above and whilst this is its main mechanism of action it also exerts some effect on the intrinsic pathway by crosstalk in the form of Bid activation, a member of the Bcl family. Bid activation causes mitochondrial instability and the release of cytochrome c increasing apoptosis. In return activation of the intrinsic pathway with chemotherapy or radiotherapy results in up-regulation of the active DR4 and DR5 TRAIL receptors [56, 57] so augmenting the action of the extrinsic pathway. Although TRAIL exerts its main effects via the apoptotic pathway it has also been shown to activate non-apoptotic pathways. It up-regulates transcription factors c-Jun and NFκB via stimulation of the JNK, p38 and IKK kinase pathways [58]. The importance of these pathways is not clearly understood nor is their mechanism of action [58, 59] although they have a predominantly anti-apoptotic role and are therefore thought to enable the cell to maintain a balance between survival and death.

The physiological functions of TRAIL are not clearly understood but it is secreted from almost all normal cells. The predominant role of this protein is thought to be in the immune surveillance of the host to tumours and virus-infected cells. TRAIL knockout mice have an increased rate of TRAIL-sensitive tumour development following application of the known carcinogen methylcholanthrene (MCA), a finding that is replicated when a neutralising anti-TRAIL antibody is used [60, 61]. This action is thought to be mediated by natural killer (NK) cells and dependent on interferon gamma (IFNɣ) [60]. NK cells, monocytes, T cells and dendritic cells have all been shown to have TRAIL dependent anti-tumour effects when stimulated with IFNɣ strengthening the role of TRAIL in NK mediated immunosurveillance against tumours [62].

1.3.2 TRAIL as an anti-tumour therapy

The use of TRAIL to activate the extrinsic apoptotic pathway is an exciting prospect in the treatment of cancers. *In vitro* data has shown that a wide number of tumours of many different tissue types exhibit reduced growth rates when treated with recombinant TRAIL whilst similar tests on normal cell types, including fibroblasts, epithelial cells, smooth muscle cells and astrocytes show no such effect [42]. Both recombinant TRAIL and monoclonal antibodies to the active TRAIL receptors (DR4 and DR5) have been shown to cause apoptosis in a variety of cancer cell lines [63, 64]. Tumour cells modified to express TRAIL undergo increased apoptosis as determined by flow cytometry [65] and induce death of neighbouring tumour cells via a bystander effect [66].

Despite promising results with both recombinant TRAIL and TRAIL receptor antibodies a number of problems have been identified. Recombinant TRAIL is delivered intravenously and has a pharmacokinetic half-life of 32 minutes [67] meaning repeated high dose systemic delivery is needed to produce the desired local effect. Monoclonal antibodies have the advantage of a receptor specific high affinity binding enabling a prolonged half-life when compared with recombinant TRAIL, but this specificity may in turn be its downfall when you consider the presence of decoy receptors whose importance is not yet clearly established. Despite these concerns both recombinant TRAIL and the monoclonal TRAIL antibodies to

DR4 and DR5 have been tested in both phase I and phase II clinical trials in both haematological malignancies and solid organ tumours with moderate effect [68-71].

The ideal aim of a clinical therapy is to deliver a therapeutically relevant dose of a treatment to a targeted area of disease with as low toxicity as possible. An ideal cancer therapy would involve a vehicle that homes to and resides at the site of the tumour and delivers a low but consistent dose of treatment that can be activated and inactivated as required. Adenoviruses have been used to allow long term stable incorporation of DNA into the host cell genome and, using this system, TRAIL has been directly injected into tumours causing a reduction in tumour growth in a number of tumour xenograft models including colon and prostate [65].

1.3.3 TRAIL in combination with other agents

In addition to its use as a single agent TRAIL has been studied in combination with a number of other agents. It would appear logical that by triggering both the intrinsic and extrinsic apoptotic pathways there would be an appropriate increase in cell death. However results from a number of *in vitro* studies suggest that there is a synergistic effect when using TRAIL in combination with other agents, a phenomenon attributed to the crosstalk between the two pathways. The mechanism behind this synergy is not clearly elucidated and a number of studies have proposed different hypotheses relating to different elements of the apoptotic pathway. Both radiotherapy and a number of different chemotherapy drugs, including doxorubicin, etoposide, paclitaxel and the vinka alkaloids have been shown to upregulate TRAIL receptors on the cell surface [72, 73] along with histone deacetylase inhibitors (HDACIs) [74]. Alternative studies have suggested that doxorubicin acts by clustering receptors into lipid rafts [75] or by down regulating inhibitors of the apoptotic pathway [76]. These chemotherapy and TRAIL combinations have been so effective that they have induced TRAIL sensitivity in lines previously known to be resistant such as malignant pleural mesothelioma. In this disease, studies looking at a number of agents including etoposide [77, 78], doxorubicin, cisplatin and gemcitabine [79] in combination

with recombinant TRAIL have implicated downstream caspase activation rather than receptor up regulation.

Although initial interest focussed on combining existing cancer treatments with TRAIL this has now widened to other agents that act directly on the downstream apoptotic pathway. New targets have been the inhibitors of apoptosis such as c-FLIP (cellular flice-like inhibitory protein) [80], Bcl2 [81] and IAP inhibitors [82] and blocking these molecules has led to increases in TRAIL induced apoptosis and blocking of the pro-apoptotic mediators with NFκB [83] and PI3K [84] inhibitors which can overcome TRAIL resistance in pancreatic cancer cells.

1.3.3.1 cFLIP and Histone Deacetylase Inhibitors

c-FLIP is currently generating significant interest as a possible mechanism of TRAIL resistance and is increasingly becoming a target for new treatments. c-FLIP has 3 splice variant forms; c-$FLIP_L$ (long 55kDa), c-$FLIP_s$ (short 26kDa) and c-$FLIP_R$ (Raji 24kDa) and the long and short forms are structurally similar to pro-caspase 8 (Figure 1.3). During death receptor mediated apoptosis, pro-caspase 8 is recruited to the DISC and cleaved to produce initially an intermediate sub-unit followed by two active sub-units. Both variants of c-FLIP have been shown to block different steps of caspase 8 activation preventing the initiation of the caspase cascade and subsequent apoptosis [85]. In addition to blocking pro-apoptotic pathways it is thought to trigger the pro-survival pathways NFκB and ERK [86] and is therefore thought to play a key role in balancing pro and anti-apoptotic signals.

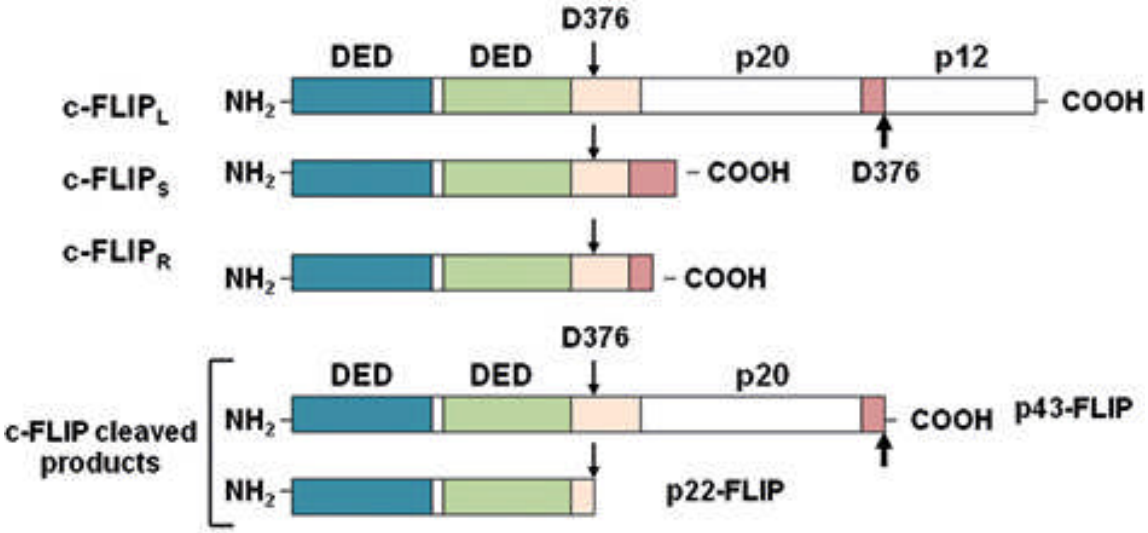

Figure 1.3 Structure of cFLIP variants. There are 3 cFLIP variants all of which contain two death effector domains (DED) at their N-terminal. cFLIP$_L$ also contains two caspase like domains and can act as an anti-apoptotic or pro-apoptotic factor depending on its interaction with the DISC. cFLIP$_S$, cFLIP$_R$ and two cFLIP cleavage products produced by cleavage of cFLIP$_L$ by pro-caspase 8, all act as anti-apoptotic proteins (adapted from [87]).

c-FLIP has been observed to be over-expressed in a number of malignancies including ovarian [88], breast [89], prostate [90] and colorectal [91] cancer cell lines and has been implicated as a possible cause of resistance to tested agents. In malignant mesothelioma c-FLIP over-expression has also been reported and silencing with siRNA results in increased Fas-induced apoptosis of the malignant cells [92] [93]. A number of conventional chemotherapy agents have been shown to alter c-FLIP expression and they either allow apoptosis alone or induce increased sensitivity to TRAIL.

Histone deacetylase inhibitors (HDACi) are an exciting class of anti-cancer drugs that have a number of biological effects that influence tumour growth and survival; including inhibition of cell cycle progression, induction of tumour cell apoptosis and suppression of angiogenesis. One of the key roles of HDACi in preclinical cancer models is the induction of apoptosis and this can occur through activation of either the intrinsic or extrinsic apoptotic pathways [94] and it has been shown that HDACi down-regulate cFLIP and other downstream regulators of the apoptotic pathways [95] such as XIAP. Whilst some *in vitro* studies have looked at the combination of HDACi and activators of the TRAIL pathway and shown significant synergistic effects, the only combination assessed in *in vivo* studies is a DR5 mAB and the HDACi, SAHA (suberoylanilide hydroxamic acid, vorinostat, Zolinza) to a syngeneic mouse model of breast cancer [96]. The mechanism of action is thought to be an increase in TRAIL sensitivity by a combination of DR5 up-regulation [97, 98] and c-FLIP down-regulation [99, 100]. SAHA has been assessed as a single agent in a phase III, randomised, double blind, placebo-controlled trial in patients with advance mesothelioma as a second line therapy (NCT00128102) but the results are not yet reported.

1.3.4 The need for better TRAIL targeting

So far the majority of studies looking at the utility of TRAIL as an anti-cancer therapy have looked at recombinant TRAIL and monoclonal antibodies to the active death receptors. The main problems with using recombinant TRAIL is that it is dependent on intravenous delivery meaning there is no specific targeting of the therapy to the site of disease. In addition the half-life of the drug is only 32 minutes [67] meaning that repeated high doses are required to produce the desired effect. The problems with the half-life have been overcome with the

use of monoclonal antibodies which bind with high specificity to their respective death receptors. The main concerns with this however is that there are five receptors of which the individual contribution to triggering apoptosis is unknown, making cell specificity a significant issue. For example it has been shown that some breast and colon cancer cell lines only trigger apoptosis with DR5 binding [101] whilst cells from chronic lymphocytic leukaemia require signalling through DR4 receptors despite the presence of both receptors [102]. The majority of monoclonal antibodies being developed currently are DR5 agonists although this is likely to reflect increased DR5 expression on tumour cells rather than any functional studies [103].

In order to improve tumour treatment, an ideal system would allow direct targeting of both primary tumours and distant metastases by long term controllable TRAIL expression. This has been achieved in both a lung metastasis [104] and glioma [105] model by the use of human adult mesenchymal stem cells.

1.4 Mesenchymal Stem Cells

A stem cell is an undifferentiated cell that has the capacity for both unlimited self-renewal and asymmetric division such that they are able not only to renew themselves but differentiate into more specialised daughter cells. There are classically two types of stem cells: embryonic and adult. Embryonic stem cells are derived from the blastocyst of the developing embryo and are pluripotent, meaning they can produce cells of any lineage (ectoderm, mesoderm and endoderm). Because of their pluripotency embryonic stem cells are attractive candidates for future therapies as given the right conditions they could differentiate into any tissue type. However the use of human embryos for scientific research has created both ethical, political and moral objections and their use is severely restricted. In addition to this their defining characteristics of unlimited cell growth and differentiation means they have high tumourigenicity and are likely to trigger immune responses within a foreign host [106].

In contrast adult stem cells are traditionally thought to be lineage restricted with daughter cells being able to differentiate into a limited number of cell types. The best characterised adult stem cells are bone marrow derived stem cells (BMSCs) which consist of haematopoietic stem cells (HSCs) and mesenchymal stem cells (MSCs). HSCs produce progenitors for mature blood cells whilst MSCs differentiate into tissue stromal cells including bone, fat and cartilage [107]. MSCs are characterised by their adherence to plastic, and their expression of the stem cell markers CD105, CD73 and CD90 and lack of expression of CD45, CD34, CD14, CD11b, CD79α, CD19 or HLA [108]. Because of their inherent properties of unlimited self-renewal and multipotency, stem cell research has been an area of intense focus both for tissue repair and regeneration and as the basis for cell therapy. Initial studies suggested that BMSCs were able to engraft as epithelial cells within the lung [109] and that the level of engraftment was increased in the presence of injury resulting in a reduction in the severity of damage [110, 111]. Whilst these findings are now thought to be due largely to artefact there remains strong evidence that BMSCs contribute to the deposition of the extracellular matrix including tissue stroma, wound healing and organ fibrosis. Data from transplantation studies have shown that over 30% of fibroblasts in a skin wound healing model were bone marrow derived [112] and in a bleomycin model of lung fibrosis 80% of type I collagen-expressing fibroblasts at the site of lung fibrosis were bone marrow in origin [113, 114].

1.4.1 Tumour stroma

Tumours consist of two main compartments, the parenchyma and the stroma. The parenchyma is made up largely of tumour cells whilst the stroma consists of a combination of cells including connective tissue, fibroblasts and inflammatory cells. The stroma also contains a specialised extracellular matrix (ECM) which contains fibroblasts and myofibroblasts and a basement membrane which is composed of molecules such as collagens, fibronectin, fibrin, proteoglycans, and hyaluronan [115]. The basement membrane regulates many processes including cell survival, proliferation, differentiation and migration, as well as providing structural support. There is significant cross talk between the parenchyma and stroma allowing intrinsic and extrinsic growth factors to

influence each other. In normal cells there is a tightly controlled equilibrium between cell renewal and cell death regulated through crosstalk between parenchyma and stroma that ensures tissue remodelling or appropriate response to injury. However, in cancer cells there is a breakdown in this communication allowing cancer cells to continuously send signals to stimulate remodelling and reorganise the stroma into a form that permits tumour development [116].

The tumour stroma consists of several mediators including cytokines and growth factors, proteolytic enzymes such as matrix metalloproteinases, extracellular matrix proteins, immune cells, endothelial cells and fibroblasts. These growth factors and proteolytic enzymes can influence the ability of tumours to invade and affect their progression [117]. Increased stroma and myofibroblast numbers have been associated with a poorer prognosis in a number of cancers [118, 119] and the proliferative capacity of stromal fibroblasts has been shown to correlate with breast cancer metastases [120]. If the myofibroblasts and fibroblasts are further activated with irradiation then the invasiveness of pancreatic cancer cells appears to increase [121].

Evidence from tracking labelled bone marrow derived cells following bone marrow transplantation has clearly demonstrated that the bone marrow contributes to the extracellular matrix in a wide range of tumour types [122-124]. The extent of this contribution is dependent both on tumour type and the site of implantation [124] and encouragingly these cells appear to be functional with the demonstration of collagen production [125].

What is less certain is the role of BMSCs in tumour neovasculogenesis – another hallmark of malignant tumour growth. There is conflicting evidence regarding this with some studies showing that intravenous delivery of Sca^{1+} bone marrow cells results in these cells being incorporated into the periphery of a glioma model causing a reduction in tumour size and increased apoptosis [126, 127]. Other studies however have shown only a minimal contribution of BMSCs to the newly formed tumour endothelium [128].

Most excitingly there is increasing *in vitro* and *in vivo* evidence that MSCs have the ability to specifically target tumour tissue. *In vitro* migration studies have demonstrated MSC migration towards both tumour cells and conditioned media from tumour cells [129-131] whilst *in vivo* MSCs have been shown to incorporate into and persist in tumours following systemic administration in a wide variety of tumour models including Kaposi's sarcoma [132], breast metastases [133] and glioma [105]. This MSC incorporation has been shown to occur when they are delivered both concurrently with tumour cells [132] and to established tumours although it is widely thought that established tumours are needed.

1.4.2 Mediators of MSC homing

One of the key features of MSCs that make them attractive as vehicles for delivery of therapeutic proteins is their ability to home to and incorporate into tumours. MSCs transduced with green fluorescent protein (eGFP) were delivered systemically into non-human primates and cells were localised within multiple tissues including lung, bone skin and thymus [134] and MSCs delivered systemically into a rat model were shown to home to non-haematopoietic tissues and proliferate within the tissue [135]. Despite consistent evidence that MSCs are able to home to injured tissue and tumours, the precise biological mechanism by which this occurs is not clearly defined. During homing the injured tissue or tumour stroma releases soluble factors from the ECM and inflammatory cells, in particular hyaluronic acid which triggers the diffusion of chemokines and growth factors that in turn stimulate the migration of cells [136] in a process reminiscent of leukocyte recruitment to areas of inflammation. HSCs are known to be reliant on the chemokine CXCL12 (SDF-1α) and its receptor CXCR4 [137] and there is some suggestion that it is important in the recruitment of BMSCs to both fibrotic lung [138, 139] and tumours [117]. In addition to SDF-1α there has been interest in the monocyte chemotactic protein-1 (MCP-1) which has been shown to be secreted from primary cultures and explants of breast tumours [140]. In ovarian cancer the toll-like receptor LL-37 has been shown to stimulate MSC homing in a dose-dependent manner [141] and LL-37 is known to be overexpressed in other tumour types.

There are in the region of 50 human chemokines which function via interaction with G-protein coupled receptors and despite numerous attempts to definitively identify the chemokines and growth factors that are essential for MSC migration, along with which receptors are present, there is as yet no consensus [142-144]. The discrepancies in results may be largely due to the heterogeneity of cell types used although most agree that MSCs express a number of chemokine receptors that are likely to be involved in their homing abilities [145] along with a combination of chemokines and growth factors that enable a maximum effect [146].

1.4.3 MSCs as vectors for cellular based therapy

MSCs have multiple characteristics that make them attractive for delivering oncological therapies such as TRAIL. They are known to home to and incorporate into a wide variety of tumours meaning they would be able deliver a therapy locally to the tumour. They can be relatively easily harvested from patients by aspirating bone marrow under a local anaesthetic in a short, minimally invasive procedure; they are readily transduced with viral vectors allowing them to be modified to carry therapeutic genes and they can be expanded in culture for many passages without altering their original properties. A key benefit to MSCs is that whilst they express major histocompatibility complex (MHC) 1 they lack both MHC2 and co-stimulatory molecules CD80, CD86 and CD40 [147] making them immunoprivileged and unable to generate an immune rejection response when injected into patients. This allows the delivery of donor unmatched allogeneic MSCs without immunomodulation making them more accessible for use in clinical practice.

This approach has already been successful with other therapies such as interferon beta (IFN-β). Human MSCs engineered to express IFN-β have been delivered to gliomas [129], metastatic breast and melanoma models resulting in reduced tumour burden and increased survival [133, 148]. IFN-ɣ and IL-12 have been used in similar ways with IL-12 producing MSCs preventing tumour development when injected prior to tumour inoculation [149] or preventing metastases from developing when injected after tumour establishment [150]. MSC-IFNɣ stimulates apoptosis and inhibits proliferation of leukaemic cells *in vitro* [151].

MSC Therapy	Disease	Model	Reference
MSC-IFNβ	Glioma Lung metastases	Murine Murine	Nakamizo et al [129] Studeny et al [133]
MSC-IL12	Lung cancer Melanoma Hepatoma	Murine Murine Murine	Chen et al [149] Chen et al [150]
MSC-IFNϒ	Chronic myelogenous leukaemia	In vitro	Li et al [151]
MSC-Ang1	Acute lung injury	Murine	Mei et al [152]
MSC-eNOS	Pulmonary hypertension	Rodent Human	Kanki-Horimoto et al [153] PHACeT Trial (NCT00469027)
MSC-VEGF	Acute myocardial infarction	Rodent	Matsumoto et al [154]

Table 1.1. Table of modified MSCs used as therapeutic delivery vectors

As well as homing to sites of tumour, MSCs also home to areas of damage and repair. This property has been exploited in diseases such as pulmonary arterial hypertension, acute lung injury and cardiovascular disease. MSCs expressing angiopoietin-1 have been shown to reduce endotoxin-mediated lung injury [152], and those with endothelial nitric oxide synthase (eNOS) reduce monocrotaline induced pulmonary arterial hypertension in rats [153]. Vascular endothelial growth factor (VEGF) expressing MSCs improve cardiac function in a murine model of myocardial infarction [154]. A phase 1 clinical trial (PHACeT) is currently underway looking at the safety of endothelial progenitor cells as vectors for the delivery of eNOS to patients with pulmonary arterial hypertension.

In addition to their use as vectors it is important to remember that MSCs are active cells that may influence other physiological and pathological processes. It has been well described that MSCs have direct immunosuppressive effects on other cells in particular T-cells, B-cells and dendritic cells resulting in a reduction in plasma cell maturation, antibody

production and antigen presentation [155-157]. MSCs also induce $CD4^+CD25^+FoxP3^+$ regulatory T-cells (Treg), which in turn limit the activation of CD4 and CD8 lymphocyte subsets, B-cells and NK cells [158]. The precise mechanism by which MSCs exert this effect is not clear but thought to involve direct cell contact and the release of soluble factors [159].

These immunosuppressive effects have been exploited in the treatment of graft versus host disease (GvHD) following bone marrow transplantation. In a phase 2 clinical trial using MSCs to treat severe, steroid-resistant GvHD 71% of patients treated exhibited either a complete or partial response. Interestingly there was no difference in outcomes or adverse events between patients receiving MSCs from either matched or unmatched donors [160]. A phase 2 trial looking at the use of MSCs to treat Crohn's disease is currently underway [161] and recruitment to a phase 2 clinical trial is ongoing for use in the treatment of chronic obstructive pulmonary disease (COPD) [162].

In addition to their immunosuppressive effects MSCs are thought to reduce damage at sites of injury, aid in repair and wound healing and exert anti-inflammatory effects. This has been exploited in clinical trials in a number of vascular diseases – most notably cardiovascular. There have been multiple clinical trials looking at the injection of MSCs, BMSCs and HSCs into the coronary arteries following acute myocardial infarction with the weight of evidence showing an improvement in cardiac function, reduction in infarct size and improved tissue remodelling [163, 164]. This improvement in cardiac function is also seen following intra-arterial injection of MSCs to patients with chronic heart disease and in claudication distance in patients with peripheral vascular disease [163, 165]. In terms of their anti-inflammatory effects MSC administration to mice with bleomycin induced lung injury led to reduced inflammation, fibrosis and collagen deposition, an effect attributed to expression of the IL-1 receptor antagonist by the MSCs resulting in downregulation of the pro-inflammatory cytokines IL-1 and TNFα [110, 111]. These paracrine effects of MSCs are thought to be responsible for improvements in other models of organ damage including hepatic failure [166], stroke [167] and acute renal injury [168].

One of the defining properties of MSCs is their ability to undergo unlimited self- renewal and asymmetric expansion. Because of these inherent cellular properties there is some concern that MSCs themselves have either the potential to undergo malignant change or to enhance the proliferation of malignant cells. MSCs co-cultured with breast cancer cells and peripheral blood mononuclear cells have been shown to shift the Th1/Th2 cytokine balance towards Th2 thereby allowing breast cancer cells to evade the immune system [169] whilst subcutaneously delivered allogeneic melanoma cells produced tumours in mice only when co-injected with MSCs – an observation that was attributed to the immunosuppressive effects of the stem cells [170]. In addition to altering the balance of the immune system they are also thought to act within the tumour microenvironment by the release of paracrine growth factors or by transforming into tumour associated fibroblasts which can enhance metastasis formation and tumour growth [171-173]. In Burkett's lymphoma cells they enhanced *in vivo* cell growth by a VEGF dependent pathway and in breast cancer models they were shown to produce the chemokine CCL5 which augmented the motility, invasion and metastatic potential of the tumours along with IL-6 [174, 175].

In contrast other groups have shown that MSCs have anti-tumorigenic properties. They arrest hepatoma, lymphoma and insulinoma cells at G0/G1 and increase cancer cell apoptosis and reduce malignant ascites in intraperitoneal hepatoma models [176]. Inhibition of tumour growth and increased survival has been seen following intratumoural MSC injection in a glioma model [177] along with reduced tumour growth and metastases in a breast tumour model [178]. MSCs release soluble factors that reduce tumour growth and progression in glioma, melanoma and lung carcinoma models [177, 179]. It is likely that the differences in results can be in part explained by the different tumour types studied, different sources of stem cells and whether the cells are used *in vitro* or *in vivo*.

To ensure that MSCs have an anti-tumorigenic effect MSCs can be modified to deliver anti-cancer therapies directly to the site of the tumour. Such strategies include delivery of anti-angiogenic proteins, immunostimulatory proteins, pro-drug converting proteins or pro-apoptotic molecules. Pro-apoptotic proteins studied include MSCs engineered to express TRAIL which have been shown to be effective in eliminating lung metastases and breast

tumours both *in vitro* and *in vivo* [104, 180] and reducing tumour burden in an animal model of glioma [105].

As for the risk of stem cells themselves undergoing malignant change, studies have shown that *in vitro* passaging of human MSCs has demonstrated the potential for the development of karyotype abnormalities [181] and murine MSCs delivery systemically have produced sarcomas [182] and osteosarcomas [183]. In another murine model *Helicobacter felis* was used to produce chronic gastric injury within which a carcinoma developed from bone marrow-derived cells [184]. In contrast a study performed to determine the potential susceptibility of human bone-marrow derived MSCs to malignant transformation showed no features to suggest this, with stable karyotypes and shortening telomeres over the 44 week culture period [185]. In addition to this *in vitro* finding MSCs have been used in multiple clinical trials over the last 10 years for treatment of a wide range of diseases including GvHD [160], cardiovascular disease, Crohn's disease, peripheral vascular disease, osteogenesis imperfecta [186] and COPD [187] with no acute or long term adverse effects reported.

1.4.4 Combining MSCs and TRAIL

The combination of MSCs and TRAIL is an exciting prospect. TRAIL has the advantage over other anti-cancer therapies as it appears to selectively affect only malignant cells. The problems with recombinant TRAIL and monoclonal antibodies to TRAIL receptors described earlier are overcome by targeting TRAIL delivery to the tumour site with MSCs, allowing low dose targeted delivery. This combination of MSCs and TRAIL has already been studied in a murine model of lung metastases where intravenous delivery of MSCTRAIL resulted in a 40% elimination of metastases [104] and in a glioma model where intratumoural MSCTRAIL injection showed a significant reduction in tumour growth [105].

1.5 Gene and Cellular therapy

Gene therapy is the use of DNA as a therapeutic agent to treat disease. Its use was first conceived in the early 1970's and the first approved clinical trial was performed 20 years

later [188] with mixed results. Since then many technical, ethical and safety issues have been addressed to allow the occurrence of a large number of clinical trials although most of these have been phase I and II with very few phase III trials [189].

Mammalian organs are evolved to protect themselves from foreign substances and a significant barrier to the success of gene therapy has been the development of delivery vectors that are able to avoid the host immune system, to achieve targeted delivery to specific cell populations and to allow sustained transgene expression. The lung has been particularly challenging in these respects [190].

1.5.1 Benefits of combined cellular and gene therapy

Cellular therapy describes the process of introducing cells into a tissue as a therapeutic agent to treat disease. Cell therapies can be used either with or without gene therapy and is an approach classically used in the field of regenerative medicine. The use of combined cell and gene therapy is not suitable for all applications but it does have a number of advantages over direct *in vivo* gene delivery. The initial optimisation of vector transfer into cells and determination of the cell responses is carried out *in vitro* so any concerns can be addressed prior to use in humans. In addition, performing gene transfer into specific cells *ex vivo* eliminates the problems of achieving cell-specific gene expression. By using autologous or non-immunogenic cells the potential problems of immune rejection can be overcome. Despite these benefits there are some challenges to performing successful gene transfer into cells *in vitro*. The majority of cells have a good defence mechanism that is designed to exclude and destroy foreign materials and the DNA and vector being used may themselves be cytotoxic. Once delivered *in vivo* cells containing foreign material may be recognised as non-self and be destroyed. In addition the viral vectors used for most gene insertions have specific safety issues that need to be overcome.

1.5.2 Pitfalls of gene transfer

Initial experiments designed to incorporate foreign DNA into a human cell line depended on the uptake of isolated extracellular DNA. This mechanism was shown to be very inefficient and did not result in stable transformation [191]. It was later discovered that some viruses were capable of integrating their genetic material into a target cell genome leading to the

idea that viruses could be used as vectors to introduce new DNA into the host cell genome [192].

Over the last 50 years our understanding of the genetic component of human disease has improved dramatically along with the ability to clone specific genes, making the potential for gene therapy in humans into a reality. In addition growing knowledge of virus biology and the ability to clone genetic sequences has enabled the development of both recombinant viral vectors and non-viral methods of gene transfer.

Non-viral methods of gene transfer use cationic lipids or polymers which form complexes with negatively charged nucleic acids and are then taken up actively by cells by endocytosis. Methods such as electroporation and microinjection can be used to improve the uptake of the nucleic acids into the cells but these methods are more useful to the *in vitro* setting and have limited use *in vivo* [193, 194].

Viral vectors use the innate ability of the virus to gain entry into and survive within the host cell nucleus to ensure continued expression of the viral genome making them popular choices as gene delivery vectors [195]. To make their use as delivery vectors feasible they have been modified significantly to produce replication-incompetent viruses with attenuated cytopathic effects and immunogenicity [195]. One of the enduring concerns over the use of viral vectors is their safety, with different safety concerns depending on the type of viral vector used. Many of these concerns have now been overcome thanks to advances in vector design. Different types of viral vectors are summarised in Table 1.2

Viral Vector	Structure	Advantages	Disadvantages
Adenovirus	Double stranded DNA	DNA incorporated into host cell nucleus Infect both dividing and quiescent cells Transient gene expression Reduced risk of genotoxicity Can carry large DNA inserts	Transient gene expression (weeks) Potentially immunogenic Early vectors associated with adverse events in patients [192]
Adeno-associated virus (AAV)	Single stranded DNA	Infect both dividing and quiescent cells Long term gene expression Non-cytotoxic Non-immunogenic	Only carry small DNA inserts
Retrovirus	Single stranded RNA	DNA incorporated into host cell genome Long term stable gene expression	Tendency to insert into oncogene promoters triggering oncogenic mutations [196]
Lentivirus	Single stranded RNA	DNA incorporated into host cell genome Long term stable gene expression Infect both dividing and quiescent cells Good safety record as virus is replication incompetent No insertion into oncogene promoters	

Table 1.2 Summary of Viral Vectors used in Gene Therapy

1.5.2.1 The use of lentiviral vectors in clinical practice

The first phase I clinical trial to use lentiviral vectors was started in 2003. In this study $CD4^+$ T lymphocytes from patients with wildtype HIV-1 infection were harvested and transduced *ex vivo* using a lentiviral vector expressing an anti-sense gene against the HIV-1 envelope. There was no evidence of the development of replication competent vector-derived HIV-1 and no evidence of insertional mutagenesis up to 3 years after administration [197]. Since then, lentiviral vectors have been used in a number of clinical trials with no adverse events recorded and some success in the treatment of x-linked adrenoleukodystrophy and β-thalassaemia [198, 199].

1.5.3 Vector choice

With the wide choice of viral vectors available for gene delivery the first step was to decide which viral vector to use for this project. As my aim was to develop a combined cell and gene therapy for malignant mesothelioma it was important to consider both the cell delivery vehicle and the vector used for genetic modification. One of the key benefits to using MSCs as delivery vehicles is that they can be expanded in vitro following transduction with a therapeutic vector. This meant that I needed vector which would allow long term stable gene expression rather than transient expression, limiting the choices to a lentivirus or AAV. Our laboratory already had significant experience in working with lentiviral vectors and our collaborator providing the viral vector worked predominantly with lentiviruses. For this reason a lentiviral vector was chosen for gene delivery.

Lentiviruses are most commonly based on the human immunodeficiency virus (HIV-1) as they are very effective in incorporating their DNA into the host genome. However, one of the main concerns regarding their use is that once incorporation into the host cell they may be able to produce replication competent lentiviruses, enabling uncontrolled replication of the HIV-1 virus and subsequent HIV infection of the host. In order to bypass the issue of host infection non-human lentiviruses can be used. Examples of these are feline immunodeficiency virus (FIV) and equine infection anaemia virus (EIAV) both of which are effective at infecting cats and horses respectively but not human cells. As MSCs have a slow population doubling time we needed a highly efficient viral vector to ensure good cell transduction with TRAIL and subsequent therapeutic effect and for this reason an HIV-1 lentivirus was used. In contrast the lentivirus used to transduce the cancer cells with luciferase was an FIV based virus as this was readily available from our collaborators. Although it has lower transduction efficiency in human cells it was suitable for cancer cell

transduction as they have a rapid population doubling time meaning that even a small number of transduced cells can develop into a pure population resulting in high levels of gene expression.

The TRAIL lentiviral vector used to transduce the MSCs had two important components; a tetracycline inducible promoter and a green fluorescent protein (GFP) reporter gene linked to the therapeutic TRAIL gene via an internal ribosome entry site (IRES), TRAIL-IRES-GFP. The benefit of using a tetracycline inducible promoter to control the expression of TRAIL was that the therapy could be activated and deactivated simply by the addition of a tetracycline antibiotic, in this case doxycycline. This means that transduced cells could be assessed for the effect of viral transduction using the same vector rather than an empty vector and that transgene expression could be activated only when needed. The presence of GFP within the viral vector was a useful tool as it allows rapid assessment of transgene production by simple methods such as fluorescent microscopy and flow cytometry. The linking of the TRAIL and GFP with IRES meant that the expression of both TRAIL and GFP were dependent on the same promoter so GFP would only be expressed if TRAIL was being produced. The expression of the protein after the IRES is often lower than expression of the protein before the IRES meaning that whilst GFP expression is a good indicator of TRAIL production it is likely to be an underestimate.

1.6 Hypothesis

Mesenchymal stem cells modified to express TRAIL can reduce tumour growth in malignant pleural mesothelioma alone and in combination with chemotherapy.

1.7 Aims

This project aims to determine whether MSCTRAIL can be used to cause death of malignant pleural mesothelioma both *in vitro* and *in vivo* and whether pre-treatment of mesothelioma cells with existing chemo and radiotherapies can sensitise previously resistant cells to the effects of MSCTRAIL. My aims were:

1. Generate MSCs expressing TRAIL using a lentiviral vector
2. Determine the *in vitro* sensitivity of multiple human malignant pleural mesothelioma cell lines to MSCTRAIL alone and in combination with existing chemotherapy agents
3. Develop a suitable *in vivo* tumour model and confirm that MSCs home to sites of tumour
4. Determine whether MSCTRAIL therapy can reduce mesothelioma growth *in vivo*

Chapter Two

Materials and Methods

2 MATERIALS AND METHODS

2.1 Chemicals, solvents and plastic ware

All chemicals used were of analytical grade or above and obtained from Sigma Aldrich (Poole, UK) unless otherwise stated. Water used for preparation of buffers was distilled and deionised (ddH_2O) using a Millipore water purification system (Millipore R010 followed by Millipore Q plus; Millipore Ltd., MA, US). Polypropylene centrifuge tubes and pipettes were obtained from Becton Dickenson (Oxford, UK).

2.2 Cell Culture

All sterile culture media, sterile tissue culture grade trypsin/EDTA, tissue culture antibiotics and fetal bovine serum (FBS) were purchased from Invitrogen (Paisley, UK) unless otherwise stated. Sterile tissue culture flasks and plates were purchased from Nunc (Roskilde, Denmark) unless otherwise stated.

Human mesothelioma cells were cultured in Dulbeccos' modified Eagle's medium (DMEM) with 4mM L-Glutamine, 50U/ml penicillin and 50µg/ml streptomycin and 10% (v/v) FBS and incubated at 37^{o}C in a humidified 5% CO_2 atmosphere. Cell lines JU77, ONE58, LO68, MSTO-211H, H28, H2052 and Met5A were kind gifts from Professor Bruce Robinson (Lung Institute of Western Australia, University of Western Australia). Hela and 293T cells were obtained from Cancer Research UK, London Research Institute (CRUK, London, UK) and kept as above. Human adult mesenchymal stem cells were provided through the Tulane Centre for Gene Therapy, MSC cell distribution centre (LA, US) and cultured in αMEM with 4mM L-Glutamine, 50U/ml penicillin and 50µg/ml streptomycin and 16% (v/v) FBS. All cell lines were incubated at 37^{o}C in a humidified 5% CO_2 atmosphere. Cells transduced with a Tet-on plasmid had FBS replaced with Tet-system approved FBS (Clontech, Paris, France).

Media was changed every 3 days. Cells were grown until approximately 80% confluent and mobilised by washing with sterile phosphate-buffered saline (PBS) followed by 0.05% trypsin in EDTA. After detachment cells were pelleted by centrifugation at 300g for 5 minutes and plated into 75 or 175 cm^2 tissue culture flasks at ratios of 1:3 to 1:10 every 5-10 days depending on rate of proliferation. Human adult MSCs were plated at 150-200 cells/cm^2 every 10-14 days depending on rate of proliferation. For long term storage of cells, harvest

and centrifugation was performed as described and the cell pellet was resuspended in 1ml of freezing medium; 50% (v/v) medium, 40% (V/V) FBS and 10% (v/v) dimethyl sulfoxide (DMSO), except MSCs which were stored in 65% medium, 30% FBS and 5% DMSO. The cell suspension was transferred to a cryovial, placed in an isopropanol freezing container and left at -80^{0}C for 24 hours to allow slow freezing. Cells were then transferred to liquid nitrogen for long term storage. For subsequent use, cryovials were removed from the liquid nitrogen and thawed rapidly in a water bath at 37^{0}C. The cell suspension was added to standard cell culture media and plated in flasks overnight to allow cells to adhere. Once cells were adherent medium was exchanged for fresh medium.

2.2.1 Stock solutions of drugs and additives

All drugs and solutions used in tissue culture were sterile filtered through a 0.22µm filter unless otherwise stated. All solvents were tissue-culture grade.

Table 2.1: Stock solutions of drugs and additives used in tissue culture

Drug/Additive	Solvent	Stock Concentration	Supplier
Polybrene	Water	4 mg/ml	Sigma Aldrich
Doxycycline Hyclate	Water	10 mg/ml	Sigma Aldrich
Hygromycin	Media	50 mg/ml	Invitrogen
D-Luciferin	PBS	10 mg/ml	Regis Technologies Inc. USA
Human recombinant TRAIL	PBS	10 µg/ml	Peprotech
Cisplatin	DMSO	1 mg/ml	Calbiochem
Pemetrexed	NaCl	25 mg/ml	Eli Lilly
SAHA	DMSO	5mM	Cayman Chemicals

2.3 Human Malignant Pleural Mesothelioma Cell Lines

Human malignant pleural mesothelioma (MPM) cell lines were a kind gift from Professor Bruce Robinson (Lung Institute of Western Australia, University of Western Australia, Perth). Six MPM cell lines; MSTO-211H, H28, H2052, JU77, ONE58, LO68 and one benign mesothelial cell line, Met 5A, were tested. All cell lines were derived from patients diagnosed with malignant pleural mesothelioma. Although all cell lines had previously been characterised some key markers were confirmed prior to use.

2.3.1 Characterisation of MPM cell lines

Clinically MPM is often difficult to diagnose even when good histological specimens are obtained. Not only does malignant disease need to be differentiated from benign disease but it also needs to be separated from other malignancies that may present in a similar clinical location. The immunohistochemical markers used for diagnosis vary depending on the histologic type of mesothelioma (epithelioid versus sarcomatoid), the location of the tumour (pleural versus peritoneal), and the type of tumour being considered in the differential diagnosis. Guidelines produced by the International Mesothelioma Interest Group suggest a panel of positive and negative immunohistochemical markers are used and they should have either a sensitivity or specificity of >80% and the location of the staining is important for diagnosis [8].

2.3.1.1 Immunocytochemistry for calretinin and WT-1

Calretinin, a positive marker is one of the most commonly tested for markers in mesothelioma and should be demonstrated in almost all epithelioid mesotheliomas. Staining should be strong and diffuse and both nuclear and cytoplasmic for a diagnosis of mesothelioma. Wilms tumour 1 (WT-1) is also a useful immunohistochemical marker for mesothelioma and 70-95% of samples show nuclear positivity. These 2 markers were used to confirm that all cell lines used were MPM. Calretinin and WT-1 antibodies were used at a 1:100 dilution. All secondary antibodies were used at a 1:300 dilution (Table 2.2).

MPM cells were plated on chamber slides (Millipore, UK) at a density of $1x10^5$ and left to adhere overnight. The following day cells were washed once with PBS and fixed with 300µl

of 4% paraformaldehyde (PFA) for 20 minutes at room temperature. 4% PFA was made by mixing 4g paraformaldehyde with 100 ml PBS and leaving to dissolve at 70-75^{0}C. Once all PFA was dissolved the solution was left to cool before using. The PFA was removed and slides were washed twice with 500 µl PBS. For antibody staining slides were blocked in blocking solution (PBS, 0.1% azide, 0.2% fish skin gelatin and 10% FBS) for 1 hour at room temperature with gentle agitation. After blocking, slides were incubated with the primary antibody in blocking solution overnight at 4^{0}C. The following day slides were washed with PBS for 5 minutes, repeated three times and then incubated with alexa fluor-conjugated secondary antibodies for 3 hours at room temperature protected from light. Slides were again washed for 5 minutes with PBS, repeated 3 times followed by incubation with DAPI for 10 minutes at room temperature again protected from light. Finally slides were washed for 5 minutes with PBS and a coverslip was mounted using 50 µl moviol.

Table 2.2: Antibodies used for immunofluorescence in characterisation of MPM cell lines and determination of TRAIL receptor status. All secondary antibodies were from Invitrogen and used at a dilution of 1:300.

Antigen	Primary Antibody	Secondary Antibody
Calretinin	Rabbit polyclonal to calretinin, Abcam, ab702, dilution 1:100	Alexa fluor 488 donkey anti-rabbit, Invitrogen, A21206
WT-1	Mouse monoclonal (6F-H2 clone, IgG_1) to WT-1, Upstate, Millipore, 05-753, dilution 1:100	Alexa fluor 555 goat anti-mouse IgG_1, Invitrogen, A21127
DR5	Goat polyclonal to TRAIL-R2, Enzo Life Sciences, ALX-210-743, dilution 1:100	Alexa fluor 488 donkey anti-goat, Invitrogen, A11055
DcR1	Rabbit polyclonal to TRAIL-R3, ProSci, PS2170, dilution 1:100	Alexa fluor 555 donkey anti-rabbit, Invitrogen, A31572

DcR2	Rabbit polyclonal to TRAIL-R4, ProSci, PS2021, dilution 1:100	Alexa fluor 555 donkey anti-rabbit, Invitrogen, A31572

2.3.1.2 Determination of TRAIL receptor status of MPM cell lines

The pro-apoptotic function of TRAIL relies on TRAIL receptor induced signalling. In order to determine whether or not MPM cells were likely to be sensitive to TRAIL induced apoptosis the first step was to determine the presence or absence of active TRAIL receptor DR5 and its decoy receptors DcR1 and DcR2. All TRAIL receptor antibodies were used at a dilution of 1:100 (Table 2.2).

Cells were plated on chamber slides and immunocytochemical staining was carried out as described above.

2.4 Production of MSCTRAIL and Firefly Luciferase Lentiviral Vectors

2.4.1 Lentiviral vector plasmids

2.4.1.1 pLenti-TRAIL-IRES-eGFP

The lentiviral vector plasmid pLenti-TRAIL-IRES-eGFP (courtesy of Dr Michael Loebinger, UCL) was used as the doxycycline-inducible lentiviral vector that would co-express TRAIL and GFP (Figure 2.1). Key components of the plasmid are the internal ribosome entry site (IRES) located between the TRAIL sequence and the eGFP which allows co-ordinated expression of both genes and enables the eGFP to be used as a surrogate marker of TRAIL expression, a human CMV promoter which is constitutively active in all mammalian cells and the woodchuck hepatitis virus post-transcriptional regulatory element which has been shown to increase transgene expression in target cells [200].

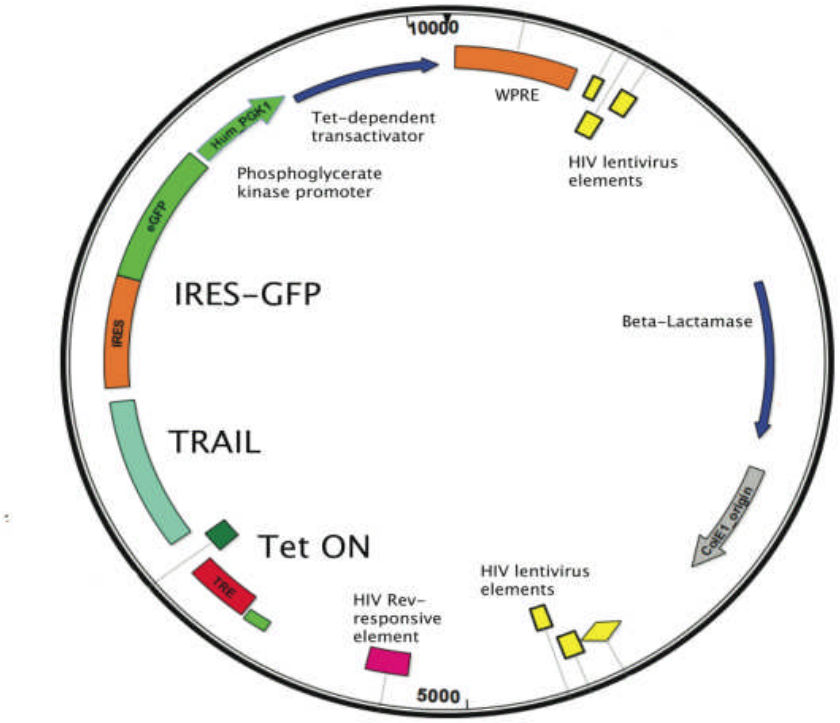

Figure 2.1: pLenti-TRAIL-IRES-eGFP lentiviral vector. Plasmid map for TRAIL-IRES-eGFP plasmid. The genome includes HIV-1 based genes, the tetracycline responsive element (TRE) and tetracycline transactivator under the control of the human phosphoglycerate kinase promoter (Hum PGK1), a human CMV promoter, human full length TRAIL, an internal ribosome entry site (IRES), enhanced green fluorescent protein (eGFP) and the woodchuck hepatitis post-transcriptional regulatory element (WPRE). The plasmid also includes a colE1 origin region and an ampicillin resistance gene to aid propagation in bacteria.

2.4.1.2 pLIONII-Hyg-Luc2YFP

The FIV based virus vector pLIONII-Hyg-Luc2YFP (courtesy of Dr Stephen Goldie, CRI, CRUK) was used to generate the lentiviral vector expressing firefly luciferase and yellow fluorescent protein (YFP). In contrast to the HIV-1 based human lentiviral vector, the pLIONII-Hyg-Luc2YFP vector is derived from the Feline Immunodeficiency Virus (FIV). The FIV virus is a compact genome that makes multiple structural and regulatory proteins essential for its replication. This plasmid constitutively expresses firefly luciferase and YFP under a CAGGS promoter and it has a hygromycin resistance gene to allow for selection of transfected cells.

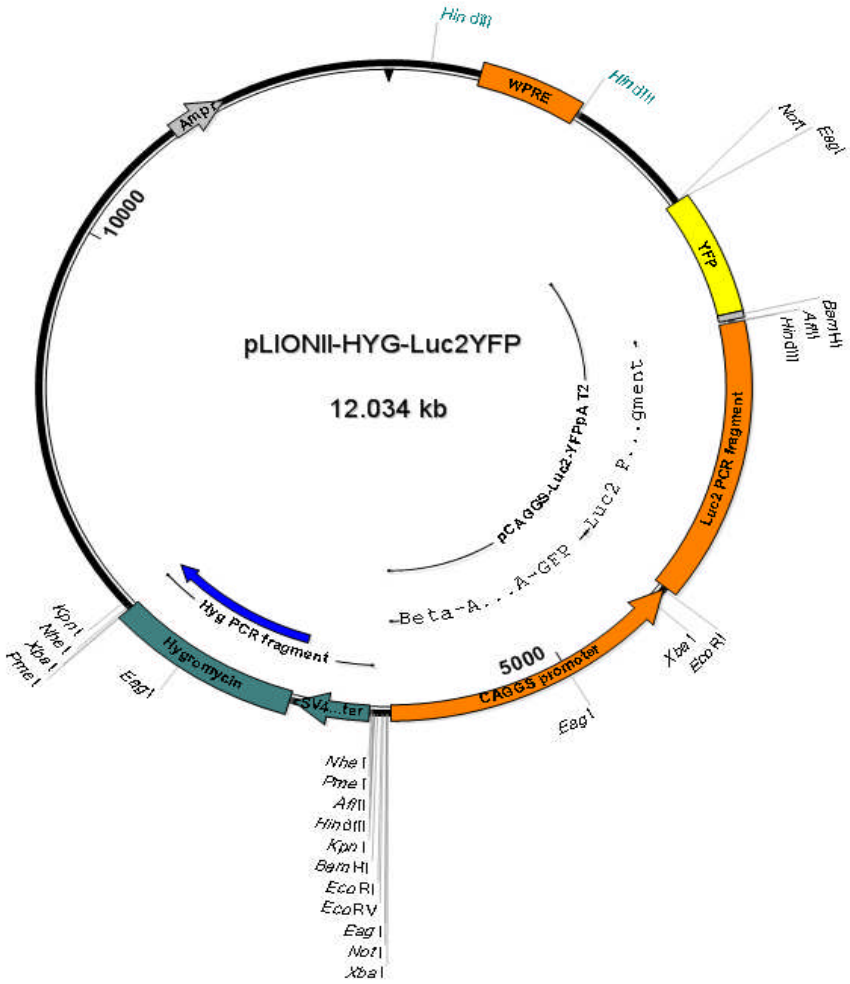

Figure 2.2 pLIONII-HYG-Luc2YFP lentiviral vector. Plasmid map for Luciferase-YFP plasmid. The genome includes FIV-1 based genes, a human CAGGS promoter, firefly luciferase and the fluorescent reporter gene YFP. The plasmid also includes the woodchuck hepatitis post-transcriptional regulatory element (WPRE), an ampicillin resistance gene to aid propagation in bacteria and a hygromycin resistance gene to allow selection of infected target cells to enable the production of a pure population.

2.4.2 Propagation of lentiviral vector plasmids using *Escherichia Coli*

Large scale production of lentiviral vectors requires significant quantities of plasmid DNA. Each plasmid contains a replication sequence and an ampicillin resistance gene to allow replication of plasmids in *Escherichia Coli (E. coli)*.

2.4.2.1 Bacterial transformation of E. Coli with plasmid DNA

Plasmids were expanded using OneShot TOP10 chemically competent *E. coli* (Invitrogen, Paisley, UK). 1µl plasmid was added to a OneShot and left on ice for 30 minutes before being heat shocked at 42^{o}C for 30 secs and returned to ice for a further 2 minutes. 250µl of SOC medium was added to the bacteria and incubated at 37^{0}C for 1 hour on a shaking incubator at 220rpm.

2.4.2.2 Production of single plasmid-transformed bacterial colonies and generation of starter cultures

LB (Luria Bertani) agar plates were made by dissolving 35g LB agar in 1L of dd$H_2$0, autoclaving at 121^{0}C for 15 minutes and cooling to approximately 50^{0}C prior to the addition of 50µg/ml carbenicillin. The LB agar was then poured into 90mm sterile petri dishes (Fisher) and cooled at 4^{0}C until the agar was set. Prior to use LB agar plates were pre-warmed at 37^{0}C.

Different volumes of transformed bacteria (from 10-100µl) were spread onto the agar plates and incubated overnight at 37^{o}C. The following day single bacterial colonies were selected using a sterile loop and used to inoculate 5ml LB broth (Fisher Scientific, Loughborough, UK) containing 50µg/ml carbenicillin in a 15ml falcon tube. LB broth was prepared by dissolving LB broth powder in dd$H_2$0 at 20g/L, autoclaving at 121^{0}C for 15 minutes and allowing to cool to approximately 50^{0}C prior to adding 50µg/ml carbenicillin. Falcon tubes containing the single bacterial colonies were incubated overnight in an orbital incubator at 37^{o}C and 220rpm.

2.4.2.3 Miniprep – Extraction of plasmid from starter cultures

To confirm that the bacteria had been successfully transformed with the plasmid DNA, extraction was performed using the FastPlasmid© Mini Kit (Eppendorf, Cambridge, UK). Individual bacterial colonies were tested as follows. 3ml of the starter culture was

centrifuged at 2000rpm for 15 minutes after which the bacterial pellet was re-suspended in 400µl lysis buffer and left for 3 minutes at room temperature. The mixture was transferred to the spin column provided and centrifuged at 13,000rpm for 1 minute, then washed with 400µl of wash buffer and re-centrifuged at the same settings. Finally 50µl of elution buffer was added to the column, incubated at room temperature for 1 minute and centrifuged at 13,000rpm for 1 minute.

2.4.2.4 Restriction digests

All restriction digests were performed using enzymes and buffers from New England Biolabs ((NEB), Hitchin, UK). Purified DNA from both pLenti-TRAIL-IRES-eGFP and pLIONII-Hyg-Luc2YFP were digested in a single enzymatic reaction using ECOR1 restriction site for the pLIONII-Hyg-Luc2YFP plasmid and ECORV and Mlu1 restriction sites for the pLenti-TRAIL-IRES-eGFP plasmid. Both enzymatic reactions were incubated at 37^0C for 1 hour and heat inactivated at 65^0C for 5 minutes. DNA was purified using the QIAquick PCR Purification Kit (Clontech, 740609.10) according to the manufacturer's protocol. The purified product was run on a 1% (w/v) agarose gel using a HyperLadder I molecular weight marker (Bioline). An ultraviolet lamp was used to demonstrate the DNA fragments.

2.4.2.5 Maxiprep - Large scale production and extraction of plasmid DNA

To multiply the plasmid the remaining 2ml of the starter culture was added to 200ml of LB broth containing 50µg/ml carbenicillin and incubated overnight in an orbital incubator at 220rpm and 37^oC. DNA was purified using the Purelink HiPure Plasmid DNA Maxiprep Kit (Invitrogen, Paisley, UK) as follows. The bacteria were harvested by centrifugation of the LB broth at 4000g for 10 minutes, the pellet was resuspended in 10ml of resuspension buffer (50mM Tris-HCl pH8, 10mM EDTA) with 20mg/ml RNase A, mixed with 10ml lysis buffer (0.2M NaOH, 1% (w/v) SDS) and left to incubate for 5 minutes to release the plasmid from the bacteria. 10ml precipitation buffer (3.1M potassium acetate pH5.5) was added to precipitate the cell debris and DNA out of solution and centrifuged at 12,000g for 10 minutes at room temperature.

Equilibration filter columns are anion exchange columns which bind negatively charged phosphate molecules on the DNA backbone. These were prepared by adding 30ml equilibration buffer and allowing the buffer to drop through under gravity. Once the

columns were prepared the supernatant containing the plasmid DNA was loaded into an equilibration column. The column was washed using 60ml wash buffer (0.1M sodium acetate pH5, 825mM NaCl) to remove RNA, proteins, carbohydrates and other impurities, and finally the plasmid DNA was eluted from the column with 15ml elution buffer (100mM Tris-HCl pH 8.5, 1.25M NaCl). DNA was precipitated by adding 10.5ml isopropanol and centrifuging for 30 minutes at 4500rpm at 4^{o}C. The plasmid DNA was then washed by re-suspending in 70% ethanol and was centrifuged for 15 minutes at 4500rpm at 4^{o}C. The DNA pellet was allowed to air dry before being resuspended in 500µl TE buffer (10mM Tris-HCl pH8, 0.1mM EDTA).

2.4.2.6 DNA Quantification

The DNA was quantified and purity checked using an Ultrospec 3000 spectrophotometer (GE Healthcare, Amersham, UK). Nucleic acids absorb ultraviolet light in a distinct pattern and the amount of light absorbed at different wavelengths is an indication of their purity. The ratio of absorbance at 260nm and 280nm (A260/A280 ratio) gives a measure of purity and a ratio of >1.8 is expected for pure DNA. DNA yield was expressed in µg/ml. For the pLIONII-Hyg-Luc2YFP plasmid the A260/A280 ratio was 1.93 with a concentration of 2.923 µg/µl and for the pLenti-TRAIL-IRES-eGFP plasmid the A260/A280 ratio was 1.90 with a concentration of 1.765 µg/µl.

2.4.3 Transient transfection of 293T cells with plasmid DNA

293T cells are a human embryonic kidney cell line and are commonly used as a packing cell for the production of lentivirus. They are ideal for this role as they are highly permissible to transfection, they contain the SV40 large T-antigen which supports the replication of plasmids containing the SV40 origin of replication and they are able to produce high levels of protein. Transient transfection of 293T cells is used to assess the function of the plasmid using a simple and rapid technique. It involves the introduction of nucleic acids into cells by non-viral methods and occurs by opening of transient pores in the cell membrane to allow uptake of the plasmid. Usually DNA is not readily taken up by cells as both DNA and the cell surface membranes are negatively charged. To overcome this, chemical transfection reagents can be used. The cationic polymer polyethylenimine (PEI) was used to perform

transient transfection with the pLenti-TRAIL-IRES-eGFP plasmid and calcium phosphate was used as the transfection reagent for the pLIONII-Hyg-Luc2YFP plasmid. Initially PEI was used as the transfection reagent for the pLIONII-Hyg-Luc2YFP plasmid however this gave low transfection rates of <30% (Figure 5.2). For this reason an alternative transfection reagent, calcium phosphate, was used when working with the pLIONII-Hyg-Luc2YFP plasmid and this produced much higher transfection rates of >85%.

2.4.3.1 Transfection using JetPEI™ for pLenti-TRAIL-IRES-eGFP plasmid

PEI is a cationic polymer which condenses DNA into positively charged particles which bind to the negatively charged particles on the surface of the cell membrane and are endocytosed. JetPEI™ is a commercially available PEI derivative which has been reported to enable very high transduction rates [201].

$1x10^6$ 293T cells were seeded in a 6-well plate and left to adhere overnight. For each well 6µl JetPEI™ was diluted in 100µl 150mM sodium chloride (NaCl) and vortexed. At the same time 3µg DNA was added to 100µl 150mM NaCl and vortexed to ensure thorough mixing. The JetPEI™ solution was then added to the DNA solution, mixed thoroughly and incubated at room temperature for 15-30 minutes. Cells had a media exchange for 1ml of fresh medium and 200µl of DNA/PEI mix was added dropwise to each well. The plates were returned to the incubator for 4 hours and media was exchanged for fresh media containing 10µg/ml doxycycline to activate TRAIL transgene expression. Cells were left with doxycycline containing medium for 48 hours and the success of transfection was assessed using GFP expression as determined by flow cytometry.

2.4.3.2 Transfection using calcium phosphate for pLIONII-Hyg-Luc2YFP

Calcium phosphate transfection was first described as a technique for transient transfection and permanent transduction in the 1960's and was modified to its current form in the early 1970's since when it has remained largely unchanged. The plasmid DNA is combined with calcium ions to form DNA precipitates which are then taken up into cells by endocytosis.

$2x10^6$ 293T cells were attached to a 6cm plate and 2µl of 50mM chloroquine was added prior to transfection. In a 15ml falcon tube 5µg structural vector (ENV), 3µg of plasmid and

2µg envelope vector (VSVG) were added to 61µl of 2M calcium chloride and 430µl sterile ddH_2O at room temperature and mixed well. 500µl of 2XHBS (Sigma, Dorset, UK) was added to the DNA mixture and bubbled over 15 seconds. The mixture was added drop wise to cells and incubated at 37^{o}C for 8 hours before exchanging for fresh media and incubating for a further 24 hours. Cells were assessed for YFP under fluorescent microscopy and by flow cytometry.

2.4.3.3 Assessment of transgene expression

Both plasmids contain fluorescent reporter proteins to allow easy detection of transgene expression by flow cytometry. For pLenti-TRAIL-IRES-eGFP flow cytometry was performed after incubating cells in media containing 10µg/ml doxycycline to activate the tetracycline dependent promoter. Flow cytometry was performed for GFP. With pLIONII-Hyg-Luc2YFP no transgene activation was required as the protein was constitutively expressed and flow cytometry was performed for YFP.

2.4.4 Production of Lentivirus

In order to manufacture functioning lentivirus additional plasmids containing envelope and structural proteins are required. Without these additional proteins the lentivirus will be unable to incorporate into the host cell genome and replicate along with its host cells. As pLenti-TRAIL-IRES-eGFP is a 3rd generation HIV-1 based lentivirus and pLIONII-Hyg-Luc2YFP is a feline based lentivirus both plasmids require different structural and packaging plasmids.

2.4.4.1 Production of lentiviral vector for pLenti-TRAIL-IRES-eGFP

In addition to the plasmid of interest, the envelope vector pMD.G2 plasmid expressing vesicular stomatitis G protein (VSV-G) and packaging vector pCMV-dR8.74 (kind gifts from Prof A Thrasher, UCL) were used for production of pLenti-TRAIL-IRES-eGFP and were produced as follows. 293T cells were seeded in a T175 flask and kept at a confluence of above 50% for the week prior to transfection and passaged on alternate days at ratios of 1:2 or 1:3 according to growth rates. 24 hours prior to transfection cells were split at a ratio of 1:2 to 1:2.5 to enable them to reach 80-90% confluence on the day of transfection. To ensure significant quantities of virus were produced 18 T175 cm^2 flasks were used.

For each T175 cm^2 flask, 50µg TRAIL plasmid, 12.5µg pMD.G2 and 37.5µg pCMV-dR8.74 were added to 1ml 150mM NaCl, vortexed and sterile filtered using a 0.22µ filter. 80µl JetPEI™ was added to the same volume of 150mM NaCl and vortexed. The PEI/NaCl mix was added to the DNA/NaCl mix and incubated at room temperature for 20 minutes. The media was removed from each flask and replaced with 13ml fresh media and 2ml DNA/PEI/NaCl mix. The cells were incubated for 4 hours at 37°C and then exchanged for 20ml fresh cellular medium and left overnight. The following day media was exchanged for 12ml normal media into which the lentivirus was secreted.

2.4.4.2 Production of lentiviral vector for PLIONII-Hyg-Luc2YFP

As this plasmid is an FIV-1 based plasmid the packaging and envelope plasmids used were pCI-VSVG and pCPRDEnv (gift from Dr Stephen Goldie, CRI, CRUK). 293T cells were seeded and prepared as described above. Calcium phosphate transduction was performed as described for transient transfection except the DNA/HBS mixture was incubated overnight rather than for 4 hours. The following day the media was exchanged for 12ml normal media into which the lentivirus was secreted.

2.4.4.3 Harvest of lentiviral vector

The following day, 48 hours after 293T transfection with the plasmid DNA, the cell supernatant containing the virus was collected and exchanged for 12ml fresh medium. The media containing the lentiviral vectors was purified by centrifugation at 300g for 10 minutes at 4°C (Allegra X-15R, Beckman, High Wycombe, UK) and filtered at 0.45µm. The filtered supernatant was transferred to Ultraclear™ centrifuge tubes (Beckman, High Wycombe, UK) and concentrated by ultracentrifugation at 17,000rpm for 2 hours at 4°C (SW28 rotor, Optima LE80K Ultracentrifuge, Beckman). The supernatant was removed, 100µl cooled optimem was added to the viral pellet and incubated on ice for 1 hour. After incubation the viral pellet was resuspended and stored in 20µl aliquots at -80°C before use. This procedure was repeated the following day resulting in two batches of lentiviral vectors.

2.4.5 Titration of lentivirus

Usually titration of lentiviral vectors is performed using HeLa cells (cervical carcinoma cell line) as they are known to be permissive to transduction. However as TRAIL is known to kill cancer cells and not healthy cells 293T cells were used for lentiviral titration in this case.

50,000 293T cells were plated into each well of a 12-well plate and left overnight to adhere. The following day the media was exchanged for 1.5ml media containing polybrene (Sigma Aldrich, Poole, UK) at a concentration of 4mg/ml and incubated for 5 minutes. This media was then exchanged for 1.5ml media containing polybrene as above and viral concentrations of 15µl, 3.75µl, 0.937µl and 0.234µl and incubated for 24 hours at 37^{o}C. After 24hrs, the media was removed and replaced with normal media and 10µg/ml doxycycline for the pLenti-TRAIL-IRES-eGFP lentiviral vector and without doxycycline for the pLIONII-Hyg-Luc2YFP lentiviral vector as appropriate. After 48 hours cells were detached using trypsin/EDTA and the percentage of GFP positive cells were determined using flow cytometry (FACSCalibur, Beckton Dickenson, Oxford, UK). Samples were gated according to forward and side scatter characteristics to exclude cell debris and doublets and a minimum of 10000 gated events were collected for each sample analysed. GFP and YFP fluorescence was detected using a blue excitation laser (488nm) and 530nm band pass filter. Sample analysis was performed using FlowJo Software (Tree Star Inc., Oregon, USA). The viral titre was calculated in infectious units/ml as below:

$$\text{Viral titre} = \frac{\text{number of cells plated x proportion of GFP positive cells}}{\text{Volume of virus in ml}}$$

2.4.6 Permanent transduction of MSCs and MPM cell lines

Whilst many cell types are easy to transduce with lentiviral vectors it is essential to ensure that the optimal amount of virus is used to obtain maximum transduction efficiency. If too few viral particles are used then low levels of transduction will occur but if too many are used then multiple copies will be incorporated into the target cell DNA and the lentiviral vectors may cause toxicity resulting in poor growth and altered morphology post

transduction. The multiplicity of infection (MOI) is the ratio of infectious viral particles to target cells and prior to permanent target cell transduction a range of MOI's should be tested to determine optimal number. For MSCs an MOI of 10 was used in accordance with previous reports [104, 183].

As both viral particles and cell surface membranes carry negative charges a cationic polymer, polybrene, was used to neutralise the charge repulsion and thereby enhance transduction efficiency.

2.4.6.1 Transduction of MSCs with pLenti-TRAIL-IRES-eGFP

Human MSCs were plated at a density of 35,000 cells per T175. 3 days after seeding (approximate confluency 20-30%) normal media was exchanged for a mix of 12ml αMEM media with 12µl polybrene (4µg/ml) and incubated for 5 minutes. This media was then removed and replaced with 12ml αMEM media with 12µl polybrene and an appropriate volume of virus to give a MOI of 10. The virus/polybrene/media mix was incubated at 37^{o}C for 24 hours after which the media was changed for 20ml media and doxycycline 10µg/ml. Cells were left to reach 80% confluence and were harvested using trypsin/EDTA and the success of MSC transduction was determined by flow cytometry (as previously described) and fluorescence microscopy using a Carl Zeiss Axiovert S100 fluorescent microscope.

2.4.6.2 Transduction of MPM cell lines with pLIONII-Hyg-Luc2YFP

Permanent transduction of mesothelioma cell lines was performed as described for MSCs. However for the luciferase transduction the lentivirus was left on for 48 hours rather than 24 hours before exchanging for normal media and then assessed for the presence of YFP under fluorescent microscopy. The luciferase lentivirus also had a hygromycin resistant gene present allowing selection of only transduced cells. 72 hours after removing the lentivirus 200µg/ml hygromycin was added to the culture media and left for 48 hours before exchanging for normal media. This was repeated until all cells were fluorescent.

2.5 Enzyme-linked immunosorbent assay (ELISA)

All absorbance was measured using a Titertec Multiscan MCC/340 plate reader (Labsystems, Turku, Finland) and an automated plate washer was used for all assays. Assays performed on cell culture samples were performed in triplicate and on those performed on murine serum were carried out in duplicate. ELISAs were performed using the human TRAIL/TNFSF10 Quantikine ELISA kit (R&D Systems, Abingdon, UK).

2.5.1 Sample collection and preparation

Cell supernatants were prepared by removing debris by centrifugation at 300g for 5 minutes. Cell lysates were prepared by washing the cells three times in cold PBS, adding the cell lysis buffer provided at 1 x 10^6 and incubating at 37^{o}C for 30 minutes with gentle shaking. Cells were then centrifuged at 500g for 15 minutes and the supernatant was retained and stored at -20^{o}C until required.

Murine serum was collected in Microvette® CB300 blood collection tubes (Sarstedt) at sacrifice. Samples were placed on ice for 30 minutes and then centrifuged at 1000g for 15 minutes. Serum was transferred to 500µl eppendorf tubes and placed at -80^{0}C until ELISA was performed.

2.5.2 BCA protein assay

To ensure equivalent amounts of protein were loaded for different samples the protein concentration of cell lysates, supernatants and serum were assessed using the bicinchoninic acid (BCA) protein assay (Thermo Fisher Scientific, IL, US). The BCA assay relies on two reactions; firstly the peptide bonds in the protein reduces Cu^{2+} to Cu^{+}, a reaction that is dependent on the amount of protein present and secondly the bicinchoninic acid is chelated with the Cu^{+} ions to produce a purple coloured solution. This colour strongly absorbs light in a linear fashion at 562nm. Standards were made by dissolving BSA in PBS at concentrations from 20µg/ml to 2000µg/ml.

20µl of each sample along with 20µl standard were added to a 96-well plate, 180µl of BCA working solution was added to each well and agitated on a plate shaker for 30 seconds. The plate was then incubated at 37^{o}C for 30 minutes before reading the absorbance at 550nm. The absorbance of the samples was compared to those of known protein concentrations to determine the protein concentration.

2.5.3 TRAIL ELISA procedure

The human TRAIL ELISA kit (R&D, Abingdon, UK) was used according to the manufacturer's instructions. 100µl of assay diluent RD1S was added to each well of a 96-well plate. 50µl of samples containing equal amounts of protein were then added and incubated for 2 hours at room temperature on a horizontal orbital plate shaker at 500rpm. The plate was washed four times with wash buffer before adding 200µl TRAIL conjugate to each well and incubating for a further 2 hours on the orbital plate shaker. The plate was washed a further four times, 200µl of a colour substrate solution was added to each well and incubated for 30 minutes at room temperature in the dark. Finally 50µl stop solution was added to each well and the absorbance was measured at 450nm using the plate reader. Readings were compared to known concentrations of human recombinant TRAIL (R&D Systems) which were used to plot a standard curve to determine the concentrations of TRAIL protein in each sample. Readings were also taken at 540nm and were subtracted from those taken at 450nm to correct for optical imperfections in the plate.

2.6 Determination of dose-response curves for chemotherapeutic agents

The half maximal inhibitory concentration (IC_{50}) of a drug is an indication of how effective that drug is at inhibiting a biological or biochemical function and allows determination of the amount of the specified drug that is required to inhibit the measured biological effect by half. The IC_{50} is determined by constructing a dose-response curve and identifying the concentration at which the measured biological function is reduced by a half. Dose-response curves were determined by measuring the effect of different concentrations of drugs on cell proliferation using a colorimetric XTT assay (AppliChem) that detects cellular

metabolic activity. During the assay the yellow tetrazolium salt XTT is reduced to a coloured formazan dye by the dehydrogenase enzymes in metabolically active cells. As this conversion only occurs in viable cells the amount of formazan produced is directly proportional to the number of viable cells. The formazan dye is soluble in aqueous solution and can be quantified by measuring absorbance at 450nm wavelength. All doses were tested in triplicate and all absorbances were measured using a Titertec Multiscan MCC/340 plate reader (Labsystems, Turku, Finland).

2.6.1 Dose response curves

Chemotherapy agents and doses tested were as follows: cisplatin 0-32µM, pemetrexed 0-200µM, SAHA 0-5µM.

10,000 MPM cells were plated in each well of a 96-well plate and left to adhere overnight. The following day media was exchanged for fresh media containing different concentrations of chemotherapy agents and incubated for 48 hours. To perform the XTT assay 0.1ml activation reagent was added to 5ml XTT reagent and 50µl of the solution was added to each well of the 96-well plate. Plates were incubated at 37^0C for 4 hours and on removal were shaken gently to ensure an even distribution of dye within the wells. Absorbance was measured at 450nm and 650nm to allow subtraction of reference absorbance.

2.7 *In vitro* co-culture experiments

Both MSCs and MPM cells have similar forward and side scatter properties on flow cytometry making identification of the different cell populations difficult. Vibrant®CM-DiI cell labelling solution (Invitrogen) is a lipophilic fluorescent stain than stains the lipid constituents of the cell membrane. It is photostable and considered suitable for long-term cell tracking [104]. In all co-culture experiments MPM cells were stained with DiI to distinguish them from MSCs on flow cytometry.

As the TRAIL lentiviral vector contains a tetracycline dependent promoter all co-culture experiments were performed using tetracycline free serum (Clontech, Paris, France) to ensure there was no TRAIL activation in the control cells.

2.7.1 Co-culture experiments

50,000 human MSCs transduced with TRAIL (MSCTRAIL) were plated in each well of a 6 well plate. MPM cells were detached, counted and resuspended in serum free media at a concentration of 1 million cells/ml. 5µl/ml of DiI was added to the MPM cell suspensions and incubated for 20 minutes at room temperature after which cells were washed twice in sterile PBS. MPM cells were then plated with the MSCTRAIL at a density of 50,000 cells per well. Cells were left to adhere overnight and then media was exchanged for either media alone, media containing doxycycline 10µg/ml or media containing 200ng/ml recombinant TRAIL (rTRAIL) with or without chemotherapy according to experimental design. Cells were incubated for 48 hours to allow maximal activation of TRAIL.

2.7.2 Apoptosis assessment

Annexin V is a 35-36kDa calcium-dependent phospholipid binding protein with a high affinity for phosphatidylserine which is located on the cytoplasmic side of the cell membrane. In living cells this is inaccessible to cell surface binding proteins but in apoptotic cells it is translocated to the outer surface of the cell membrane enabling the binding of annexin V. In addition to this annexin V can travel through the porous cell membrane of dead cells and bind to phosphatidylserine on the cytoplasmic cell surface although these cells will also stain with DAPI, a cell impermeant dead cell stain. With this system Annexin V^- /$DAPI^-$ cells were considered alive, annexin V^+/$DAPI^-$ cells were apoptotic and annexin V^+/$DAPI^+$ were considered dead having completed apoptosis.

Media including floating cells were collected and placed into a FACS tube. Adherent cells were washed twice with PBS, detached with trypsin as previously described and added to the FACS tube. Samples were centrifuged at 300g for 5 minutes. The supernatant was discarded, and the cell pellet was resuspended in 100µl Annexin binding buffer (1X) with 3µl Annexin V-AlexaFluor 647 (Invitrogen, Paisley, UK) and incubated for 40 minutes on ice. After incubation a further 400µl of annexin binding buffer was added and samples were filtered through a 100µm cell strainer. 2µg/ml DAPI was added to each sample immediately prior to flow cytometry analysis.

Samples were analysed on an LSR2 machine (Beckton Dickenson, Oxford, UK) and electronic compensation was performed to minimise overlap of emission spectra. Samples were gated according to forward and side scatter to exclude cell doublets and debris and a minimum of 10,000 gated events were collected and analysed. Sample analysis and quantification was performed using FlowJo software. GFP fluorescence was detected using a blue excitation laser (488nm) and 530/30 band pass filter. The secondary antibody AlexaFluor 647 was detected using a red excitation laser (635nm) and 660/20 band pass filter, DiI labelling was detected using a blue excitation laser and 575/25 band pass filter whilst DAPI detection was achieved with an ultraviolet excitation laser (355nm) and a band pass filter at 440/40.

2.8 *In vivo* models

2.8.1 Animals

Human tumour xenograft models are a well-established mode of determining the efficacy of anti-cancer therapies. In order to successfully establish human tumours in a murine model the animals need to be immunosuppressed to prevent rejection of cancer cells. NOD/SCID mice (NOD.CB17-Prkdc^{scid}) have the severe combined immunodeficiency mutation on a non-obese non-diabetic background resulting in a lack of functioning B and T-lymphocytes, lymphopaenia and hypogammaglobulinaemia.

Eight to ten week old NOD/SCID mice (Charles Rivers) were kept in individually ventilated cages at the Central Biological Services Unit at University College London. Animals were kept on a 12 hours light/dark cycle at 20-25^{o}C and were provided with autoclaved food and water *ad libitum.* When mice needed doxycycline this was given in their autoclaved drinking water at a concentration of 2g/L with 3% (w/v) sucrose and administered via black water bottles to protect from light. All animal studies were approved by the University College London Biological Services Ethical Review Committee and licensed under the UK Home Office regulations and the Evidence for the Operation of Animals (Scientific Procedures) Act 1986 (Home Office, London, UK).

2.8.2 *In vivo* tumour xenograft models

Luciferase transduced MSTO-211H (MSTO-211HLuc) cells were used to generate all tumour xenografts. All cells were detached from flasks using trypsin/EDTA, neutralised with serum containing medium and the cell suspension was counted. Cells were centrifuged at 300g for 5 minutes and the cell pellet was resuspended to the required cell concentration in 100µl sterile PBS. Cells were kept on ice prior to injection. All animals were weighed prior to tumour cell inoculation and twice weekly thereafter. Animals were sacrificed when they reached >20% weight loss or if they showed other signs of distress such as piloerection, hunching or being cold to touch.

2.8.2.1 Intrapleural tumour xenograft model

Intrapleural tumours were obtained by injecting cell concentrations from $8x10^4$ to $2x10^5$ into the pleural cavity. Animals were stilled using isofluorane anaesthesia (3% in 2l/min oxygen); the right thoracic wall was shaved and cleaned with 2% chlorhexidine. A 5mm incision was made through the skin and subcutaneous tissue on the right chest wall exposing the intercostal space underneath. Cells were injected using an insulin needle through the intercostal space into the pleural cavity.

2.8.3 Demonstration of MSCs homing to MPM tumours

In order to track MSCs homing to tumours *in vivo* dual modality fluorescent and bioluminescent imaging were used. Fluorescence can be difficult to use *in vivo* as fluorophores with wavelengths <600nm will be absorbed by the animal tissue thereby reducing the fluorescent signal detected. In order to be useful, both the excitation and emission spectra of any fluorophore would need to be >600nm. Firefly luciferase has a peak emission wavelength of approximately 560nm with a spectra from 450-650nm. To ensure no overlap of signal between the bioluminescence and fluorescence an ideal fluorophore would have excitation and emission wavelengths >650nm. DiR is a member of the long chain dialkylcarbocyanine family along with Vibrant®CM-DiI cell labelling solution and has an emission spectra of 710-800nm making it suitable for *in vivo* use. Whilst DiR is a suitable choice for *in vivo* imaging it would not be easy to identify on tissue sections as both the confocal and fluorescent microscopes available for use were unable to detect fluorophores

with this emission spectra. To enable cells to be imaged both *in vivo* and *in vitro* cells were dual stained with DiR and DiI.

Intrapleural tumours were established using $2x10^5$ MSTO-211HLuc cells as described above (2.8.2.1) and allowed to establish for 6 days. MSCs were harvested and after counting were resuspended in serum free medium to a concentration of $1x10^6$ cells/ml. 1 µl of a 100mM stock solution of DiR was added to the MSC cell pellet along with 5 µl of DiI and incubated at room temperature in the dark for 20 minutes. The cell pellet was then washed twice with PBS, centrifuged at 300g for 5 minutes and resuspended in a final volume of 100 µl sterile PBS for intrapleural delivery or 200 µl for intravenous delivery into the lateral tail vein. Following *in vivo* delivery cells were tracked for 24 hours to determine the location of the MSCs.

2.8.4 Therapeutic use of MSCTRAIL

Intrapleural tumours were established using $8x10^4$ cells as described in section 2.8.2.1 and allowed to establish for 5 days. Both MSCTRAIL and MSC were harvested and stained with DiI. For intrapleural MSC delivery cells were resuspended to a final concentration of $1x10^6$ cells in 100 µl sterile PBS and for intravenous delivery cells were resuspended to a final concentration of $1x10^6$ cells in 200 µl sterile PBS. MSCTRAIL and MSC were delivered on days 5, 9, 12, 15 and 18 during tumour development and bioluminescent imaging was performed twice weekly. To enable an accurate determination of tumour cell proliferation 200 µl 5-bromo-2'-deoxyuridine (BrdU; Invitrogen 00-0103; 10mg/ml) was administered 1 hour prior to sacrifice

MSCTRAIL cells were cultured in doxycycline prior to *in vivo* delivery to ensure maximal TRAIL expression and all animals were given doxycycline in their drinking water throughout the duration of the experiment.

2.8.5 Extended MSC homing

Intrapleural tumours were established using $2x10^5$ MSTO-211HLuc cells and allowed to develop for 10 days. MSCs were stained with DiR and DiI as described in section 2.8.3 and resuspended in sterile PBS as previously described. Cells were delivered both intrapleurally

and intravenously into the lateral tail vein. Following MSC delivery cells were tracked and imaged daily for 6 days.

2.9 Bioluminescent and fluorescent imaging

Bioluminescence is the production and emission of light by living organisms and is naturally occurring in fireflies, anglerfish and some species of squid. Luciferase belongs to a family of oxidative enzymes which in the presence of the substrate D-luciferin catalyse its conversion to oxyluciferin and light.

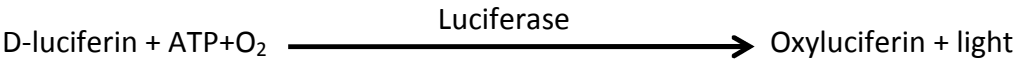

Cells can be transduced with a lentiviral vector containing firefly luciferase and can be used to detect cells both *in vitro* and *in vivo*. In this thesis bioluminescent imaging was used both to identify tumours and as a longitudinal marker of tumour burden.

All imaging was performed using an IVIS® Lumina II imaging system (Caliper Life Sciences). This system uses a sensitive charge-coupled device camera which is cooled to -90^{0}C. This camera converts the photons of light emitted from subjects within a dark sealed imaging chamber into electronic charge and can detect the rate of emission of photons of light over the course of an exposure. All images were obtained using an automatic exposure time, a medium binning resolution with an F-stop setting of 1. Grey-scale images were acquired prior to bioluminescence images to ensure correct positioning of subjects.

In addition to measuring a bioluminescent signal the IVIS can also detect fluorescence at varying wavelengths. All fluorescent images were reliant on the DiR fluorophore and therefore acquired using a 745nm emission filter and ICG detection filter. An automatic exposure time was used along with F-stop of 1 and medium binning resolution.

Data was analysed using Living Image 4.1 software (Xenogen, Caliper Life Sciences, Runcorn, UK), areas of bioluminescence were selected using the region of interest (ROI) tool and bioluminescent or fluorescent counts were determined as appropriate. ROI's were kept

constant between subjects throughout individual experiments. The tumour volume for each group was expressed as the total photon count within the dedicated region of interest.

2.9.1 *In vitro* bioluminescent and fluorescent imaging

In order to confirm successful luciferase transduction of MPM cells and that expression directly correlates to photon count cells were plated at increasing cell densities in a 12-well plate. Cells were allowed to adhere overnight and the following day medium was exchanged for medium containing D-luciferin at a concentration of 150 µg/ml immediately prior to imaging. Cells were placed in the imaging chamber and images were acquired using automatic exposure settings, medium sensitivity binning and F-stop 1.

To confirm successful MSC staining with DiR and to determine the correct filter settings required for imaging cells were stained as described in section 2.8.3 with either DiI or DiR alone or in combination and plated at a density of $1x10^5$ cells in each well of a 6-well plate. Cells were left to adhere overnight and imaged the following day using multiple filter sets.

2.9.2 *In vivo* bioluminescent and fluorescent imaging

D-luciferin is a small molecule that freely diffuses across cell membranes. When injected intraperitoneally D-luciferin is not excreted but slowly absorbed into the circulation, perfuses the tissues and is ultimately excreted by the kidneys. This means the luciferin concentration within the body is related to the pharmacokinetics of substrate inflow vs substrate outflow. As the substrate is being injected the inflow is greater that the outflow resulting in a slowly increasing bioluminescent signal. Once the substrate reaches equilibrium in the body (inflow and outflow are equal) there is a plateau in the bioluminescent signal and the counts can be used as a reliable measure of cell number. Finally the excretion of substrate is greater that the inflow resulting in a gradual reduction of bioluminescent signal. In order for bioluminescent counts to be reliable and comparable images must be taken during the plateau phase which is cell line dependent.

Animals injected with MPM-Luc were imaged 2 hours after initial cell injection and twice weekly thereafter. Prior to imaging animals were given an intraperitoneal injection of 200 µl D-Luciferin (10mg/ml) and stilled using isofluorane anaesthesia throughout image

acquisition and placed on a heated stage to ensure they maintained an appropriate body temperature throughout anaesthesia. An initial experiment was performed to determine the luciferase kinetics of the MSTO-211HLuc tumours and identify the optimal time between D-luciferin delivery and imaging. Images were acquired every 5 minutes after D-luciferin injection and photon count was determined at each time point. For all subsequent imaging experiments D-luciferin was administered intraperitoneally 15 minutes prior to imaging. At the end of the study organs were imaged for bioluminescence and examined for macroscopic evidence of tumours.

2.10 Histological preparation of tissue

Mice were sacrificed using intraperitoneal injection of pentobarbital followed by laparotomy and exsanguination. Visible tumours were identified and removed along with bioluminescent regions detected on imaging. If lung insufflation was required, the thoracic cavity was opened, trachea exposed and cannulated with a 22G cannula. The lungs were insufflated with 10% neutral buffered formalin (Sigma, Dorset, UK) at a pressure of 25cm H_2O and the trachea was ligated. The heart and lungs were removed *en bloc* and placed in 10% neutral buffered formalin overnight at 4^{o}C. If insufflation was not required heart and lungs were removed *en bloc*, weighed and placed in 10% neutral buffered formalin overnight. The following day formalin was exchanged for 70% ethanol and kept at 4^{o}C until processed. Specimens were placed in processing cassettes, dehydrated using a Leica TP 1050 tissue processor which exposes samples to a serial alcohol gradient. The tissue was then embedded in paraffin wax and 3µm sections were cut from the paraffin embedded sections using a microtome. Sections were mounted on polylysine slides (VWR, Leicestershire, UK) for staining. Prior to all staining sections were de-waxed in xylene and rehydrated through decreasing concentrations of ethanol through to water before being washed twice in PBS.

2.10.1 Immunofluorescence

2.10.1.1 Calretinin

The primary antibody used was a rabbit polyclonal antibody to calretinin (ab702, Abcam, Cambridge, UK) at a dilution of 1:100. The secondary antibody used was AlexaFluor 555 donkey anti-rabbit (Invitrogen, Paisley, UK) at a dilution of 1:300.

Firstly the antigen was unmasked by immersing sections in 1xEDTA (pH9.0 (12g TRIS base, 1g EDTA, 3.5ml HCl, 500ml H_2O)) and microwaving at high power for two periods of 10 minutes. The sections were then cooled for 15 minutes, washed twice in PBS and blocked for 1 hour with blocking solution (PBS, 10% FBS, and 0.2% fish skin gelatin) to prevent non-specific antibody binding. The blocking solution was removed and the primary antibody diluted in blocking solution to the appropriate dilution was added and incubated overnight at 4^oC. The following day slides were washed three times in PBS for 5 minutes each and then incubated with secondary antibody diluted in blocking solution (1 in 300 dilutions) for 3 hours at room temperature. The slides were then drained and stained with DAPI (1µl DAPI in 10ml PBS) for 5 minutes. Finally the slides were washed in PBS for 5 minutes and coverslips were applied using moviol.

2.10.1.2 Luciferase

Primary antibody used was a rabbit polyclonal antibody to firefly luciferase (ab21176, Abcam, UK) at a dilution of 1:2000. Secondary antibody was an Alexa fluor 555 or 488-conjugated donkey anti rabbit (Invitrogen) at a dilution of 1:300. The choice of secondary antibody was determined by whether single or dual staining was being performed.

Sections were dewaxed as before but no antigen retrieval step was required. Sections were washed twice in PBS then left to block in PBS with 10% FBS and 0.2% fish skin gelatin for 1 hour at room temperature. Slides were incubated overnight at 4^0C with the primary antibody diluted in blocking solution and then washed three times with PBS. Sections were then incubated with the secondary antibody for 3 hours at room temperature protected from light. Finally slides were washed three times with PBS, incubated for DAPI for 5 minutes as described above and coverslips were mounted using moviol.

2.10.1.3 Visualisation of DiI-labelled cells

DiI-labelled cells could be visualised directly using microscopy as long as they were in an aqueous phase. Sections were dewaxed, stained with DAPI as already described and coverslips were mounted using moviol.

2.10.1.4 TUNEL staining

Terminal deoxynucleotidyl transferase dUTP nick end labelling (TUNEL) is a histological technique for detecting fragmented DNA due to apoptosis by labelling nicks in the DNA that are recognised the enzyme terminal deoxynucleotidyl transferase (TdT). TUNEL is one of the main methods for determining programmed cell death due to apoptosis and if used correctly will only label cells undergoing apoptosis and not necrosis.

In order to quantify the amount of apoptosis within tumour samples dual staining was performed with TUNEL and luciferase. TUNEL positive cells are visualised in the 488nm channel so for luciferase staining the primary antibody used was a rabbit polyclonal antibody to firefly luciferase (Abcam, UK) at a dilution of 1:2000 and the secondary antibody was Alexa fluor 555-conjugated donkey anti-rabbit (A31572, Invitrogen) at a dilution of 1:300. TUNEL assay was performed in accordance with the manufacturer's protocol (G3250, Promega, UK)

Slides were dewaxed, washed once in 0.85% NaCl for 5 minutes and once in PBS. Sections were then fixed in 4% PFA for 15 minutes at room temperature and washed three times with PBS for 5 minutes each. 100 µl proteinase K (20 µg/ml concentration) was added drop wise to each section to permeabilise the tissue and incubated for 8 minutes at room temperature. Slides were washed again with PBS twice followed by a further 5 minute fixation in 4% PFA and a final wash in PBS. Slides were drained and the tissue was covered with 100 µl equilibration buffer and left to incubate for 10 minutes. During this incubation a nucleotide master mix was made up on ice and kept protected from light. For each slide the nucleotide mix contained 45 µl equilibration buffer, 5 µl nucleotide mix and 1 µl TdT enzyme. For the negative control the TdT enzyme was replaced with 1 µl ddH_2O. The equilibration buffer was removed and 50 µl rTDT incubation buffer was added to the section, covered with a plastic coverslip to ensure even distribution of the mixture and

incubated for 1 hour at room temperature in the dark. Incubation was stopped by immersing the slides in a 2x saline-sodium citrate (SSC) solution for 15 minutes at room temperature and sections were washed three times in PBS. Blocking was then performed by incubating slides in blocking solution (described above in section 2.10.1.1) for 1 hour at room temperature and then incubated overnight with the primary antibody diluted in blocking solution. Slides were washed three times in PBS and incubated with the secondary antibody diluted in blocking solution for 3 hours at room temperature. Slides were drained, washed once with PBS and stained with DAPI for 5 minutes. Slides were washed again with PBS and coverslips were mounted using moviol.

2.10.1.5 BrdU staining

5-bromo 2-deoxyuridine (BrdU) is a thymidine analogue commonly used for cell proliferation assays. It is incorporated into DNA during the synthesis phase of the cell-cycle as a substitute for thymidine and thereby serves as a marker for proliferation. BrdU (Invitrogen, 00-0103) was delivered by intraperitoneal injection to each mouse 1 hour prior to sacrifice. The primary antibody used was a rat monoclonal antibody to BrdU (MCA2060, AbD Serotec, Oxford, UK) at a dilution of 1:100. The secondary antibody used was AlexaFluor 555 goat anti-rat (A21434, Invitrogen, Paisley, UK) at a dilution of 1:300. Slides were dewaxed and antigen retrieval was performed by incubating in 2M HCl for 30 mins at 37^0C. Slides were washed twice in PBS and blocking and staining was carried out as described in section 2.10.1.2.

2.11 Tumour digestion for flow cytometry

In order to determine the proportion of MSCs that home to and incorporate within the tumour, enzymatic digestion of tumour tissue was performed for flow cytometry. Firstly, bioluminescent tumours were identified on open cavity imaging at sacrifice and removed with as little lung tissue as possible. Tumour fragments were placed into a falcon tube containing 2 ml of digest medium consisting of 2 ml RPMI-1640 (Invitrogen) with 1mg/ml collagenase (Sigma) and DNase I (Roche; 10 μg/ml) for 1 hour at 37 ^{0}C. Samples were then passed through a 70 μm filter and tissue was homogenised to ensure no large fragments

remained. Samples were centrifuged at 300g for 5 minutes and the supernatant was discarded. Cell pellets were resuspended in 1 ml red blood cell lysis buffer (Sigma) for 1 minute and then neutralized with 30 ml RPMI. Samples were centrifuged again at 300g for 5 minutes and the cell pellet was resuspended in 500 µl RPMI-1640 for analysis by flow cytometry. Flow cytometry (LSR Fortessa, Beckton Dickinson) was performed for YFP using a 488nm laser and 525/50 wavelength filter set to detect tumour cells and DiR using a 633nm laser and 780/60 wavelength filter set to detect MSCs.

2.12 Microscopy and Images

Light microscopy was performed using an Olympus BX 40 light microscope and fluorescent microscopy of slides was carried out using a Carl Zeiss Axioskop 2 fluorescent microscope and an Axioscope Lumar V12 Stereo microscope. Microscopy of cells was performed using a Zeiss Axiovert S100 inverted microscope. Images were acquired using a QImaging camera linked to QCapture Pro 6.0 software or Axiovision 4.8 and merging of fluorescent images was performed using Adobe Photoshop CS4. BrdU and TUNEL positive cells were quantified using Volocity software.

2.13 Statistical analysis

Statistical analysis was performed using GraphPad Prism (GraphPad Software, CA, USA) and Microsoft Excel. Students t-test was used to analyse differences between two groups whilst the analysis of variance (ANOVA) test with a Tukey post-hoc analysis was used to analyse differences between three groups. For multiple groups measured over multiple time points repeated measures ANOVA was used. Results were considered statistically significant for $p \leq 0.05$. All *in vitro* tests were performed in triplicate and repeated 3 times and all data are represented as mean values ± standard error of mean unless otherwise stated.

Chapter Three

Generation of MSCs expressing TNF-related apoptosis inducing ligand and characterisation of malignant pleural mesothelioma cell lines

3 Generation of MSCs expressing TRAIL and characterisation of malignant pleural mesothelioma cell lines

The first aim of this project was to successfully transduce MSCs with TRAIL and to characterise malignant pleural mesothelioma cell lines to ensure they expressed characteristic mesothelioma markers and to determine their TRAIL receptor status. Initially a protocol for the production of HIV-1 lentiviral vectors producing TRAIL-IRES-eGFP under doxycycline control was optimised. Human bone marrow-derived MSCs were transduced using this vector and TRAIL expression was confirmed. Simultaneously, six human malignant pleural mesothelioma cell lines were examined for expression of calretinin and WT-1 and their TRAIL receptor status was determined. In addition, dose response curves were performed for multiple chemotherapeutic agents to determine the dosage to be used for subsequent *in vitro* co-culture experiments.

3.1 Production and titration of TRAIL-IRES-eGFP lentiviral vector

The TRAIL-IRES-eGFP plasmid was first propagated by transformation of chemically competent *E.coli* bacteria, growth of infected bacteria and subsequent extraction of the DNA plasmid. The production of the correct DNA plasmid was confirmed by the presence of appropriate sized bands on the restriction digest gels. Lentivirus was produced by co-transfecting 293T cells with pLenti-TRAIL-IRES-eGFP plasmid and with envelope and packaging vectors and the virus was harvested and concentrated by ultracentrifugation. Viral titration was performed using 293T transductions and finally MSCs were stably transduced with the lentiviral vector.

3.1.1 Lentiviral titration of 293T cells with pLenti-TRAIL-IRES-eGFP

Usually after concentration of lentiviral vectors the titre of the virus is determined using transduction of HeLa cells. This both confirms that the process of lentivirus production has been successful and allows the calculation of multiplicities of infection for target cell transduction. HeLa cells are usually used for this as they are highly permissible to lentivirus transduction and with the pLenti-TRAIL-IRES-eGFP virus the proportion of cells expressing GFP can be easily determined by flow cytometry and used to estimate the viral titre. However, HeLa cells are a cervical cancer cell line and are known to undergo apoptosis in the presence of TRAIL. 293T cells are also readily permissible to lentivirus transduction and as a non-malignant cell line are known to be resistant to the apoptotic effects of TRAIL. For this reason lentiviral titration was performed using 293T cells. As the production of lentivirus is variable over time, a separate viral titration was performed for both the day 1 and day 2 viral harvests. $5x10^4$ 293T cells were transduced with a dilution series of viral vectors, cells were exposed to doxycycline for 48 hours to induce transgene expression and flow cytometry for GFP was performed to determine the proportion of GFP transduced cells (Figure 3.1).

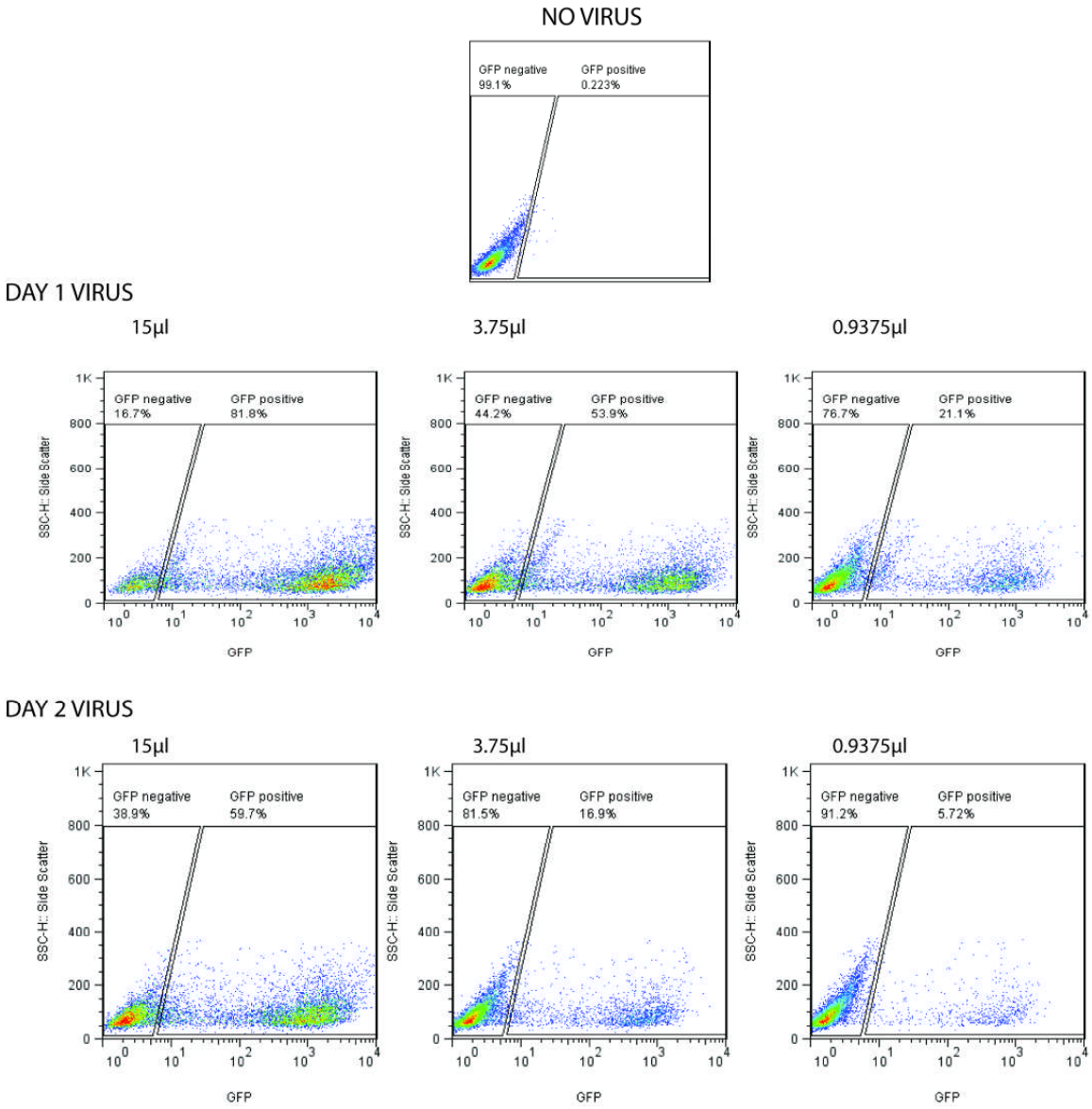

Figure 3.1 Titration of TRAIL lentivirus by transduction of 293T cells. 293T cells were transduced using a dilution series of concentrated lentiviral vectors. Doxycycline was added for 48 hours to activate transgene expression and flow cytometry was performed to determine the proportion of cells expressing GFP. Examples of flow cytometry plots showing GFP expression for a range of viral concentrations, volumes of virus shown indicates the volume of concentrated viral vector used for transduction

By using the proportion of 293T cells expressing GFP and the number of cells exposed to the lentiviral vector the number of cells successfully transduced by a known volume of virus can be determined. The different concentrations of virus on different collection days achieved ratios of 81.8 to 2.36% GFP positive cells. Higher ratios of GFP positive and therefore virally infected cells are likely to represent multiple copies of plasmids per cell and calculations using these numbers would result in an underestimate of viral titres. For this reason the viral titre was calculated using the concentration of virus that resulted in transduction rates of 10-20% where there would be fewer cells transduced with multiple copies. Using the equation:

$$\text{Viral titre} = \frac{\text{number of cells plated x proportion of GFP positive cells}}{\text{Volume of virus in ml}}$$

and the examples from figure 3.1 there were 1.2×10^7 infectious units/ml in the day 1 virus and 2×10^6 viral particles in the day 2 virus.

3.2 MSCs transduced to stably express TRAIL under doxycycline control

Once the concentration of the pLenti-TRAIL-IRES-eGFP lentiviral vector had been determined the next step was to stably transduce the MSCs with TRAIL. Work done previously within our group had determined that a multiplicity of infection (MOI) of 10 was optimal for transducing MSCs [104]. MSCs were transduced in a T175 cm^2 flask and once the virus had been removed cells were allowed to become confluent prior to performing flow cytometry. This is because MSCs can only be expanded for a limited number of passages and their homing capabilities are thought to reduce with increasing passage. Once cells were transduced it was essential for them to be expanded prior to harvesting and using for further experiments. Using an MOI of 10, 96% of cells were successfully transduced with GFP as determined by flow cytometry (Figure 3.2).

3.2.1 Confirmation of doxycycline inducible expression of GFP and simultaneous TRAIL production

In order to confirm doxycycline inducible GFP expression in TRAIL transduced MSCs, transduced cells were activated by exposure to doxycycline for 48 hours and GFP expression was determined by flow cytometry. To ensure the GFP expression was not leaky, the percentage of GFP expressing cells were compared to TRAIL transduced MSCs that were cultured in the absence of doxycycline and to the untransduced parental MSC cells. As the TRAIL lentiviral vector contains an IRES element the expression of TRAIL and GFP are linked. In order to confirm that TRAIL protein production occurred along with GFP expression a TRAIL ELISA was performed on cell lysates from untransduced cells, transduced cells cultured in standard culture media and transduced cells cultured in doxycycline for 48 hours (Figure 3.2C).

Flow cytometry showed a significant increase in GFP positive MSCs in transduced cells cultured in doxycycline containing media compared to untransduced cells. The ELISA could not detect TRAIL in untransduced cells. Cell lysates from transduced cells not exposed to doxycycline showed very low levels of TRAIL expression (6 pg TRAIL/µg total protein) whilst lysate from transduced cells exposed to doxycycline showed a significant increase in the TRAIL protein production (232 pg TRAIL/µg total protein; $p=<0.0001$; Figure 3.2E). There was also a significant increase in TRAIL production in the cell supernatant from transduced cells treated with doxycycline compared to those not treated with doxycycline. This confirms that doxycycline treatment of transduced cells results in TRAIL production. It was expected that low levels of TRAIL would be found in the cell supernatant as it is known that whilst the majority of TRAIL is membrane bound low levels are excreted into the supernatant which would explain why TRAIL acts both by cell-cell contact and by paracrine mechanisms.

Previous time course experiments had established that the TRAIL transgene was turned on within 24 hours of doxycycline exposure *in vitro* and reached near maximal production after 48 hours but took up to 7 days for TRAIL production to cease after doxycycline removal. This showed that the transgene could be successfully regulated by doxycycline administration and that 48 hours of drug administration was required for maximal TRAIL production [104].

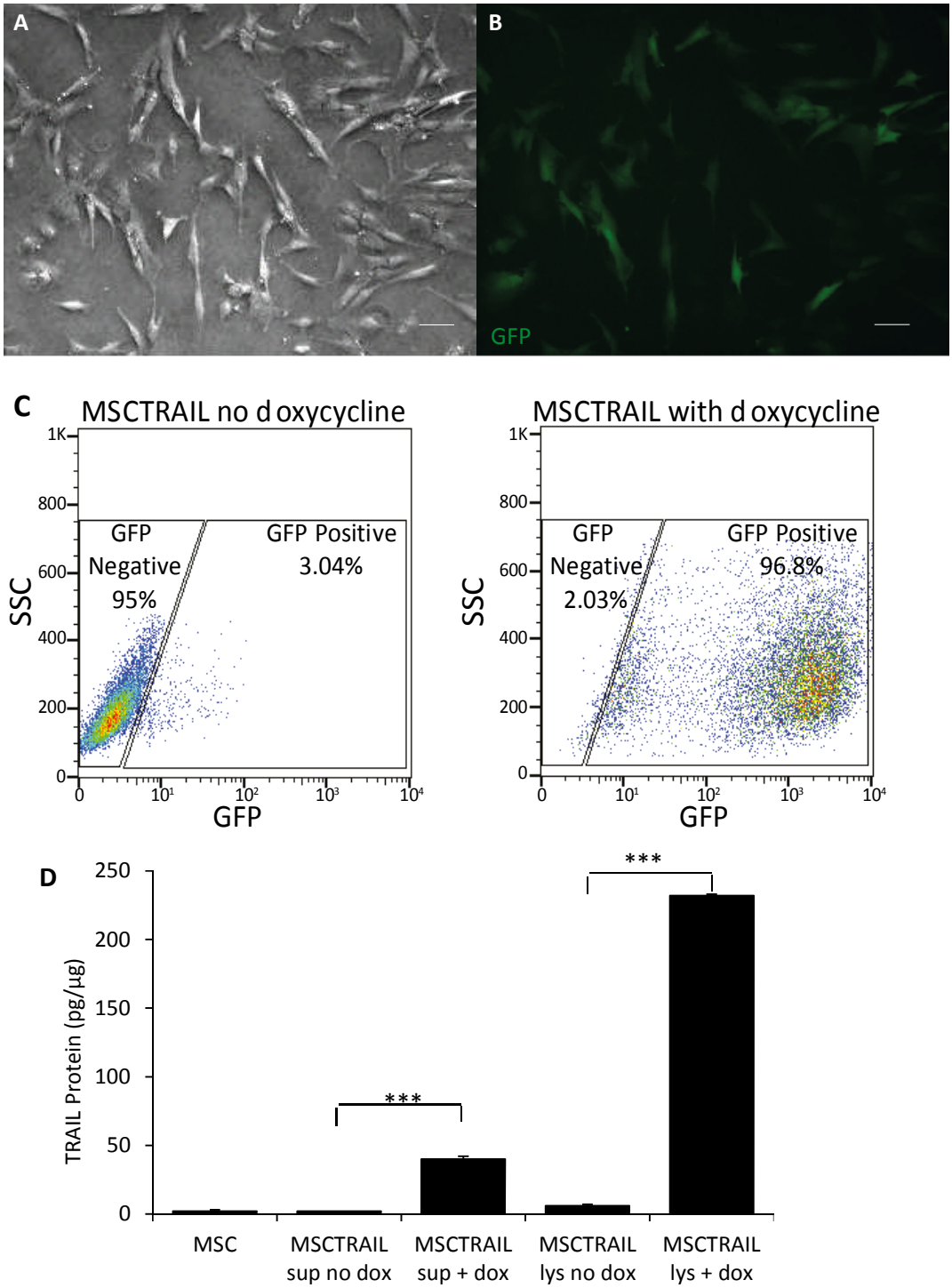

Figure 3.2 MSC Transduction. A, Bright field and B, fluorescence microscopy to confirm GFP expression following transduction of MSC with TRAIL-IRES-eGFP lentivirus and activation with doxycycline (10 µg/ml) (magnification x5; scale bar 20 µm). C, Flow cytometry plots confirming efficiency of MSC transduction following TRAIL activation with doxycycline and D, TRAIL ELISA of MSC cell supernatant (sup) and lysate (lys) demonstrating the production of TRAIL protein following MSCTRAIL activation with doxycycline (*** $p<0.0001$). There is minimal TRAIL production following MSC transduction in the absence of doxycycline and low levels in cell supernatant from activated MSCTRAIL.

3.3 Characterisation of malignant pleural mesothelioma cell lines

Six malignant pleural mesothelioma cell lines (MSTO-211H, H28, H2052, JU77, ONE58 and LO68) and one control benign mesothelial cell line (Met5A) were assessed for the presence of characteristic markers of malignant mesothelioma. Cells were plated on chamber slides and immunofluorescence was performed for calretinin and WT-1 antigen. All MPM cell lines showed characteristic nuclear and cytoplasmic staining for calretinin and nuclear staining for WT-1 antigen and images from representative cell lines are shown in Figure 3.3. In addition cell lines were positive for the active TRAIL receptor DR5 suggesting that they would be sensitive to treatment with TRAIL (Figure 3.4).

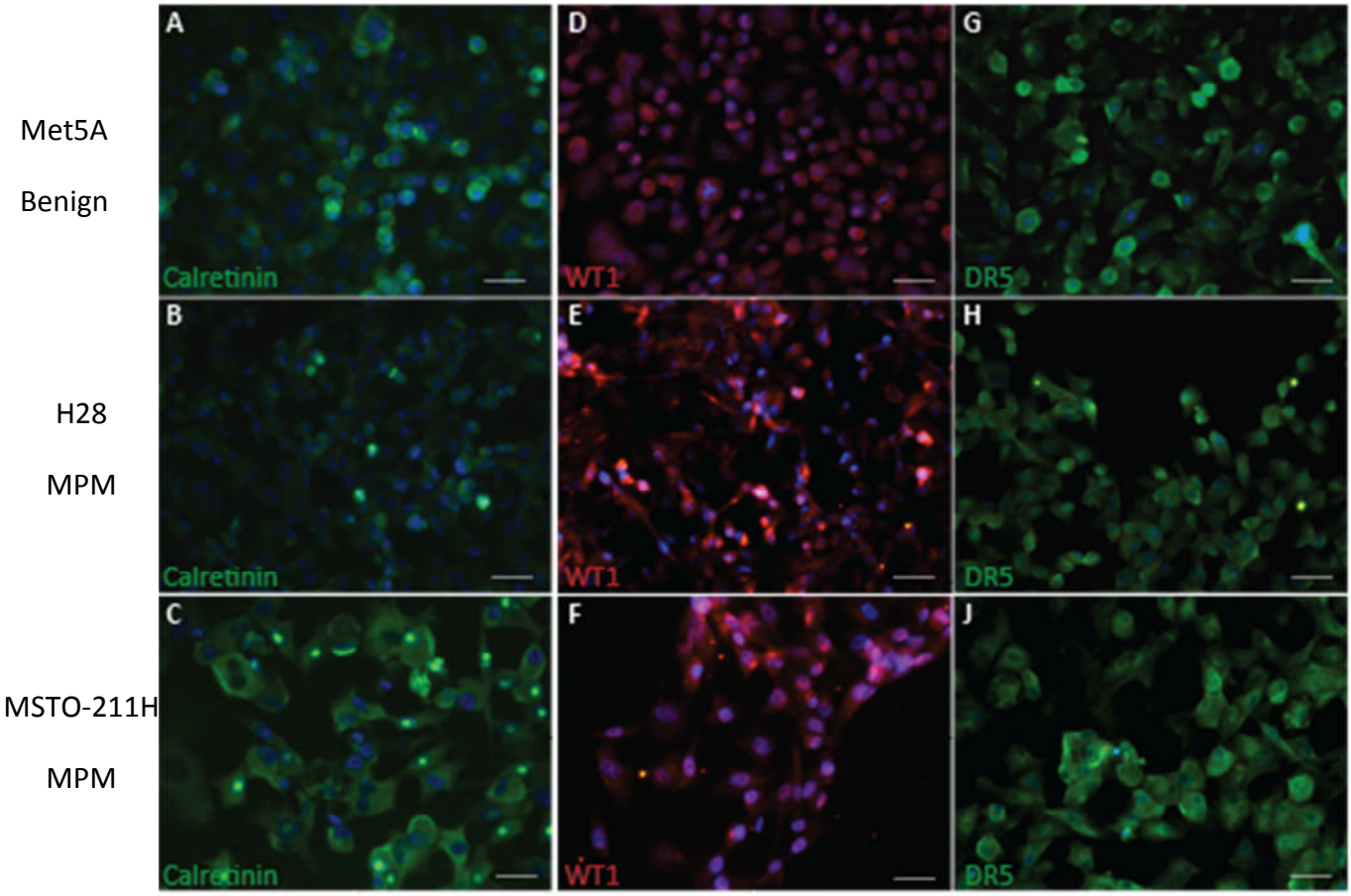

Figure 3.3. Mesothelioma Cell Line Characterisation. A-C, immunofluorescence confirms the presence of calretinin and D-F, WT1 antigen in human MPM cell lines H28 and MSTO-211H and human benign mesothelial cell line Met5A. G-J, both MPM and the benign mesothelial cell lines show the presence of the active TRAIL death receptor DR5 (magnification x20, bar 40 μm).

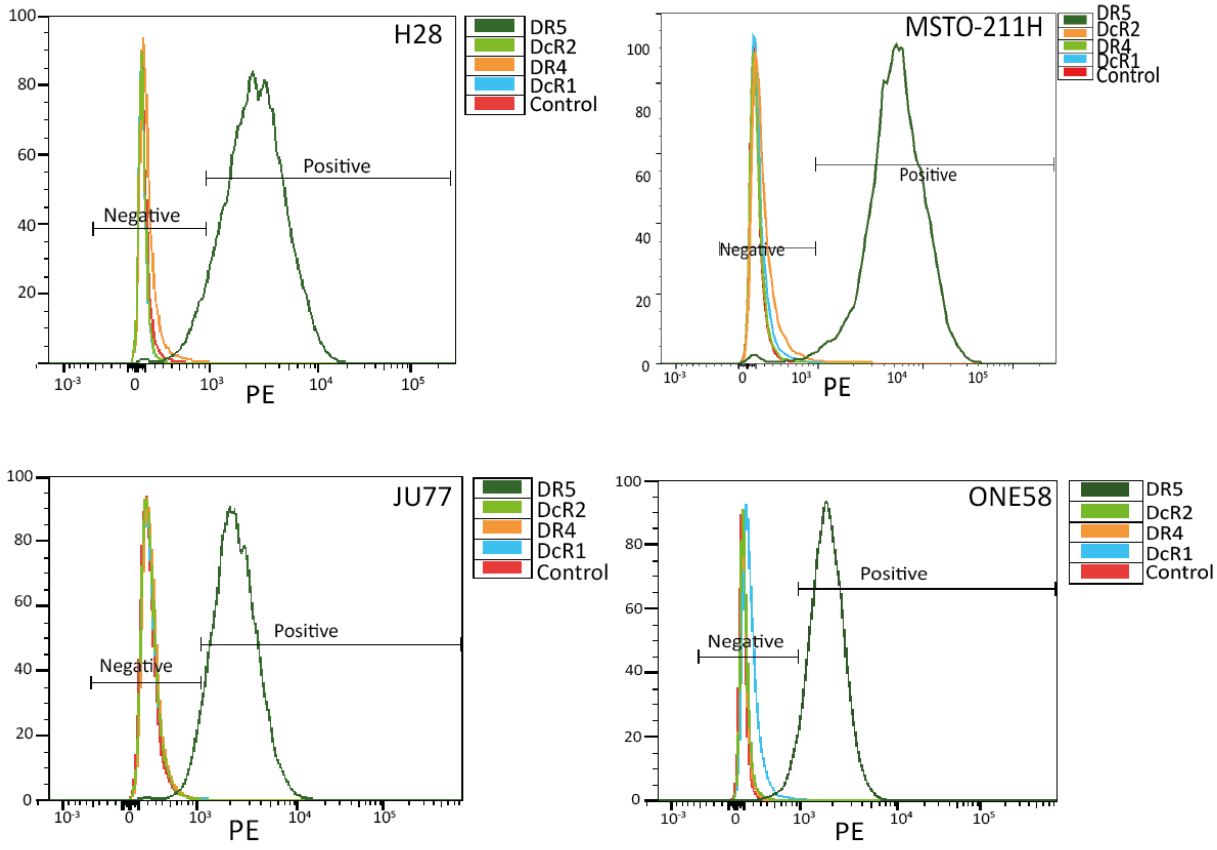

Figure 3.4: MPM cell lines show the presence of the active TRAIL receptor DR5. Flow cytometry histograms of H28, JU77, MSTO-211H and ONE58 MPM cell lines showing the presence of the active TRAIL death receptor DR5. MPM cells were harvested and resuspended at a concentration of $1x10^6$ cells/ml, then incubated with antibodies against the four TRAIL receptors or an isotype control, followed by biotinylated secondary goat anti-mouse IgG1 and streptavidin-PE. Flow cytometry was performed to detect PE. There are low levels of DR4 and the decoy receptors, DcR1 and DcR2 which suggests that in the case of these MPM cell lines, TRAIL signals predominantly by the DR5 receptor.

3.4 Determination of dose-response curves for chemotherapeutic agents

The idea behind combining chemotherapeutic agents with MSCTRAIL is that by targeting both the intrinsic and extrinsic apoptotic pathways there would be a synergistic effect on apoptosis. For any drug to be clinically acceptable it is preferable to use the lowest possible dose required to produce a therapeutic effect, thereby limiting potential side effects. For this reason we first performed dose-response curves for each agent by testing the effects of chemotherapy on cell proliferation and from this data selected the drug dosage that inhibited growth by 30%. Dose ranges assessed were in accordance with data already published and were as follows: cisplatin 0-32 μM, pemetrexed 0-200 μM, and SAHA 0-10 μM [202] [203]. Treatment of four MPM cell lines with cisplatin, pemetrexed and SAHA showed dose-dependent cytotoxicity (Figure 3.5).

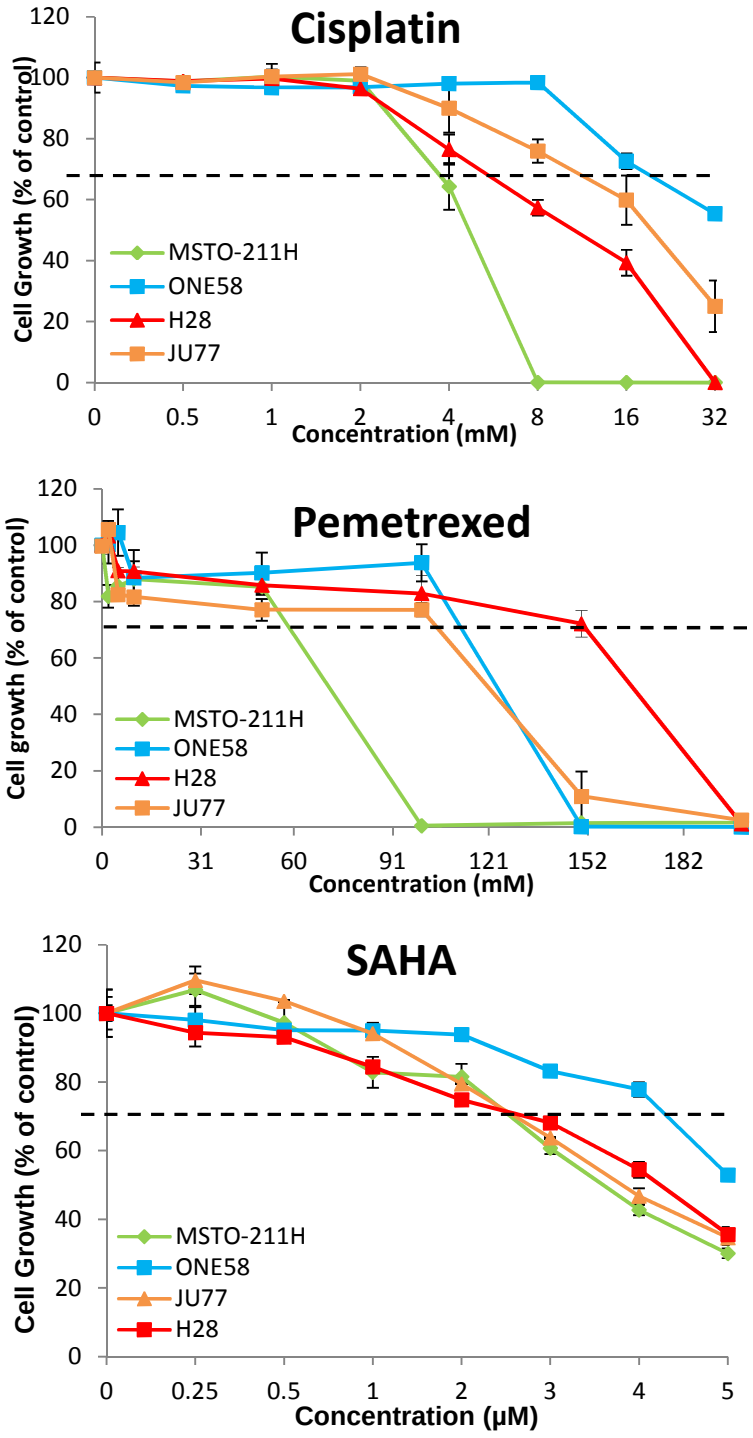

Figure 3.5: Dose response curves for chemotherapy agents for malignant mesothelioma. MPM cell lines were treated with varying doses of cisplatin (0-32 µM), pemetrexed (0-200 µM) and SAHA (0-5 µM) and cell proliferation was determined by XTT assay after 48 hrs. Absorbance values obtained with untreated cells were taken as 100%. The dose required to reduce cell growth by 30% (shown by a dotted line) was determined and used for future co-culture experiments.

The IC_{70} for SAHA ranged from 2.5-4.5 μM but that range was much larger for both cisplatin and pemetrexed with doses ranging from 4-16 μM for cisplatin and from 60-160 μM for pemetrexed. This reflects the heterogeneous nature of MPM that is seen clinically and can explain why patients have such a varied response to treatment with chemotherapy. SAHA was chosen to take forward for *in vitro* and *in vivo* testing for a two main reasons; firstly for its inhibitory effect on c-FLIP which would potentially increase the effect of TRAIL on cancer cell apoptosis and secondly, as the cell lines tested had a similar response to a narrow range of drug concentrations it may be more likely to have therapeutic efficacy in a larger patient population.

3.5 Discussion

3.5.1 Titration of lentiviral vectors

Transduction of 293T cells with a dilution series of viral concentrations was used to estimate the titres of the lentiviral vectors. Usually HeLa cells are used for this purpose as they are highly permissible to transduction but as this is a cervical cancer cell line it was likely that these cells would die when exposed to TRAIL and thereby reduce the accuracy of the titration results. Estimation of lentiviral vector titres are based on the number of cells transduced following exposure to a known amount of virus, but does not discriminate between single and multiple copies of vector incorporating within the host cell. This could lead to an underestimate of the viral titre. There are other methods that can be used to determined lentiviral vector titres such as measurement of the amount of p24 viral capsid protein by ELISA, or viral RNA by qRT-PCR. However these techniques may overestimate viral titres by detecting protein or RNA from defective particles [204].

3.5.2 MSC transduction using pLenti-TRAIL-IRES-eGFP

Human MSCs were successfully transduced using the pLenti-TRAIL-IRES-eGFP lentiviral vector. Using an MOI of 10 over 90% of MSCs were transduced as determined by flow cytometry for GFP. Previous studies have used lentiviral vectors to transduce MSCs with either fluorescent markers or other gene therapies and an MOI of 10 is used consistently to achieve transduction rates of >70% [104, 205] . To confirm that expression of GFP was associated with production of TRAIL an ELISA was performed on cell lysates of untransduced cells, transduced cells not exposed to doxycycline and transduced cells following exposure to doxycycline. The ELISA confirmed that transduced cells activated with doxycycline produced both GFP and high levels of TRAIL protein.

3.5.3 Characterisation of MPM cell lines

Malignant mesothelioma is a very heterogeneous disease and in some circumstances can be challenging to diagnose in patients. The mainstay of diagnosis clinically is immunohistochemical staining with a panel of negative and positive markers that aim to both identify the cells as mesothelial in origin along with their malignant nature, and to differentiate them from other types of cells that may undergo malignant transformation

within the same body cavity. In the case of malignant pleural mesothelioma it is important to differentiate between malignant mesothelioma and adenocarcinomas and squamous cell carcinomas of both primary lung and metastatic origin. Within a clinical setting, the most common differential diagnosis when considering a malignant pleural mesothelioma is a lung carcinoma. The consensus statement from the International Mesothelioma Interest Group (IMIG) suggests that in addition to pancytokeratin tumours should be tested for 2 mesothelioma markers and 2 carcinoma markers and if the results are concordant then a diagnosis can be confirmed [8].

There are a number of issues relating to the use of cell lines rather than primary cells for *in vitro* studies. One concern is that as cells divide in culture they can develop genetic and epigenetic alterations with the natural selection of altered cells potentially resulting in overgrowth of abnormal, culture-generated cells which may have different characteristics to the original parent population [206]. In addition, another significant concern is that cell lines can become cross-contaminated resulting in a mixed cell population with some groups suggesting that 15-20% of studies using cell lines are done so with cross-contaminated cells [207, 208]. To try and combat this we authenticated the MPM cells prior to use in all *in vitro* experiments. Using some of the immunohistochemical markers recommended by the IMIG we successfully demonstrated that all our MPM cell lines were positive for calretinin, WT-1 and pancytokeratin (data not shown), providing us with reassurance that our lines were representative of MPM.

3.5.4 TRAIL receptor status of MPM cell lines

In addition to confirming the presence of mesothelioma markers it was important to assess whether or not our cell lines expressed TRAIL death receptors and therefore whether or not they were likely to be sensitive to our MSCTRAIL therapy. TRAIL is able to interact with five different death receptors; two active receptors DR4 and DR5 and three decoy receptors DcR1, DcR2 and osteoprotegerin. The two active receptors are type I transmembrane proteins containing a cytoplasmic domain that contains a death domain that binds to pro-caspases resulting in the formation of a death-inducing signalling complex (DISC). On formation of the DISC there is downstream activation of a caspase cascade that ultimately results in cellular apoptosis. The decoy receptors share the same extracellular construction

as the active receptors but DcR1 has no intracellular domain whilst DcR2 has a truncated intracellular domain preventing either receptor from forming a DISC and the subsequent activation of the caspase cascade. Whilst it would seem logical that cell sensitivity to TRAIL may be directly regulated by the presence or absence of the death receptors this is not the case and post-translational modification by means of glycosylation and palmitoylation of the receptors is a more likely mechanism. Studies have shown a correlation between the expression of the enzyme initiating GALNT14 glycosylation and TRAIL sensitivity in pancreatic carcinoma, lung cancer and malignant melanoma cell lines which seems to effect the receptor oligomerisation in response to TRAIL binding rather than its expression [209].

The MPM cell lines studied expressed very low levels of DR4, DcR1 and DcR2 on immunohistochemical staining (data not shown) but good levels of DR5 and flow cytometry confirmed the presence of DR5 receptors suggesting that TRAIL induced apoptosis was a feasible mechanism for inducing MPM cell death.

3.5.5 Chemotherapy dose-response curves

Dose response curves were determined for three different chemotherapeutic agents: cisplatin, pemetrexed and SAHA. These agents were chosen as the current first line treatment for MPM is cisplatin in combination with pemetrexed and SAHA has shown promising pre-clinical activity in killing MPM and is currently in phase III clinical trials as a second line single agent therapy. Our results show that there is large variability in the response of MPM to chemotherapy agents – particularly cisplatin and pemetrexed, but that the response to SAHA may be more uniform. For this reason we selected SAHA as the combination agent to test both *in vitro* and *in vivo* and the dose selected was 2.5 μM. This dose showed some therapeutic efficacy as shown by a reduction in cell proliferation but is a low enough dose that toxicity would be potentially limited.

3.6 Summary

- HIV-1 based lentiviral vectors expressing TRAIL and GFP under the control of doxycycline can be generated by co-transfection of 293T cells with the lentiviral vector plasmid along with envelope and packaging plasmids
- Human MSCs can be successfully transduced with these lentiviral vectors achieving excellent transduction rates of >90%
- Expression of GFP is regulated by exposure to doxycycline and that expression of GFP is associated with TRAIL protein production
- All MPM cell lines express characteristic markers of mesothelioma and the active TRAIL death receptors required for TRAIL binding
- Different MPM cell lines have a differing response to chemotherapeutic agents as shown by dose response curves
- The dosages of different chemotherapeutic agents required to reduce cell growth by 30% varies greatly for cisplatin and pemetrexed but is much narrower for SAHA

Chapter 4

Determination of the *in vitro* effects of MSCTRAIL on MPM cells both alone and in combination with chemotherapy

4 Determination of the *in vitro* effects of MSCTRAIL on MPM cells both alone and in combination

This chapter describes the results of experiments performed to address aim 2 (section 1.7) 'to determine the *in vitro* sensitivity of multiple human malignant pleural mesothelioma cell lines to MSCTRAIL alone and in combination with existing chemotherapy agents'. Whilst many cancer cell lines are known to undergo apoptosis when treated with rTRAIL and MSCTRAIL there are also some cancer cell lines that are known to be resistant. Clinically the recommended first line treatment for malignant mesothelioma is pemetrexed and cisplatin, however new drugs such as SAHA are in phase 3 clinical trials. Experiments were therefore carried out to determine the sensitivity of all MPM cell lines to rTRAIL and MSCTRAIL and selected cell lines were tested for their response to combinations of pemetrexed, cisplatin and SAHA with MSCTRAIL and rTRAIL.

4.1 Demonstrating the biological activity of MSCTRAIL and rTRAIL as single agents in MPM

Once the MSCs had been successfully transduced with TRAIL the next step was to determine their biological activity against malignant mesothelioma cells *in vitro*. In order to demonstrate this co-culture experiments were performed. Mesothelioma cells were plated in equal ratios with MSCTRAIL or with 200ng/ml rTRAIL and cell death and apoptosis was assessed using Annexin V/DAPI flow cytometry. A schematic of the experimental set up is shown in figure 4.1.

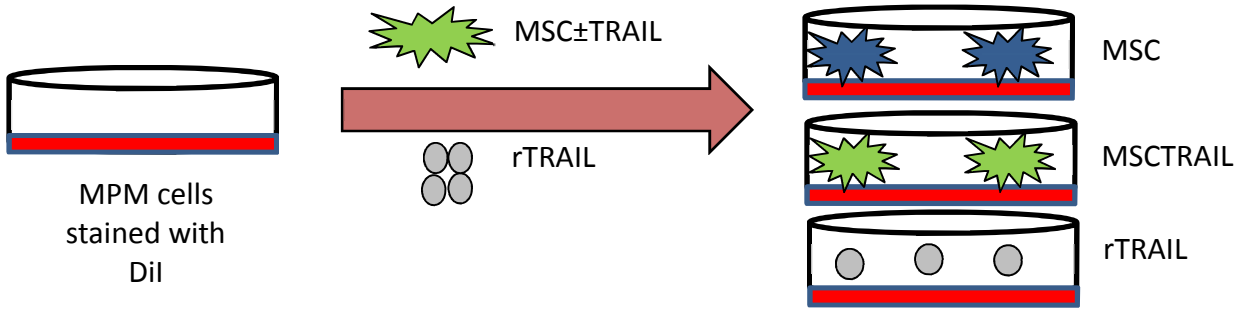

Figure 4.1: Schematic to show co-culture experiments to assess the biological activity of MSCTRAIL and rTRAIL on MPM cell lines. MPM cells were labelled with DiI and plated at a density of 50,000 cells per well along with 50,000 MSCTRAIL cells according to experimental design. After 24 hours medium was exchanged for either normal culture medium, medium containing 10 µg/ml doxycycline or 200 ng/ml rTRAIL. After 48 hours cells and supernatant were collected, stained for annexin V and DAPI and flow cytometry was performed.

Six different mesothelioma cell lines were tested for their sensitivity to MSCTRAIL and whilst both apoptosis and death increased with the addition of doxycycline and activation of TRAIL in all cell lines, the percentage of cells dying varied greatly. During analysis gating was used to include only DiI positive MPM cells and exclude all DiI negative MSCs from further analysis. DiI positive cells were then gated according to annexin V and DAPI staining with alive cells being annexin V-/DAPI-, apoptotic cells being annexin V+/DAPI- and dead cells being annexin V+/DAPI+. Representative flow cytometry plots of MSTO-211H, H28 and Met5A are shown in Figure 4.2.

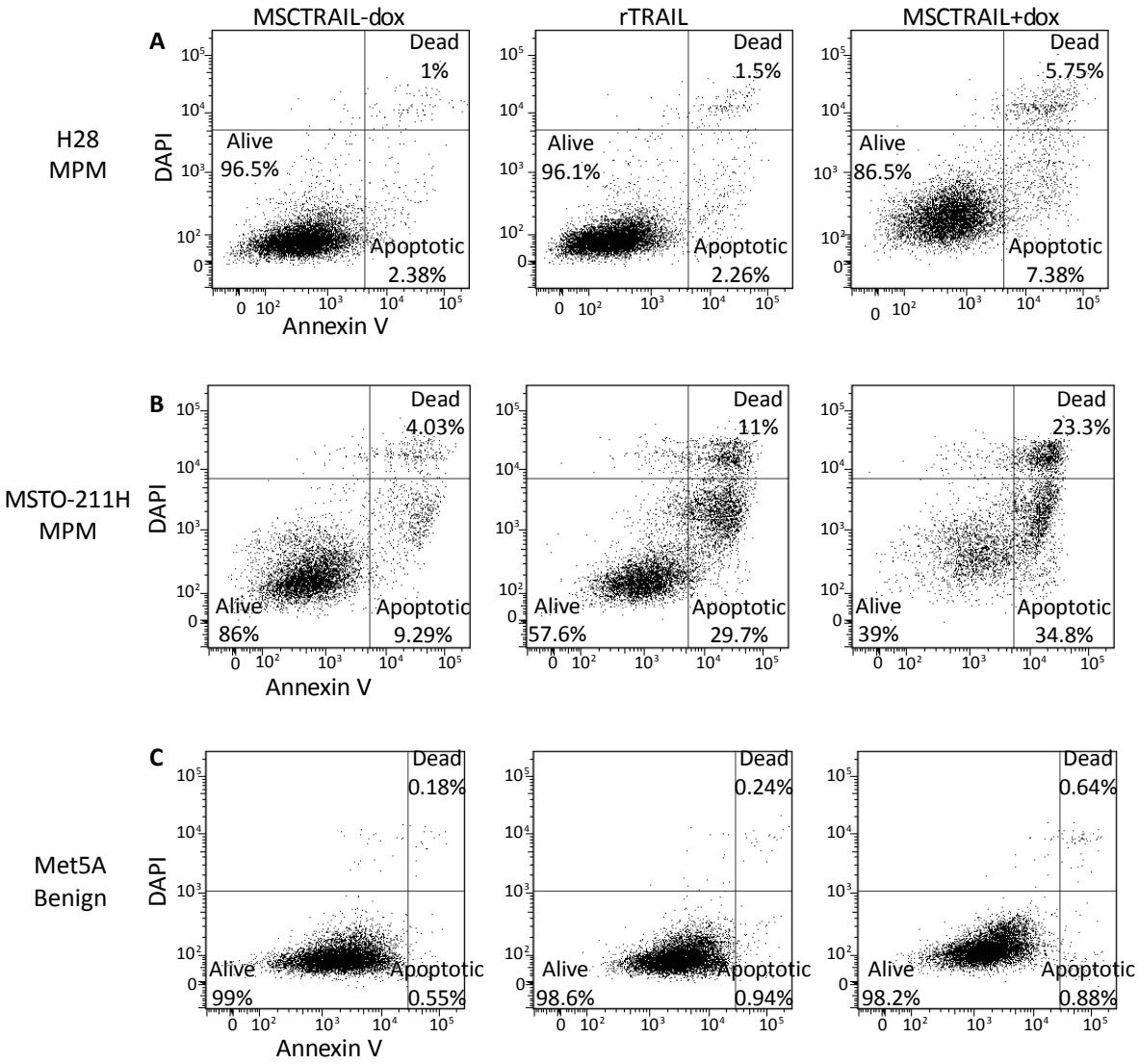

Figure 4.2: Representative flow cytometry plots showing death and apoptosis of MPM cell lines. Flow cytometry plots showing increased apoptosis and cell death following treatment with rTRAIL and MSCTRAIL + dox in A, H28 and B, MSTO-211H cell lines. Control benign mesothelial cells Met 5A, C, shows no significant increase in death or apoptosis when treated with rTRAIL or MSCTRAIL + dox.

MSTO-211H and ONE58 both showed significant sensitivity to treatment with MSCTRAIL with an increase in combined apoptosis and cell death from 12.86 ± 0.8% to 58.15 ± 1.2% ($p<0.0001$) with and without doxycycline respectively in MSTO-211H and from 3.84 ±0.6% to 22.32 ± 0.7% ($p<0.0001$) in ONE58. MSTO-211H was significantly more sensitive to MSCTRAIL than rTRAIL with apoptosis and death in rTRAIL being 42.57 ± 4.2% ($p<0.01$), whilst ONE58 was more sensitive to rTRAIL than MSCTRAIL (38.58 ± 1.2% vs 22.32 ± 0.7%; $p<0.0001$). H28 showed a smaller but still significant increase in cell death when comparing inactivated MSCTRAIL to activated MSCTRAIL from 3.37 ± 0.1% to 11.33 ± 0.7%; $p<0.0001$) and in this cell line there was no significant difference between inactivated MSCTRAIL and rTRAIL (3.37 ± 0.1% vs 3.59 ± 0.1%; ns). The cell line JU77 was also less sensitive to TRAIL with an increase in death and apoptosis from 3.58 ± 0.6% with inactivated MSCTRAIL to 7.99 ± 1.4% with activated MSCTRAIL ($p<0.001$). Treatment with rTRAIL resulted in 4.89 ± 0.2% cell death which is significantly less than with MSCTRAIL ($p<0.05$). A similar result was seen with LO68 which showed an increase from 3.04 ± 0.2% to 9.08 ± 0.9% ($p<0.0001$) with rTRAIL showing similar results to MSCTRAIL no doxycycline (3.44 ± 0.1%). H2052 showed a significant increase in cell death with rTRAIL compared to inactivated MSCTRAIL (from 3.6 ± 0.4% to 5.92 ± 0.9%; $p<0.05$) and a larger increase when compared to treatment with activated MSCTRAIL (3.6 ± 0.4% to 7.31 ± 0.6%; $p<0.001$). Figure 4.3 shows percentages of apoptosis/death in all cell lines.

The control cell line, Met5A, which is a benign mesothelial cell line showed no significant increase in cell death or apoptosis following treatment with either MSCTRAIL or rTRAIL (0.79 ± 0.05% vs 1.87 ± 1.1% and 1.5 ± 0.2% respectively; ns). Our results would be consistent with previous data showing that only malignant cells are sensitive to TRAIL induced apoptosis whilst normal cells are resistant [42].

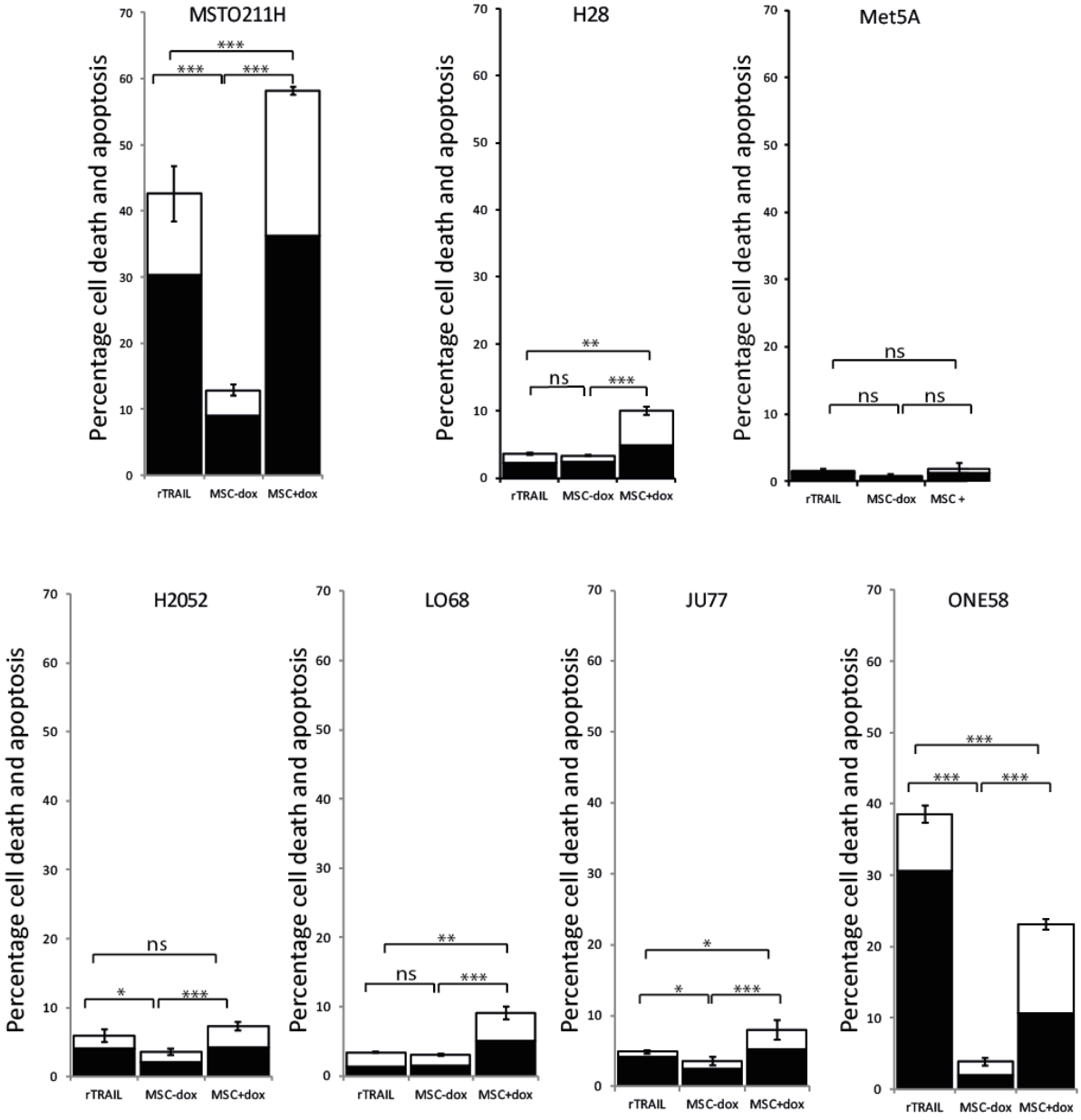

Figure 4.3: Human MPM exhibit variable sensitivity to MSCTRAIL and rTRAIL *in vitro*. Histograms showing flow cytometry data from co-culture experiments showing an increase in cell death and apoptosis in cell lines A, H28 and MSTO-211H whilst there is no significant increase in death and apoptosis in the benign control cell line Met 5A. B, Histograms showing flow cytometry data from co-culture experiments in cell lines ONE58, JU77, H2052 and LO68 that demonstrates a variable response to both rTRAIL and MSCTRAIL. (* $p<0.05$; ** $p<0.001$; *** $p<0.0001$)

Doxycycline has previously been reported to have cytostatic effects on multiple tumour cell lines including malignant mesothelioma [210]. To assess the effect of doxycycline on the MPM cell lines we plated cells in a 6 well plate and left them to adhere overnight. Medium was changed the following day for medium containing 10 µg/ml doxycycline and left for 48 hours. Cells were trypsinised and collected along with the supernatant, stained for annexin V and DAPI as before and flow cytometry was performed. The results are shown in Figure 4.4.

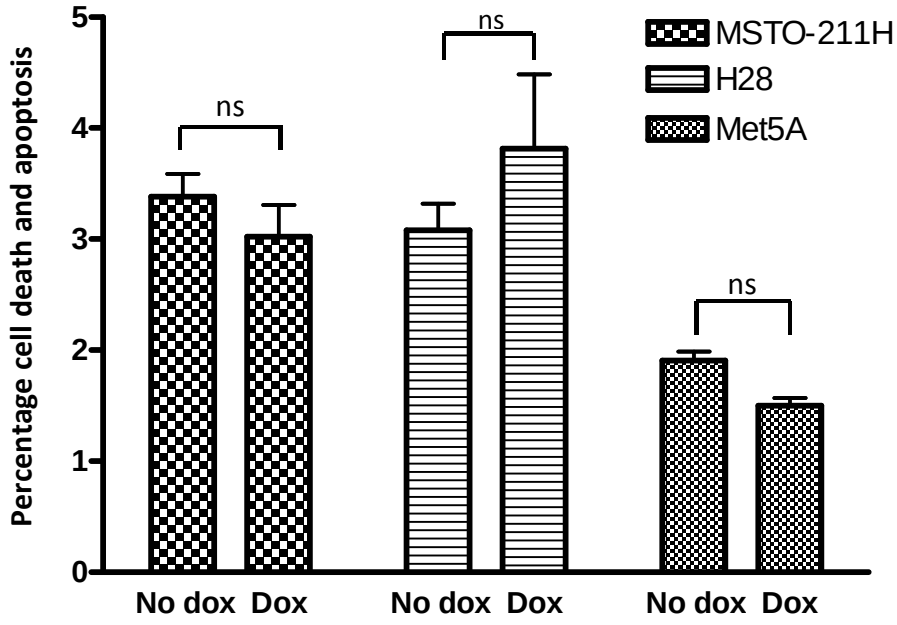

Figure 4.4: Doxycycline has no effect on cell death and apoptosis. Flow cytometry for annexin V and DAPI was carried out on MPM cells exposed to 10 µg/ml doxycycline for 48 hours. There was no significant difference between the percentage of dead and apoptotic cells in MSTO-211H and Met5A cell lines.

4.2 MSCTRAIL in combination with chemotherapy agents

From the results of the co-culture experiments assessing the response of MPM cell lines to treatment with single agent MSCTRAIL or rTRAIL it was clear that whilst all cell lines showed a significant increase in cell death and apoptosis on treatment with MSCTRAIL there was huge variability in the percentage apoptosis seen between cell lines. This is not entirely surprising and would be consistent with the clinical course of this disease. It is well known that mesothelioma is a heterogeneous disease and there is variability in patients' response to treatment. To determine whether combining MSCTRAIL therapy with existing chemotherapy agents would result in a synergistic increase in apoptosis and cell death, co-culture experiments were repeated as before but using chemotherapeutics in combination with MSCTRAIL as the experimental design dictated. To make the study as clinically relevant as possible, three chemotherapy agents were chosen for co-culture experiments; pemetrexed and cisplatin as these are the current gold standard treatment for malignant mesothelioma and SAHA the HDAC inhibitor that is being assessed in phase 3 clinical trials for second line treatment. Because of the great variability in results from initial co-culture experiments one cell line with 'high TRAIL sensitivity' and one with 'low TRAIL sensitivity' were selected for further work. MSTO-211H was selected from the high TRAIL sensitivity group and H28 was selected from the low TRAIL sensitivity group. Met5A was kept as the benign control cell line.

4.2.1 The effect of SAHA on MSCs

Prior to starting combination treatment with SAHA and MSCTRAIL the effects of SAHA on MSCs alone were tested. This was done to ensure that MSCs were not killed by SAHA which would make further use of this combination impractical. MSCs were plated at a density of 50,000 cells per well in a 6-well plate and left to adhere for 24 hours. Medium was exchanged for medium containing 2.5 μM SAHA and cells were left for 48 hours. Cells were assessed for apoptosis and death as before (section 4.1) and flow cytometry analysis showed there was no significant difference in cell death and apoptosis between untreated MSCs and those treated with SAHA (Figure 4.5).

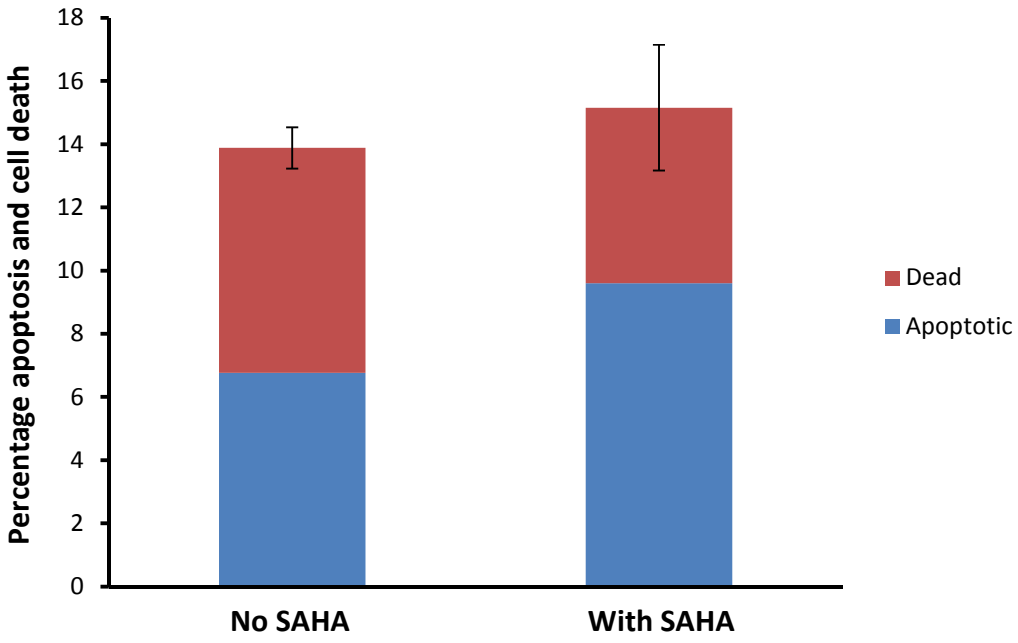

Figure 4.5: SAHA has no effect on MSC apoptosis and death. Flow cytometry for annexin V and DAPI was performed on MSCs exposed to 5 µM SAHA for 48 hours. Bar chart shows the percentage of apoptosis and cell death in cells incubated with and without SAHA and reveals no significant difference between the two groups.

4.2.2 Determining the biological effect of MSCTRAIL in combination with SAHA on MPM

Once it had been established that SAHA did not result in MSC death the next step in the *in vitro* assessment of MSCTRAIL was to combine SAHA and MSCTRAIL therapy. The experimental design was as before (section 4.1 and Figure 4.1) with the alteration that 24 hours after cell plating, medium was exchanged for culture medium containing; doxycycline alone, SAHA alone, rTRAIL alone, rTRAIL and SAHA or doxycycline and SAHA. The SAHA dose used was 2.5 μM. Plates were left for 48 hours as before and apoptosis and death were measured as previously described.

Both MPM cell lines showed a significant increase in death and apoptosis when treated with MSCTRAIL in combination with SAHA compared to either treatment alone. In the MSTO-211H cell line which has 'high TRAIL sensitivity' the levels of apoptosis and cell death when treated with single agents rTRAIL and MSCTRAIL were similar to the levels seen in previous experiments, 40.57 ± 3.3% and 55.97 ± 0.5% respectively (Figure 4.6). Treatment with SAHA alone showed significantly higher levels of apoptosis and death than either with rTRAIL alone or MSCTRAIL alone, 87.41 ± 3.4% for SAHA vs 40.57 ± 3.3% and 55.97 ± 0.5% respectively ($p<0.001$). When the effect of combination treatment was assessed there was no significant increase in cell death when comparing SAHA alone (87.41 ± 3.4%) to SAHA with rTRAIL (88.2 ± 2.2%) but there was a significant increase when compared to rTRAIL alone (87.41 ± 3.4% vs 40.57 ± 3.3%; $p<0.001$). Combining MSCTRAIL with SAHA again showed a significant increase in apoptosis and cell death compared with MSCTRAIL alone (75.97 ± 1.5 vs 55.97 ± 0.5%; $p<0.001$) but there was no significant difference between treatment with SAHA+rTRAIL and SAHA+MSCTRAIL. Whilst this would suggest that our combination of SAHA and MSCTRAIL provided no additional therapeutic benefit over SAHA and rTRAIL there would still be the added benefit of having targeted delivery of MSCTRAIL directly to the site of the tumour and would avoid the problems with the short half-life of rTRAIL.

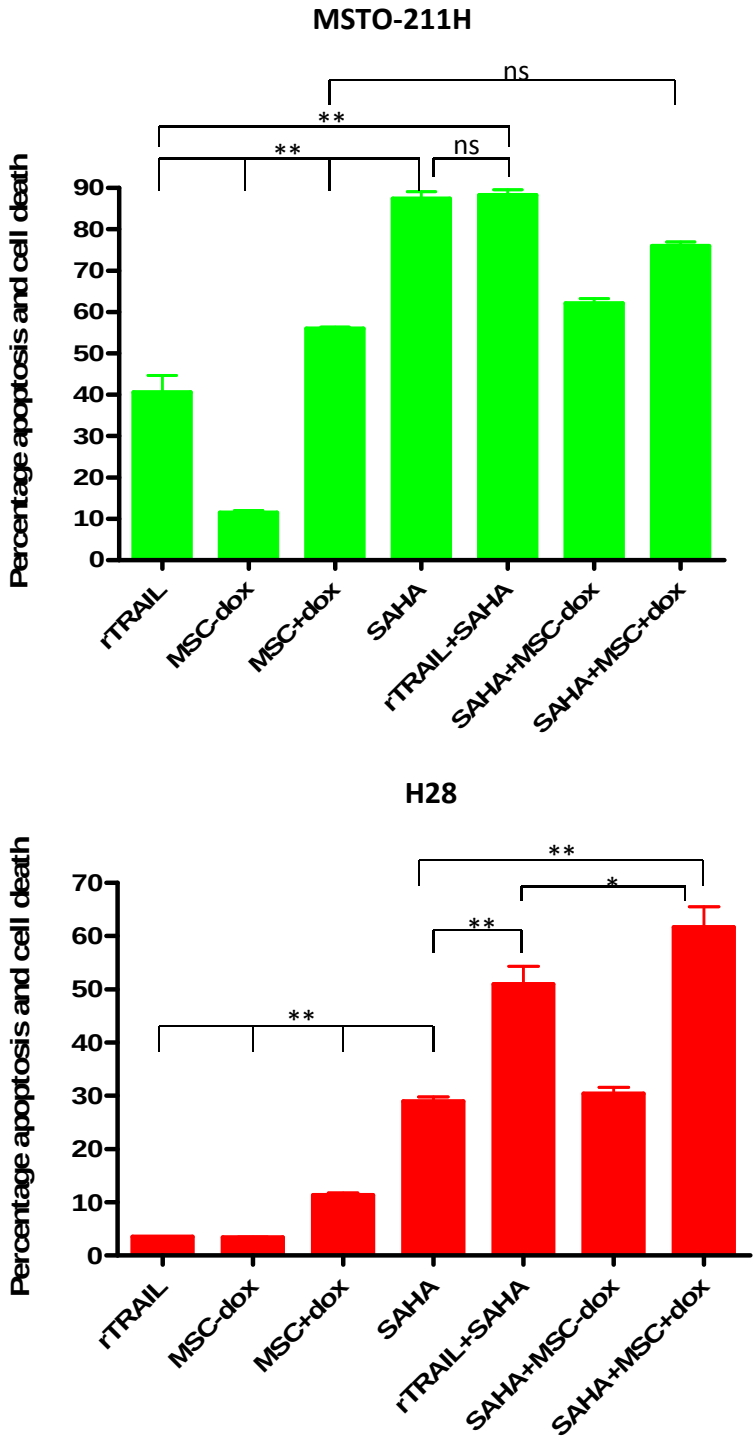

Figure 4.6: Percentage apoptosis and cell death of MPM cell lines following treatment with SAHA and MSCTRAIL. The percentage of cells undergoing apoptosis and cell death following treatment with SAHA and either rTRAIL or MSCTRAIL were assessed in MSTO-211H and H28 using flow cytometry for Annexin V and DAPI. Statistical analysis was performed using one-way analysis of variance with Bonferroni's multiple comparison test (* $p<0.05$; ** $p<0.001$).

H28 is an MPM cell line with 'low TRAIL sensitivity' and therefore it is possible that there will be a greater benefit in combining chemotherapy and TRAIL compared to single agent treatment. For this cell line treatment with SAHA alone resulted in higher levels of apoptosis and cell death than treatment with either MSCTRAIL alone or rTRAIL alone (28.97 ± 2.7% for SAHA alone vs 11.33 ± 0.7% or 3.59 ± 0.1% respectively; $p<0.001$) (Figure 4.6). When rTRAIL treatment was combined with SAHA there was a significant increase in death and apoptosis when compared to SAHA alone (3.59 ± 0.1% to 51.1 ± 2.9%; $p<0.001$) and the same was seen when MSCTRAIL was combined with SAHA vs SAHA alone (11.33 ± 0.7% to 59 ± 9.1%; $p<0.001$). For this cell line treatment with MSCTRAIL and SAHA also resulted in significantly higher levels of death and apoptosis than treatment with rTRAIL and SAHA (59 ± 9.1% vs 51.1 ± 2.9%; $p<0.05$). This means that treatment with MSCTRAIL and SAHA is the most effective combination therapy for this cell line.

4.2.3 Determining the biological effect of MSCTRAIL in combination with SAHA on non-malignant mesothelial cells

Combination treatments are not a novel concept in the treatment of cancer and whilst the benefits of treatment with dual agents may be significantly greater than with either single agent alone there is also the risk of increased adverse events as there are side effects from two drugs to be aware of. One of the proposed benefits of MSCTRAIL therapy is that it targets only cancer cells whilst leaving healthy cells unaffected, a finding confirmed in previous experiments (section 4.1 and Figure 4.2). The next step was to confirm whether treatment with SAHA and MSCTRAIL in combination resulted in an increase in apoptosis and cell death of the benign mesothelial cells, Met5A.

Experimental design was the same as in section 4.2.2 and as for all previous co-culture experiments and results are shown in Figure 4.7

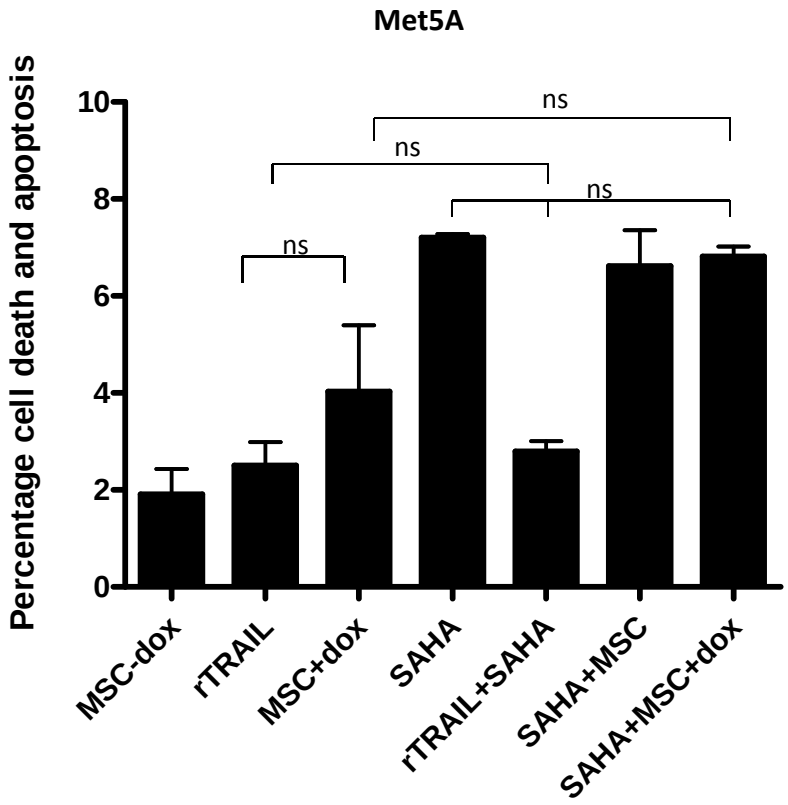

Figure 4.7: Percentage apoptosis and cell death of Met5A following treatment with SAHA and MSCTRAIL. The percentage of cells undergoing apoptosis and cell death following treatment with SAHA and either rTRAIL or MSCTRAIL were assessed in Met5A using flow cytometry for Annexin V and DAPI. Statistical analysis was performed using one-way analysis of variance with Bonferroni's multiple comparison test. There was no significant difference between treatment with rTRAIL compared to MSCTRAIL, rTRAIL vs SAHA+rTRAIL, SAHA vs either rTRAIL+SAHA or MSCTRAIL+SAHA. There was also no significant increase in death and apoptosis between treatment with MSCTRAIL and SAHA+MSCTRAIL.

As shown previously there is no significant difference in apoptosis and cell death in Met5A when treated with rTRAIL or MSCTRAIL alone. There was also no significant difference between treatment with rTRAIL alone or MSCTRAIL alone when compared to treatment with rTRAIL and SAHA (3.51 ± 0.4% or 4.88 ± 0.9% respectively vs 2.8 ±0.2%; ns). Treatment with MSCTRAIL and SAHA in combination showed no significant difference in cell death and apoptosis when compared with MSCTRAIL alone (6.81 ± 0.2% vs 4.88 ± 0.9%; ns) or SAHA alone (6.81 ± 0.2% vs 7.73 ± 0.7%; ns). This would suggest that whilst there are low levels of apoptosis and cell death in benign mesothelial cells with all treatments there is no significant effect of either single or dual agent treatment confirming the selective apoptosis of cancer cells whilst having no such effect on healthy cells.

4.3 Discussion

4.3.1 Biological activity of rTRAIL and MSCTRAIL on MPM cell lines

The biological activity of MSCTRAIL was demonstrated by *in vitro* co-culture experiments where cancer cells were plated in a 1:1 ratio with MSCTRAIL cells and TRAIL expression was activated by the addition of doxycycline for 48 hours. The death induced by MSCTRAIL was compared to that induced by MSC and rTRAIL and six different cancer cell lines were tested. An increase in death and apoptosis was seen in all malignant cell lines when treated with MSCTRAIL when compared to MSCs alone and in 4 of the 6 cell lines treatment with MSCTRAIL resulted in greater killing than with rTRAIL. Ideally it would be useful to compare the dose of rTRAIL with the amount of TRAIL delivered via the MSCs. However, this is technically difficult and unlikely to be accurate as the levels of TRAIL delivered by the MSCs will be dependent on the transduction efficiency of the cells with the viral vector and on the protocol used to extract the TRAIL protein from the cell lysate. Only 1 cell line was more sensitive to treatment with rTRAIL and the other showed similar death with MSCTRAIL and rTRAIL. Despite all cell lines being sensitive to MSCTRAIL it was noted that there was a large degree of variation between the different cell lines with two being highly sensitive to MSCTRAIL therapy and the remaining showing low sensitivity. This is not entirely surprising and would be consistent with what is seen in the clinical setting. Mesothelioma is an extremely heterogeneous disease with patients having different responses to chemotherapy and different disease courses.

Whilst all of the cancer cell lines were sensitive to treatment with MSCTRAIL the benign control cell line Met5A showed no significant increase in death and apoptosis on treatment with either MSCTRAIL or rTRAIL. This is reassuring as one of the key reasons for assessing MSCTRAIL as a therapeutic option for cancer is its selectivity for malignant cells whilst leaving healthy cells unaffected.

The *in vitro* co-culture studies performed were using a 1:1 ratio of cancer cells to MSCs and it is unlikely that within an *in vivo* or clinical setting this treatment ratio would be achieved. However, under tissue culture conditions MPM cells proliferate at a much faster rate than MSCs with a doubling time of 20 hours for MSTO-211H compared to 60 hours for MSCs.

This would mean over the 72 hours duration of the co-culture experiment the ratio of MSCs to cancer cells would increase to 1:3.6. In addition to this previous experiments performed within our lab have shown that cancer cell treatment with MSCTRAIL results in a significant increase in death and apoptosis at starting ratios of 1:16 [104]. Within early phase clinical trials most studies have looked at the safety of MSC delivery with doses ranging from 0.5-10 x 10^6 cells/kg and if MSCTRAIL was to be assessed as a treatment for patients with stage IV lung cancer then the phase I clinical trial would use increasing doses within this range to assess safety and efficacy.

4.3.2 The effect of doxycycline on MPM cell death *in vitro*

Doxycycline is a member of the tetracycline family of antibiotics that inhibits bacterial protein synthesis and is used routinely in clinical practice to treat multiple infections including those of the respiratory tract, genito-urinary tract and Lyme disease. At doses lower than those used for an anti-microbial effect, doxycycline inhibits matrix metalloproteases (MMPs) and has been shown to reduce the *in vitro* growth of human breast and prostate cancer cell lines possibly by arresting the cells in the G1 phase of the cell cycle [211, 212]. In addition to reducing cell growth, there are some reports of cell death following exposure to doxycycline, predominantly in macrophages and monocytes but also in some cancer cell lines, however this is thought to be cell line specific as cells from mesenchymal lineage appear to be unaffected [213-215]. In our cell lines tested, treatment with doxycycline did not result in an increase in cell death and apoptosis of MPM cells and so for all our *in vitro* experiments 10 µg/ml doxycycline was used to induce transgene expression. As each cage housed animals from all treatment groups all mice will have received doxycycline in the drinking water to ensure continual TRAIL transgene expression throughout the duration of the experiment.

4.3.3 Combining chemotherapy with MSCTRAIL

The first step in the activation of the extrinsic TRAIL pathway by death ligand binding is the recruitment of the FAS associated death domain (FADD) along with pro-caspases 8 and 10 by the receptor homotrimer. This first critical step in apoptosis is tightly regulated by cFLIP which works as a negative regulator of the pathway. Many cancers are known to overexpress cFLIP including malignant mesothelioma [92, 93] and targeting this molecule to

induce mesothelioma cell death is an attractive option. Pre-clinical studies looking at the effect of SAHA *in vitro* have shown that treatment with SAHA results in increased apoptosis in multiple mesothelioma cell lines and a phase 3 clinical trial has recently completed using SAHA (vorinostat) as a second line treatment for patients with malignant mesothelioma (NCT00128102). Whilst the results of using SAHA as a single agent have been promising the combination of MSCTRAIL with SAHA on MPM has not been tested.

Prior to combining SAHA and MSCTRAIL as a therapy it was important to determine whether SAHA had any effect on the viability of MSC cells and their ability to produce TRAIL. Our co-culture results show that there is no significant difference in the levels of background MSC cell death when treated with SAHA compared to no treatment.

Once it had been established that treatment with SAHA had no significant effect on MSC viability co-culture experiments were performed to determine the biological effect of combination therapy. In TRAIL sensitive cells (MSTO-211H) treatment with SAHA in combination with either rTRAIL or MSCTRAIL produced greater cell death that either rTRAIL or MSCTRAIL alone. The combination of rTRAIL with SAHA was slightly more effective in inducing apoptosis and death compared to SAHA and MSCTRAIL together but this was not statistically significant. When assessing the effect of combination therapy on cells with 'low sensitivity' to TRAIL (H28) the results were more promising suggesting that combining SAHA with MSCTRAIL has a synergistic effect on tumour cell death. In this cell line, treatment with MSCTRAIL and SAHA was most effective. The benefit of using MSCs to deliver TRAIL therapy is that MSCs deliver therapy directly to the site of the tumour and it is encouraging from a therapeutic perspective that this treatment would deliver high enough doses of TRAIL to induce levels of tumour cell death that are as good or better than those delivered systemically. It was reassuring that combination treatment with either rTRAIL or MSCTRAIL in addition to SAHA showed no significant toxic effects on the benign mesothelial cell lines – suggesting that toxicity to non-cancerous cells would remain low and help to reduce any adverse effects. When considering translation to the clinic, one of the main problems with chemotherapy is its toxicity. This is largely due to death of healthy cells, particularly those with a rapid turnover such as GI tract, skin and hair cells which accounts for symptoms of nausea and alopecia. If healthy cells remain unaffected by MSCTRAIL both alone and in

combination with chemotherapy this would likely result in a significantly improved side effect profile in the clinical setting.

4.4 Summary

- All MPM cell lines tested showed increased apoptosis and death when treated with MSCTRAIL but the percentage of cells dying varied between cell lines with two showing 'high TRAIL sensitivity' and two showing 'low TRAIL sensitivity'
- Doxycycline itself does not induce MPM cell death
- Combination treatment with MSCTRAIL and SAHA of the cell line with low TRAIL sensitivity is more effective than either agent alone whilst the cell line with high TRAIL sensitivity does not show increased death with the combination therapy
- Neither MSCTRAIL alone nor MSCTRAIL and SAHA in combination cause significant cell death in benign mesothelial cells suggesting that the effects on healthy cells are likely to be limited

Chapter 5

Develop a suitable *in vivo* tumour model and confirm that MSCs home to tumours

5 Development of an appropriate tumour model and tracking of MSC homing to tumours

This chapter describes the results of experiments carried out to address aim 3 (section 1.9) 'to develop a suitable *in vivo* tumour model and confirm that MSCs home to sites of tumour'. One of the key properties of an MSC that make it an attractive vehicle for cellular therapies is that it homes to and incorporates into tumours regardless of the route of delivery. In the clinical setting patients with malignant mesothelioma invariably require the insertion of an intercostal chest drain which provides direct and easy access to the pleural space where mesothelioma is located. To determine whether cells would be able to home to pleurally based mesothelioma, experiments were performed to track the fate of both systemically and topically delivered MSCs. The first step in this process was to develop a reliable tumour model and once this was established, cell labelling and tracking techniques were used to assess MSC homing.

5.1 *In vivo* mesothelioma model

Human tumour xenograft models are a well-established mode of determining the efficacy of anti-cancer therapies. In order to successfully establish human tumours in a murine model the animals need to be immunosuppressed to prevent rejection of cancer cells. NOD/SCID mice (NOD.CB17-Prkdc^{scid}) have the severe combined immunodeficiency mutation on a non-obese non-diabetic background resulting in a lack of functioning B and T-lymphocytes, lymphopaenia and hypogammaglobulinaemia [193].

One of the main problems with xenograft models of malignant mesothelioma is the setting of suitable end points and accurate measurement of disease burden. Previous studies looking at mesothelioma growth *in vivo* have used both subcutaneous, intraperitoneal and intrapleural methods of delivery, all with their individual problems. Whilst subcutaneous delivery is straightforward, the developing tumours can be easily measured with callipers and tumour weight and volume can be used as reliable end points, this model doesn't mimic human disease. For this reason intrapleural and intraperitoneal models are favoured. Both models reflect the human disease in terms of distribution of tumour deposits and development of ascites and pleural fluid, intraperitoneal cell delivery is straightforward and easily repeatable and whilst intrapleural delivery is more intricate it is well tolerated. The main concern with both of these models is that it is difficult to accurately monitor tumour burden and determine end points. Tumour deposits are often multiple and widespread and often adherent to nearby tissue including the pleura, heart, mediastinum and mesenteric tissues. Previous studies have used body weight as a surrogate marker for disease progression and tumour weight and volume as end points.

5.1.1 Intrapleural delivery of MSTO211H and H28 mesothelioma cells

The first step was to determine whether intrapleural delivery of different mesothelioma cells was feasible, the time course of tumour development without treatment and to define clear end points to use in measuring disease burden. The current widely accepted measures are body weight as a surrogate marker of disease development with 20% loss of body weight considered the point of sacrifice and also tumour weight and volume for end point quantification of disease burden. I chose MSTO-211H as a cell line with high TRAIL

sensitivity and H28 as a cell line with low TRAIL sensitivity. Initially 1.5 million MSTO-211H cells and 7.5 million H28 cells were resuspended in 100µl sterile PBS and injected intrapleurally. More H28 cells were delivered as this cell line has not previously been reported as tumorigenic using lower cell numbers. Body weight was measured twice weekly and animals were sacrificed when they reached 20% weight loss or after 60 days.

All animals were successfully injected with mesothelioma cells intrapleurally and recovered well from anaesthesia with no complications. Animals given MSTO-211H cells developed significant weight loss after 15 days and were sacrificed on day 20 whilst those given H28 did not lose weight and were culled after 60 days (Figure 5.1). This is in contrast to previous studies using NOD/SCID and nude mice which have needed up to 40 days for MSTO-211H cells to cause significant tumour development whilst H28 has not been previously reported to be tumorigenic *in vivo* [216-218]. In this experiment both cell lines produced macroscopically visible tumours despite only one group having documented weight loss. Tumours in animals with MSTO-211H cells had multiple small tumour deposits throughout the pleural cavity often adherent to the lung and cardiac tissue making it extremely difficult to dissect and quantify each individual tumour deposit and accurately determine a tumour weight or volume. Tumours caused by H28 cells were fewer in number but still adherent to organs. Microscopically, all tumours had some level of invasion with adjacent tissue and tumours were confirmed to be malignant mesothelioma using calretinin staining. These results show that weight loss is an unreliable marker of tumour development/burden and that tumour weight and volume is inaccurate as an end point measurement. In view of these results, we decided to use bioluminescence in the form of firefly luciferase to track tumour growth *in vivo*.

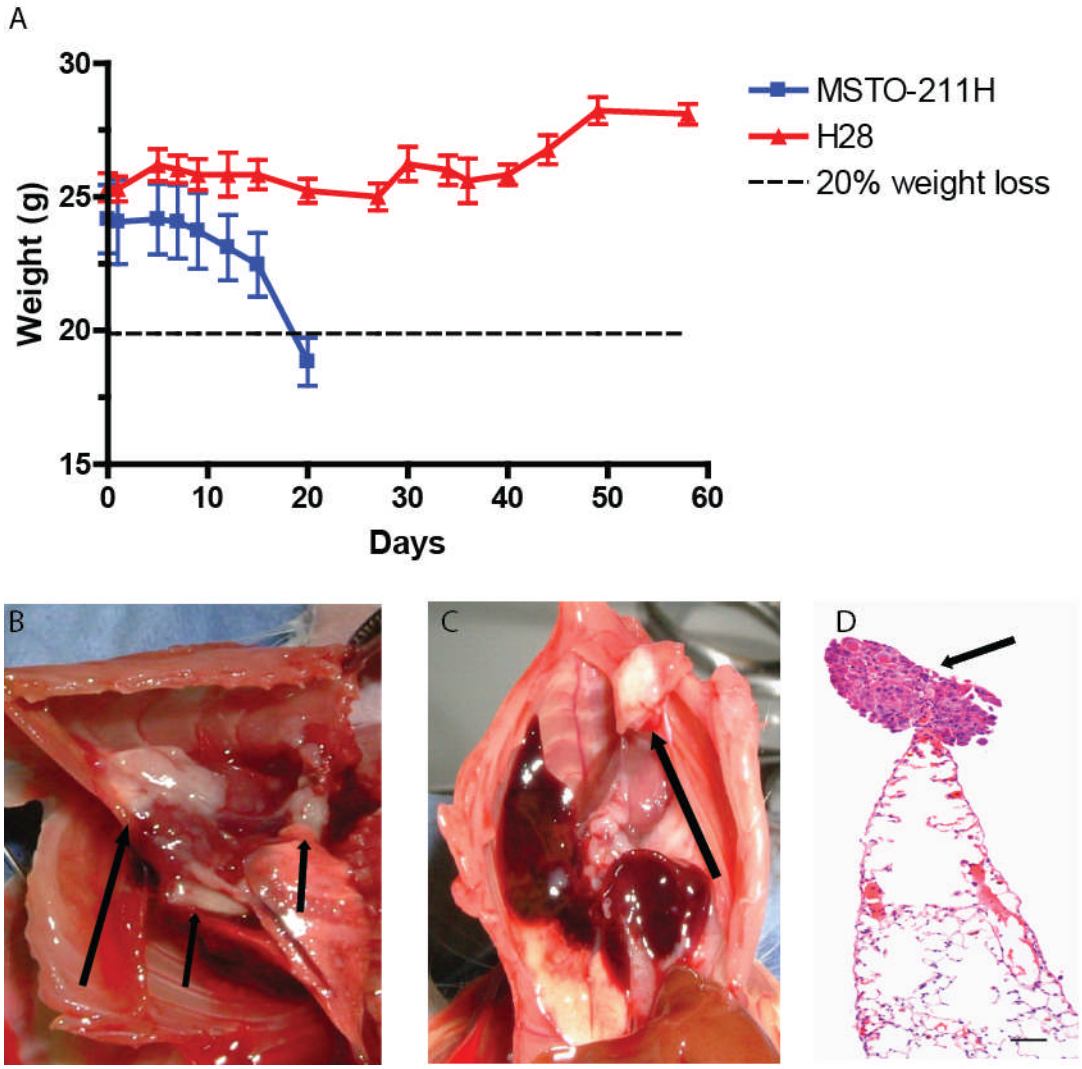

Figure 5.1: Intrapleural mesothelioma delivery. Mice were injected with either MSTO-211H or H28 cells in 100 µl PBS via intrapleural injection and body weight was measured twice weekly. A, Weight loss shows a significant reduction in weight by day 20 in animals receiving MSTO-211H cells whilst those injected with H28 cells showed no weight loss over 60 days. Macroscopic appearance of tumours in animals receiving B, MSTO-211H and C, H28 cells with black arrows showing macroscopically visible tumours. D, H&E examination of tissues confirmed mesothelioma in all animals with black arrow pointing to tumour histologically consistent with malignant pleural mesothelioma (representative H&E section shown, magnification 10x, scale bar 100 µm).

5.1.1.1 Transient transfection of 293T cells with pLIONII-Hyg-Luc2YFP

Human embryonic 293T kidney cells were transiently transfected with the luciferase-YFP plasmid and efficiency was assessed by flow cytometry. Using this method I achieved very low transfection rates of up to 35%. Because the luciferase plasmid was based on a feline virus I used the calcium phosphate method of transfection and achieved transfection rates of 87.6% using a DNA: calcium phosphate ratio of 1:3 and 85.6% using a 1:1 ratio (Figure 5.2 A & B).

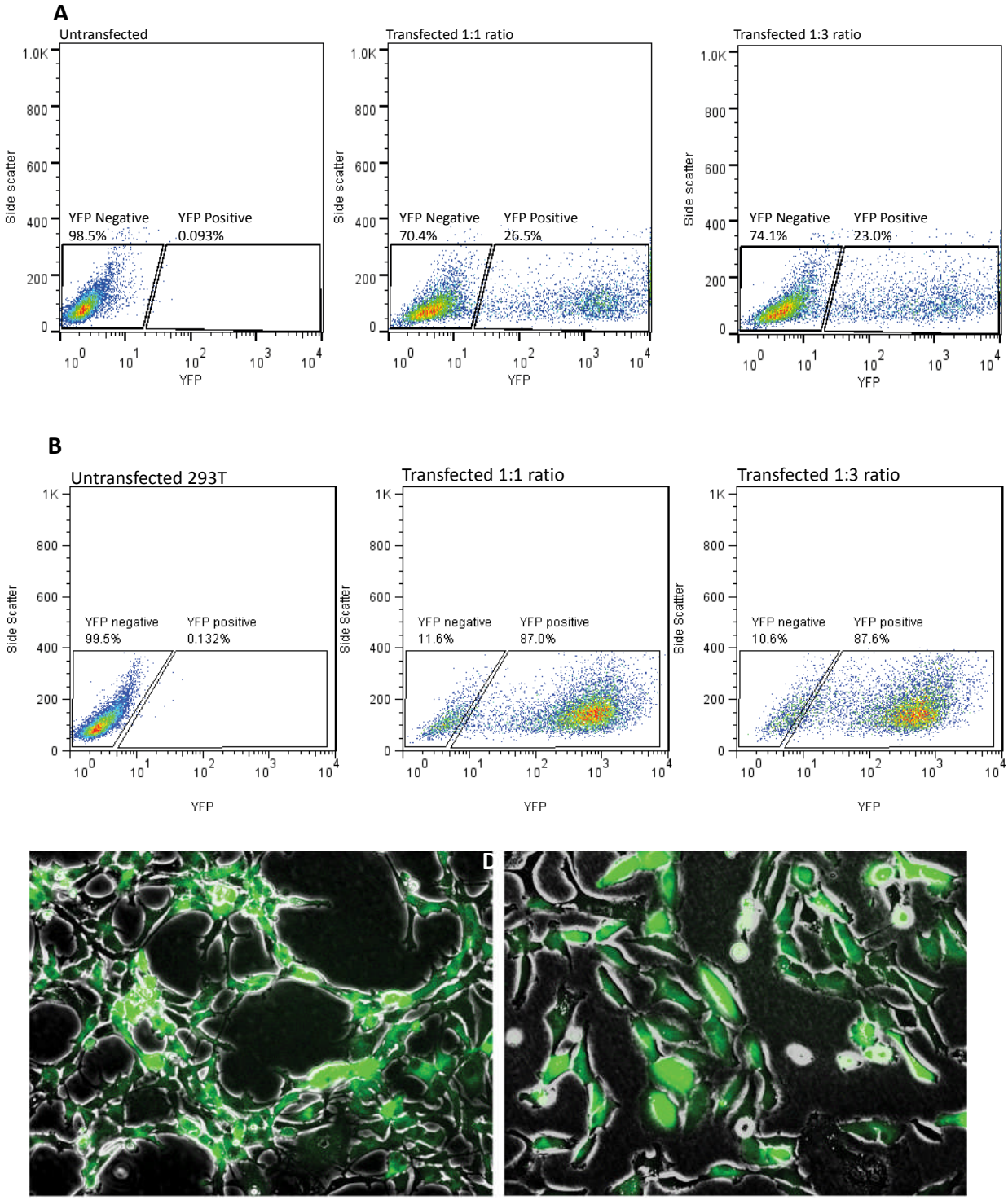

Figure 5.2: Luciferase transduction of mesothelioma cells. 293T cells were transfected with pLIONII-HYG-Luc2YFP plasmid and YFP expression was assessed using flow cytometry and fluorescence microscopy. Flow cytometry plots of YFP expression in 293T cells following A, PEI transfection showing low transfection rates of <35% and B, calcium phosphate transfection which achieves higher rates of transfection at >85%. Fluorescence microscopy showing luciferase-YFP transduced C, MSTO-211H and D, H28 mesothelioma cells.

5.1.1.2 Permanent transduction of mesothelioma cells

As the transfection rates were much higher with the calcium phosphate method when compared to using PEI, calcium phosphate was used as the transfection reagent to produce the luciferase lentivirus. Once the lentivirus had been produced the number of infectious units per ml was determined and mesothelioma cells were transduced as previously described. The success of transduction was confirmed initially on fluorescent microscopy and then cells were selected on the basis of their resistance to hygromycin using 200 µg/ml hygromycin. I successfully transduced all 6 mesothelioma cell lines (Figure 5.2 C & D) and all cell lines were selected with hygromycin until a pure population was achieved, as confirmed by fluorescence.

5.1.2 Confirmation of luciferase expression in MSTO-211H luciferase transduced cells *in vitro*

Confirmation of successful transduction of MSTO-211H and other MPM cell lines was performed using flow cytometry and fluorescent microscopy for YFP. Prior to using these cells *in vivo* bioluminescence emission was confirmed using IVIS® imaging. Luciferase transduced MSTO-211H (MSTO-211HLuc) cells were plated at increasing cell densities from 5×10^3 to 5×10^4 in a 12- well plate and left to adhere. Once cells were adherent, medium was exchanged for standard cell culture media containing D-luciferin at a concentration of 150 µg/ml. The plate was transferred to the IVIS® and imaged using an automatic exposure time. Cells emitted a good bioluminescent signal and there was a strong correlation between increasing cell density and increasing bioluminescent emission (R^2 0.9999; Figure 5.3). This result suggests that bioluminescence is a reliable marker of cell number.

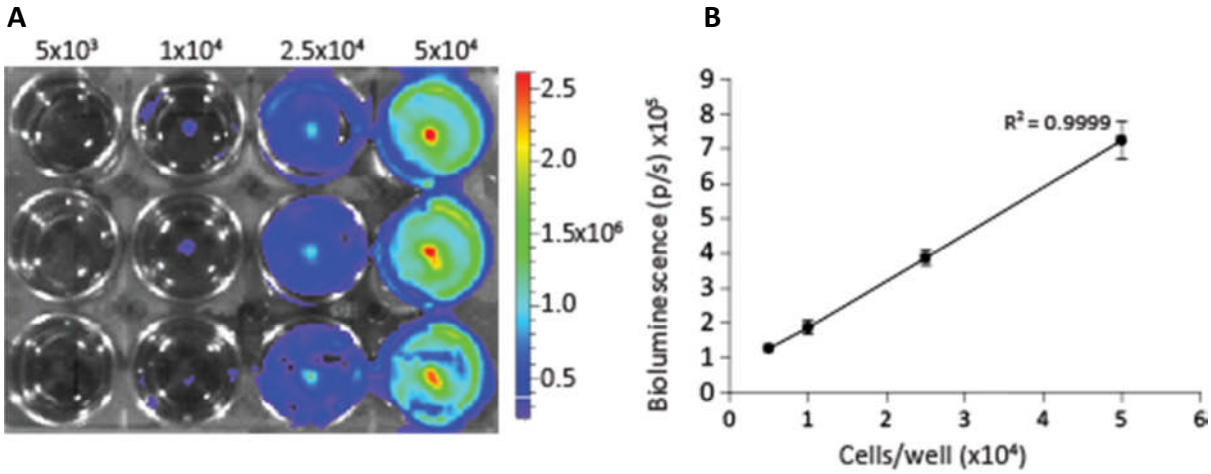

Figure 5.3: Bioluminescent imaging of MSTO-211H cells transduced with pLIONII-HYG-Luc2YFP lentiviral vector. MSTO-211H cells were transduced and plated in triplicate at increasing cell densities from 5 x 10^3 to 5 x 10^4. Once cells were adherent, 150 µg/ml D-luciferin was added to the culture medium and imaging was performed using IVIS®. The bioluminescent signal was measured using the region of interest (ROI) tool and total flux within each ROI was calculated. A) Bioluminescent imaging of plates with increasing cell density, colour bar shows bioluminescence in photons/second/cm^2/steradian. B) Linear relationship between increasing cell density and increasing bioluminescent signal showing excellent correlation with R^2 0.9999.

5.1.3 Kinetics of bioluminescence emission after exposure of MSTO-211HLuc cells to luciferin *in vivo*

Before starting the main *in vivo* imaging experiments, it was essential to determine the pharmacokinetics of intraperitoneal administration of D-luciferin. 24 hours after tumour cell delivery animals were given an intraperitoneal injection of 200 µl D-luciferin (10 mg/ml). Imaging was performed every 5 minutes for 25 minutes until the bioluminescent signal started to reduce. Bioluminescence was clearly detectable after 5 minutes and the counts increased to reach a plateau between 10 and 20 minutes (Figure 5.4). After 25 minutes the signal started to reduce. From this experiment, 15 minutes was chosen as the optimal imaging time after D-luciferin injection although anywhere between 10 and 20 minutes was acceptable as the variation in counts was very small. This allowed for any errors or problems with the running of the machine and for any problems occurring on anaesthetizing the animals.

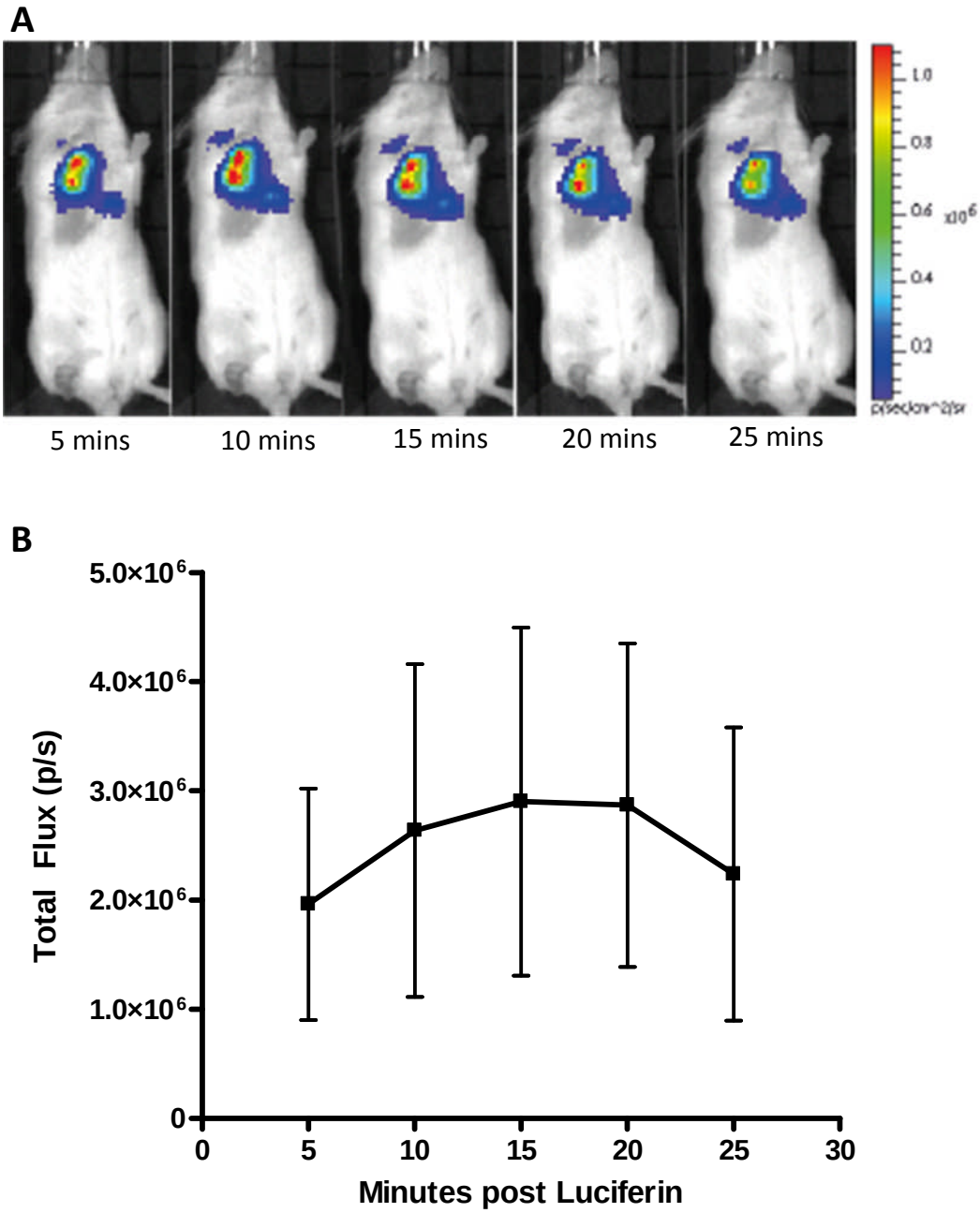

Figure 5.4: Time course of bioluminescence emission from intrapleural MSTO-211HLuc cells *in vivo* following intraperitoneal administration of luciferin. MSTO-211HLuc cells were injected intrapleurally to establish tumours. Bioluminescence was measured 24 hours post cell injection using IVIS® imaging at 5 minute intervals following intraperitoneal injection of D-luciferin. A) Images of representative mouse at 5 minute intervals following intraperitoneal luciferin injection. B) Bioluminescent measurements at 5 minute intervals following luciferin injection. Mean values are shown for 3 mice.

5.1.4 Bioluminescent tracking of intrapleural and intraperitoneal mesothelioma using MSTO-211HLuc cells

In order to determine whether I could monitor bioluminescence *in vivo* and determine whether photon emission correlated to tumour growth I injected mice with either 1,000 or 10,000 MSTO-211HLuc cells intraperitoneally or 10,000 or 100,000 cells intrapleurally and imaged them twice weekly. All animals had bioluminescent signal detected immediately following mesothelioma cell injection and the bioluminescent signal increased over time (Figure 5.5 A, B). All four models had similar growth curves but the peritoneal models were most reliable with lowest intra-experimental variability and the 10,000 cell number being the most reproducible (Figure 5.5 C). When bioluminescence was correlated with weight loss it was shown that there was no loss until the bioluminescent signal was reaching a plateau (Figure 5.5 D). This suggests the period of most rapid tumour growth cannot be detected by weight loss and that weight loss is not a reliable measure of tumour burden.

In order to ensure that the areas of highest photon emission correlated with tumour deposits, bioluminescence was measured prior to sacrificing the animals and again during dissection (Figure 5.6 A-C). Images taken during dissection show that photon emission is closely correlated to tumour growth with the highest counts being at sites of visible tumours. Bioluminescent areas were also seen at sites where there were no macroscopically visible tumours so these areas were also removed and processed along with other samples. H&E staining was consistent with mesothelioma and immunohistochemistry for calretinin showed positive cytoplasmic staining in areas of tumour (Figure 5.6 D, E) with no staining in normal lung tissue or other normal tissues.

As all models tested showed low intra-experimental variability and good reproducibility an intrapleural model of cell delivery was chosen for future experiments to have a clear relevance to the human disease process and 10,000 cells were delivered. Having established that the most rapid period of tumour growth is within the first 10 days following mesothelioma cell injection it was decided that the MSCTRAIL therapy should be started on day 5 after tumour cell inoculation and delivered every 4 days during treatment to target the rapidly dividing tumour cells aggressively.

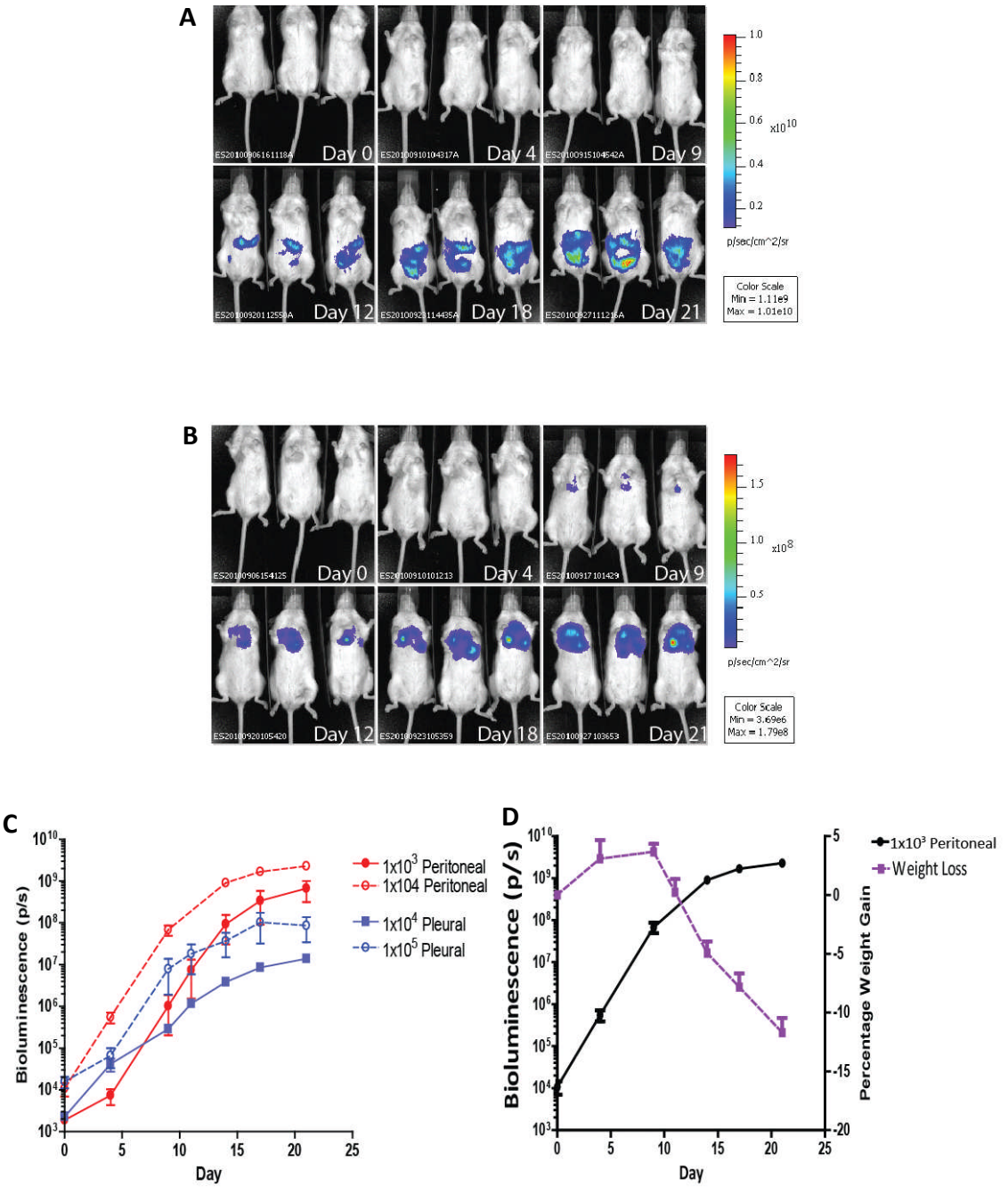

Figure 5.5: Luciferase transduced MSTO-211H cells can be tracked longitudinally and bioluminescence corresponds to tumour growth. A, Intraperitoneal and B, intrapleural delivery of luciferase transduced MSTO-211H cells results in an increase in bioluminescent signal over time in a reproducible and reliable model, C. D, The most rapid increase in bioluminescent signal occurs within the first 10 days following tumour cell inoculation suggesting this is a time of rapid tumour growth but weight loss does not start until tumour growth starts to stabilise. n=3 per group.

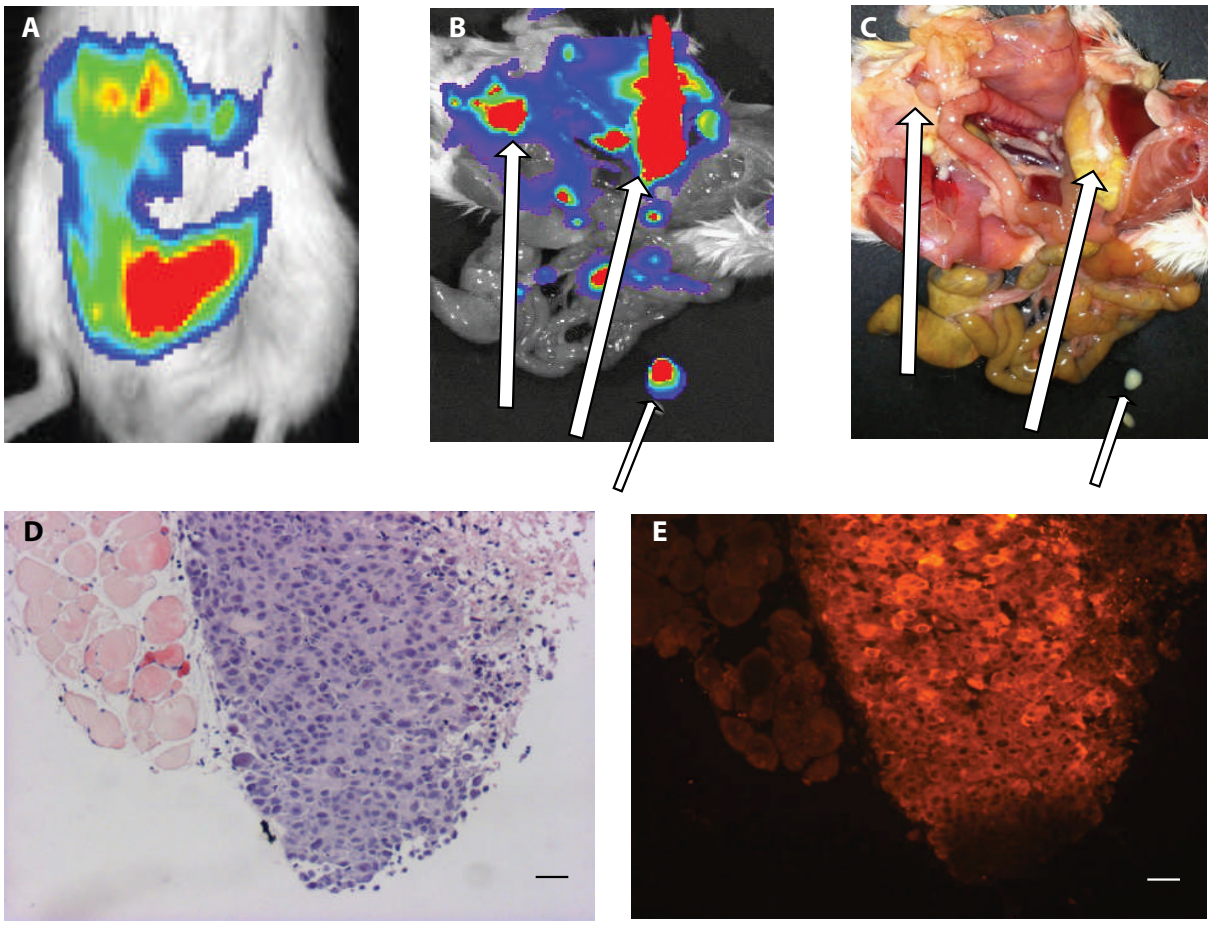

Figure 5.6: Bioluminescent imaging is a more sensitive method of tracking tumour growth than weight loss. A, Bioluminescent emission is a sensitive marker of tumour growth and can be used to detect both B&C, macroscopic and microscopic tumour deposits that would otherwise be missed under direct vision. D, H&E section of dissected tumour consistent with mesothelioma and confirmed with E, immunofluorescence staining showing positivity for calretinin whilst neighbouring non-tumour areas are negative (magnification 10x, scale bar 100 µm).

5.2 Homing of MSCs to tumours *in vivo*

Once a suitable tumour model had been established the next step was to determine whether MSCs were able to home to tumours *in vivo*. Previous *in vivo* studies have shown that systemically delivered MSCs are found within lung metastases [104] and that MSCs delivered directly into the brain can be detected in tumours located in the contralateral cerebral hemisphere [105]. This has been shown using immunofluorescence on fixed post-mortem tissue but our aim was to demonstrate for the first time using live imaging that MSCs can home to and incorporate within tumours and to assess whether homing is dependent on the route of delivery.

5.2.1 MSC detection *in vitro* using fluorescence imaging

Before assessing the ability of MSCs to home to tumours *in vivo* it was important to ensure that MSCs could be successfully stained with both DiR and DiI together and to identify the optimum fluorescent filter settings on the IVIS® imager. Both stains were used as DiR has a higher wavelength making *in vivo* tracking by IVIS feasible and DiI has a lower wavelength that can be detected on the fluorescent filters on the microscope to allow for identification of MSCs in tissue sections. MSCs were first stained with both DiR and DiI (section 2.8.3), then $1x10^5$ cells were plated in each well of a 6-well plate and left to adhere overnight. The following day plates were transported to the IVIS® and images were taken using 2 different filter sets; 710/ICG and 745/ICG as determined by the emission spectra of DiR. Imaging showed that DiR can be detected well by both 710/ICG and 745/ICG filter sets but there is a higher radiant efficiency count when cells are imaged using the 745/ICG filter set (Figure 5.7). It is also important to note that dual staining with DiR and DiI does not affect the fluorescent signal detected.

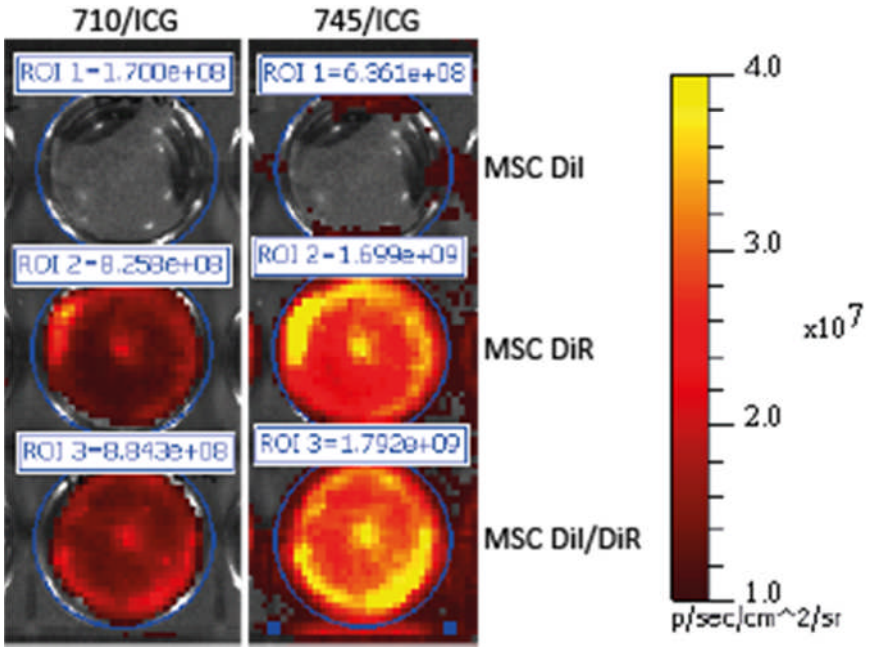

Figure 5.7: Fluorescence imaging of DiI and DiR labelled MSCs. MSCs were stained with DiI alone, DiR alone or both DiI and DiR and plated in a 6-well plate. Once adherent, cells were transferred to IVIS® for fluorescent imaging using two filter sets 710/ICG and 745/ICG to determine the optimal fluorescent settings for MSC imaging. Cells stained with DiR but not DiI were detected using both filter sets but the total fluorescent count was higher using the 754/ICG filter set. Co-staining with DiI and DiR did not affect the fluorescence counts.

5.2.2 Assessment of topical delivery of MSCs ability to home to tumours *in vivo*

To assess whether topically delivered MSCs are able to home to tumours *in vivo*, intrapleural tumours were set up as described in section 2.8.3. On day 6, $1x10^6$ DiR and DiI stained MSCs were injected intrapleurally at the same site as the tumour cells were delivered. Animals were imaged using dual bioluminescence to detect the luciferase signal and fluorescence to detect the DiR signal from the MSCs and images were compared to determine the location of the MSCs in comparison to the tumours. Animals were left for 24 hours and the imaging was repeated to establish whether the MSCs persisted. Animals were then sacrificed and dissected, open cavity imaging was performed to determine the precise location of both the tumours and MSCs and tumour samples were taken for digestion and flow cytometry and tumours and lungs were taken for fixing and histological processing.

Pleural tumours were clearly visible on bioluminescent imaging (Figure 5.8 A&B) and fluorescence clearly demonstrated MSC localisation to the site of the tumours (Figure 5.8 E). No animals developed pleural effusions so all fluorescent and bioluminescent images were representative of solid tumours. Control animals that received no MSCs showed no fluorescent signal confirming that any signal detected by the ICG filter was representative of MSCs with no bleed through of the luciferase-YFP (Figure 5.8 D). In pathological specimens tumours were detected using an anti-luciferase antibody and MSCs identified by DiI. Immunofluorescence confirmed that DiI labelled MSCs were located within the tumour stroma when delivered topically (Figure 5.8 G&H).

5.2.3 Systemic delivery of MSCs to assess the ability of MSCs to home to tumours

To determine whether MSCs were able to home to tumours when delivered systemically intrapleural tumours were established as described in section 5.2.1 and MSCs were delivered intravenously rather than intrapleurally. Imaging was performed at the same time points and tissue samples were processed using the same techniques.

Again tumours were confirmed using bioluminescent imaging (figure 5.8 C) and intravenously delivered fluorescent MSCs were identified co-localising with tumour deposits (Figure 5.8 F). Immunofluorescence confirmed that DiI labelled MSCs are identified within the tumour deposit (Figure 5.8 J).

These experiments suggest that MSCs are able to home to and incorporate within tumours when delivered either topically or systemically. From the fluorescent imaging it is possible that MSCs not only home to the tumours themselves but are also present within the lung tissue. It is possible that in addition to homing to tumours, MSCs also remain within healthy lung tissue following intravenous administration as they are trapped within lung capillaries. If this were the case then MSCs could exert a dual therapeutic effect by delivering TRAIL directly to the tumour to induce apoptosis but also to produce a bystander effect from locally secreted TRAIL.

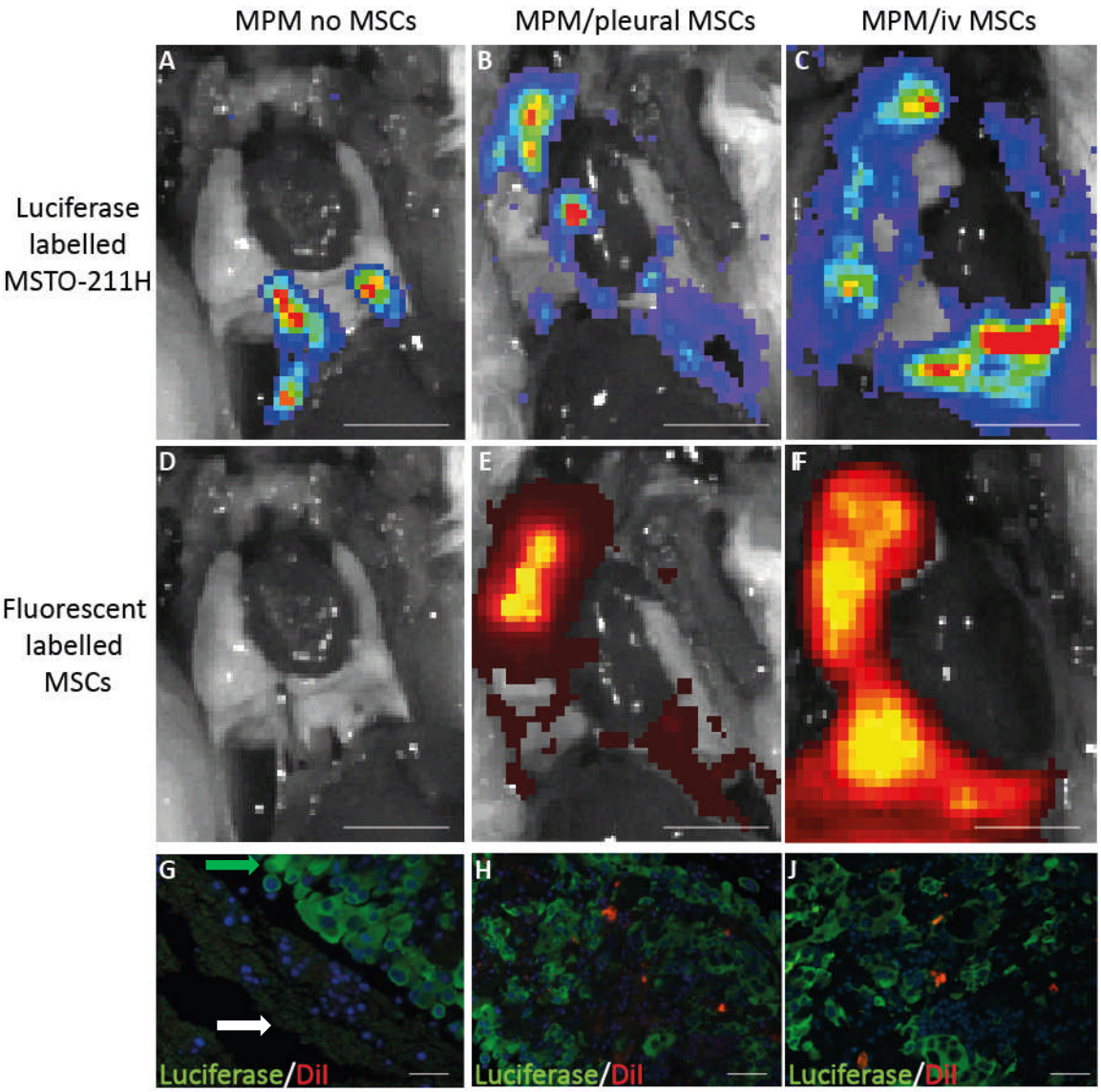

Figure 5.8: Human MSCs home to an *in vivo* model of MPM when delivered both ip and iv. A-C, IVIS images of animals with intrapleural bioluminescent MSTO-211HLuc tumour cells D, lack of fluorescent signal in control animal with no DiR labelled MSCs whilst animals receiving E, pleural MSCs and F, intravenous MSCs show co-localisation of fluorescent MSCs at the sites of tumour (scale bar 5mm). G, Immunofluorescence images confirm the absence of DiI labelled MSCs (red) within luciferase positive tumour cells (green arrow shows luciferase positive tumour and white arrow show luciferase negative smooth muscle tissue) whilst DiI labelled MSCs are visible within the luciferase positive tumours following both H, intrapleural and J, intravenous MSC delivery (magnification x20; bar 60µm).

5.3 Discussion

5.3.1 *In vivo* mesothelioma tumour models

A robust *in vivo* experimental model for malignant mesothelioma is essential to assess the efficacy of novel therapies. There are two broad categories of tumour models, syngeneic and human xenograft. Syngeneic tumour models describe a murine tumour growing in mice of the strain in which the tumour originated. They have a number of advantages in that they are relatively low cost, allow the use of immunocompetent hosts so the contribution of the immune system can be assessed and are usually non-immunogenic and very reproducible. The main disadvantages however are that the tumour cells are murine and so express the mouse homologues of the studied targets and the behaviour of the tumours may not reflect that seen in human disease. As more targeted therapeutics are being assessed the homology between murine and human targets can limit the utility of syngeneic models.

An alternative model is the human xenograft model whereby human tumour cells are delivered to an immunodeficient mouse. The benefits to this model are that the resulting tumour is human, they are reliable reproducible models and a wide variety of tumour cell lines are available for tumour induction. The main disadvantage to this model is that due to the immunodeficient nature of the mouse any interactions with the immune system cannot be studied. Initial xenograft models tended to use non-natural sites such as subcutaneous as the resultant tumours were easy to visualise and measure longitudinally. However, most groups prefer to use orthotopic sites i.e. those from where the cell line was derived as this allows better simulation of human disease. The main disadvantages of orthotopic xenograft models is that surgical techniques can often be complicated resulting in small numbers of animals used and if tumours are internal then tumour growth and response to treatment can be difficult to monitor longitudinally without using large numbers of animals to allow time point assessments. This means that end points are usually death or weight loss making accurate estimation of tumour volume difficult.

5.3.1.1 Establishing a suitable *in vivo* tumour xenograft model

As my main aims were to determine the suitability of MSCTRAIL as a novel targeted therapy for the treatment of human disease, all our *in vitro* assays had been performed using human MSCs. To ensure continuity of results and maintain the potential for clinical translation we used an orthotopic tumour xenograft model of malignant pleural mesothelioma. Initially two cell lines were assessed, MSTO-211H and H28. These were chosen as they were representative of high and low TRAIL sensitivity and were known to be tumourigenic *in vivo* [217].

Both cell lines successfully produced pleural tumours consistent with malignant mesothelioma as confirmed by H&E and immunostaining for calretinin. However, one of the main concerns from preliminary experiments was that tumour growth longitudinally was difficult to monitor and that the traditional measure of tumour burden, weight loss, was unreliable. In addition, on dissection it was clear that the pattern of tumour growth resulted in multiple small tumour deposits throughout the pleural cavity making an accurate measure of tumour burden impossible.

5.3.2 *In vivo* cell tracking techniques

A key factor in developing effective gene and cellular therapies for cancer is to understand the migration, biodistribution and lifespan of exogenously delivered cells and to accurately determine the effect of their therapeutic gene on the targeted tumour. Traditionally, the majority of cell tracking techniques have not allowed longitudinal tracking in live animals, for example immunohistochemistry for marker proteins and flow cytometry for fluorescent reporter proteins and fluorophores. These techniques are useful for providing information about the location of labelled cells at a fixed time point but do not allow longitudinal cell tracking in an individual animal. Because of these limitations there has been significant development in novel imaging techniques involving both indirect and direct cell labelling that allow non-invasive, longitudinal imaging in preclinical studies [219].

Direct labelling techniques use labels such as lipophilic dyes, radioactive molecules or nanoparticles that can be directly taken up by the cells and do not require genetic modification. As such they are usually easier to apply and are accomplished more rapidly

but the disadvantage is that the label is not permanently located within the cell and is likely to be slowly lost over time, diluted during cell division and taken up by other cells such as phagocytes. Because of these limitations direct labelling techniques are less suitable for long-term tracking studies. Indirect labelling techniques involve the introduction of a reporter gene such as a fluorescent protein or enzyme through genetic modification of the host cell. Because any labelling involves genetic modification the techniques tend to be more time consuming but any label should by expressed by both parent and daughter cells and only by live cells, making them more suitable for long term cell tracking and providing information about cell number, location and viability. I use both indirect and direct labelling techniques to allow us to track both tumour cells and MSCs.

5.3.2.1 Non-invasive bioluminescent imaging using luciferase transduced MPM

Bioluminescent imaging was chosen as a label to track MPM cells as it was important to have an accurate measure of live cell number over a long period of time. Using lentiviral transduction of MPM cells it was possible to accurately measure tumour burden throughout the course of each experiment, thus reducing the number of animals needed. Once I had successfully transduced MPM cells to express luciferase via a lentiviral vector I confirmed that there was an excellent correlation between increasing cell number and increasing bioluminescence as measured by photo count.

The first step was to determine which orthotopic model was most suitable for the *in vivo* experimental work. In humans MPM is found predominantly in the pleura but is also well known to develop in the peritoneal cavity. Whilst intrapleural MPM was felt to be more clinically translatable pleural delivery of cells requires mice to be anaesthetised and undergo minor surgery making repeated cell delivery by this route more risky. In addition there was concern that animals could develop pneumothoraces resulting in death. Intraperitoneal cell delivery has the benefit of being less invasive than intrapleural delivery and better tolerated for multiple doses. Therefore both intrapleural and intraperitoneal delivery of MPM Luc cells were assessed prior to performing a treatment experiment. Both delivery routes were well tolerated with no adverse events seen and both tumour models showed efficient tumour formation with similar patterns of increasing bioluminescence throughout the experimental period. On dissection intrapleural MPM showed more discreet tumour

deposits that were easier to dissect and often adherent to the lung tissue making lung weights a valid additional measure of determining tumour burden. For this reason and because the procedure was well tolerated intrapleural delivery of MPM was used for all subsequent experiments.

5.3.3 Homing and engrafting of MSCs within MPM tumours

One of the key characteristics of MSCs that make them attractive candidates as vectors for cellular therapy is their ability to home to multiple tumour types. MSC homing is defined as the arrest of MSCs within the vasculature of a tissue followed by transmigration across the endothelium. It is not known precisely what controls MSC homing and it is certainly not as well characterised as the leukocyte homing mechanism but it is thought to involve multiple chemokines and their receptors. Until recently the majority of studies looking at MSC homing have used either *in vitro* cell migration assays or direct cell labelling techniques within *ex vivo* samples to demonstrate localisation of MSCs at sites of interest. Real-time imaging of MSCs is therefore of particular interest and intravital microscopy has been used to demonstrate MSC rolling and diapedesis within specific tissues [220, 221].

Initial experiments were designed to demonstrate whether MSCs would home to MPM tumours when delivered either topically or systemically. Using luciferase transduced MPM cells and fluorescently labelled MSCs I showed that MSCs successfully homed to tumour deposits following both routes of delivery and were incorporated within the tumour stroma (Figure 5.8). Chemokine levels and receptor expression in the cells used in this study was not assessed but it could be evaluated in future work. If there are differences in chemokine or receptor expression this could be exploited in future experiments to improve the efficiency of MSC homing to tumours. This difference could be important when translating pre-clinical work into clinical trials as route of delivery could be critical for therapeutic efficacy.

5.4 Summary

- Both MSTO-211H and H28 cell lines are tumorigenic *in vivo* but weight loss is a poor marker of tumour burden
- MPM cell lines can be successfully transduced with luciferase lentivirus and on IVIS® imaging there is a good correlation between cell number and bioluminescent signal
- Intrapleural MSTO-211HLuc injection produces fewer more discreet tumour deposits than intraperitoneal MSTO-211HLuc injection
- MSTO-211HLuc can be tracked longitudinally after intrapleural delivery in mice using bioluminescent imaging
- DiI and DiR co-staining can be used to track MSCs using fluorescent imaging
- MSCs delivered both topically and systemically home to intrapleural tumours *in vivo* and can be demonstrated using dual bioluminescent and fluorescent imaging

Chapter 6

Assessment of therapeutic effect of MSCTRAIL delivery in a murine model of MPM both alone and in conjunction with chemotherapy

6 Assessment of therapeutic effects of MSCTRAIL delivery in a murine model of MPM both alone and in combination with chemotherapy

This chapter describes the results of experiments carried out to address aim 4 'determine whether MSCTRAIL therapy can reduce mesothelioma growth *in vivo*'. Intrapleural tumours were established and mice were given TRAIL-transduced MSCs, untransduced parental MSCs or PBS as controls. Both topical and intravenous routes were used as routes of therapeutic delivery. Cells were delivered at regular intervals during the most rapid phase of tumour growth and tumour burden was measured longitudinally using bioluminescent imaging. End-points were total bioluminescent count and lung weights along with biomarkers of response consistent with the mechanism by which TRAIL could affect tumour growth such as apoptosis and cell proliferation.

6.1 Malignant pleural mesothelioma – route of delivery for treatment

Clinically MPM often presents with a pleural effusion, fluid that builds up between the visceral and parietal pleura that line the lung and chest wall respectively. The presence of this fluid can cause significant symptoms of breathlessness and can significantly reduce a patient's quality of life. To treat a pleural effusion, thoracentesis is performed, in which a needle is inserted through the intercostal space and the fluid is drained out of the pleural space. Patients with MPM are likely to have recurrent pleural effusions and will require either repeated drainage using a chest drain or the insertion of a longer term indwelling catheter that can be accessed when fluid drainage is required.

In addition to providing symptomatic relief from the pleural effusion the presence of a chest drain allows direct access to the site of the malignant tumour. The advantage of direct tumour access has already been utilised in the case of MPM and other peritoneal tumours with existing chemotherapy agents being delivered directly to the intraperitoneal cavity [194]. A great advantage of direct access is that is allows targeted and topical delivery without the need for systemic therapies with their associated side effects.

6.2 Effects of intrapleural delivery of MSCTRAIL to a murine model of malignant pleural mesothelioma

I first assessed the intrapleural delivery of MSCs in a pleural model of MPM. Intrapleural tumours were established as previously described (section 2.8.4) and $1x10^6$ MSCTRAIL were delivered intrapleurally on days 5, 9, 12, 15 and 18 (Figure 6.1 A). Control groups received either PBS or $1x10^6$ untransduced parental MSCs (n=8 per group) and bioluminescent imaging was performed twice weekly. All groups received doxycycline in their drinking water to ensure continuous expression of TRAIL. All animals developed tumours as expected but there was no significant difference in bioluminescence between any of the treatment groups (Figure 6.1 B&C). There was also no significant difference in lung weights between any of the treatment groups (Figure 6.1 D).

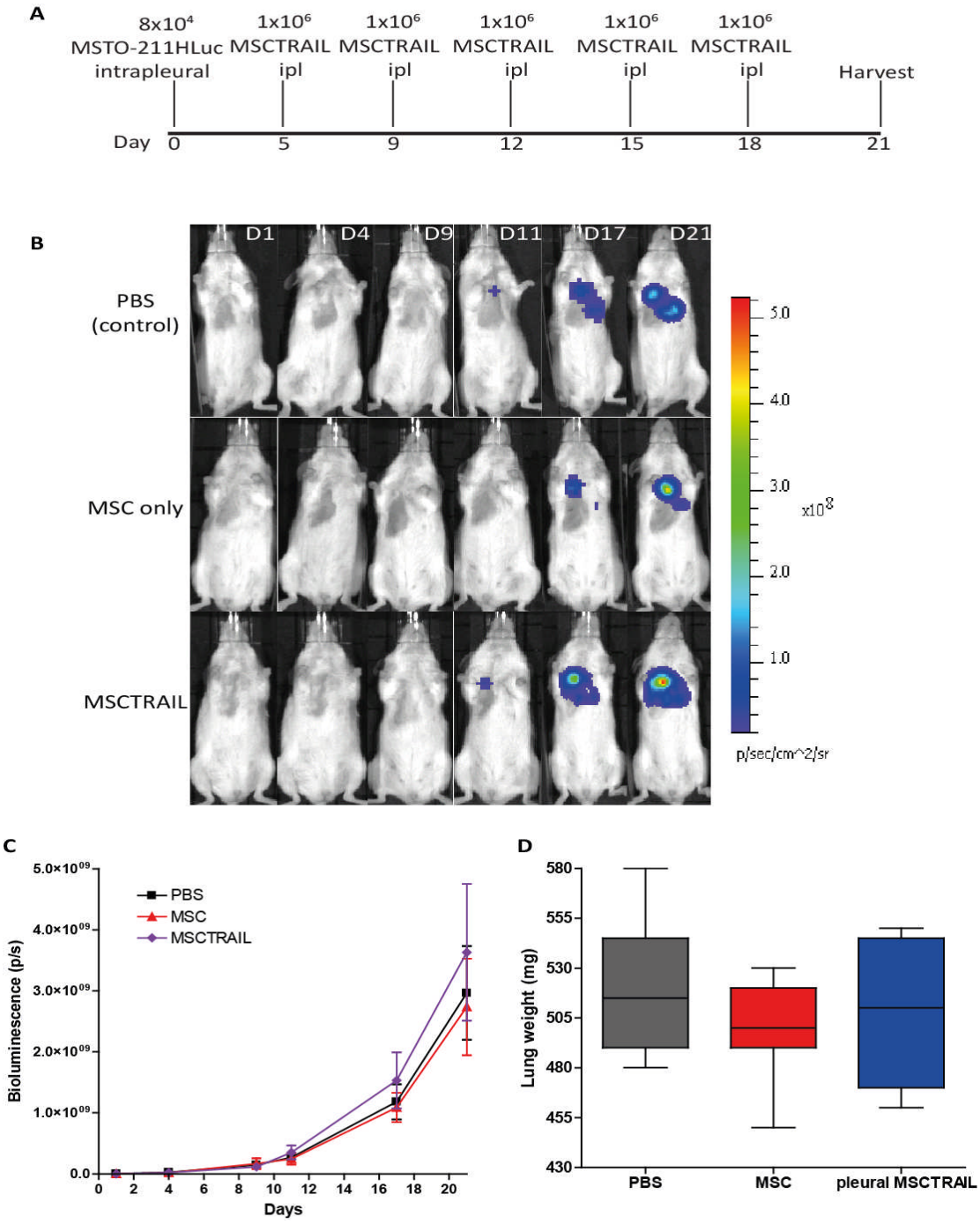

Figure 6.1: MSCTRAIL delivered intrapleurally shows no significant reduction in tumour burden. A, $8x10^4$ MSTO-211HLuc cells were delivered intrapleurally on day 0 to generate MPM tumours and $1x10^6$ MSCTRAIL cells were delivered by intrapleural injection on days 5, 9, 12, 15 and 18. Bioluminescent imaging was performed twice weekly to monitor tumour growth and animals were sacrificed on day 21 (n=8). B) Representative longitudinal IVIS® images from each treatment group showing no clear difference in bioluminescent signal between any of the groups. C) Line graph of longitudinal bioluminescent counts shows no significant difference between PBS, MSC alone or MSCTRAIL. D) Box and whiskers plot shows no significant difference in lung weights between any of the treatment groups.

6.3 Effects of intravenous delivery of MSCTRAIL to a murine model of MPM

MPM is increasingly being recognised as a metastatic disease with data showing that over half of patients with this disease have extra-thoracic metastases [5]. Previous studies have shown that intravenous delivery of MSCTRAIL can reduce tumour growth in a glioma model [105] and in some cases eliminate lung metastases [104] making it an attractive option for treating disseminated cancer. For this reason I set out to determine the effect of intravenously delivered MSCTRAIL on MPM. Intrapleural tumours were again established as described previously (section 2.8.4) and $1x10^6$ MSCTRAIL were delivered intravenously on days 5, 9, 12, 15 and 18 with control groups receiving either $1x10^6$ untransduced parental MSCs or PBS (n=8 per group, Figure 6.2 A). All mice received doxycycline administered in the drinking water and animals were imaged using IVIS® twice weekly. On day 21 animals were imaged, then sacrificed and dissected and open imaging was performed to identify tumour deposits. Heart and lungs were removed and weighed and samples were fixed for histological processing.

Bioluminescent imaging demonstrated a significant reduction in tumour growth in the group treated with MSCTRAIL compared to the PBS and untransduced MSC groups ($p<0.05$, repeated measures ANOVA; Figure 6.2 B and 6.2C). In addition to a reduction in bioluminescence there was a significant reduction in lung weights in mice treated with iv MSCTRAIL ($p<0.05$; Figure 6.2D).

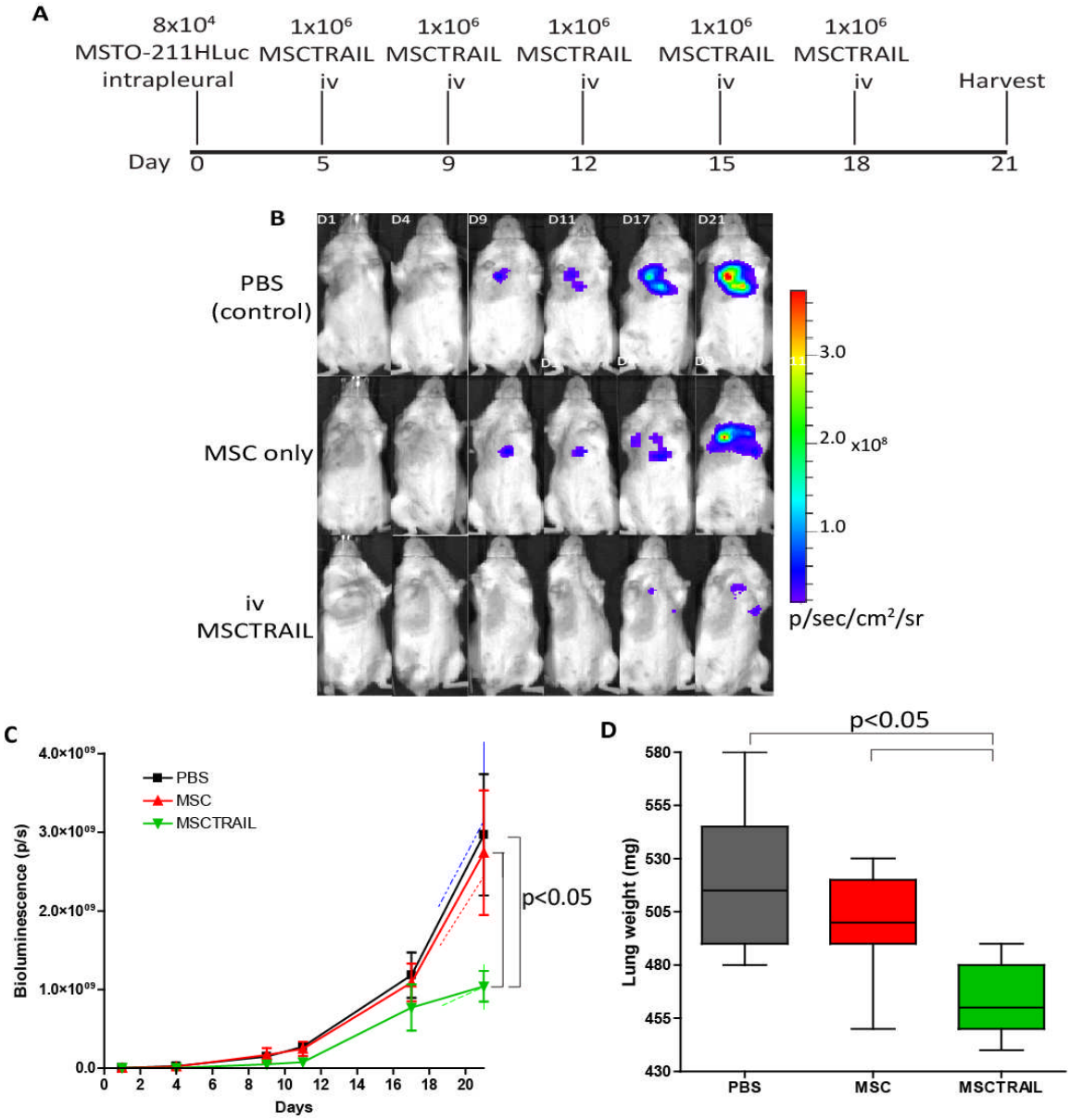

Figure 6.2: MSCTRAIL delivered intravenously causes a significant reduction in tumour burden. A) $8x10^4$ MSTO-211HLuc cells were delivered on day 0 to generate MPM tumours and $1x10^6$ MSCTRAIL were delivered via intravenous injection on days 5, 9, 12, 15 and 18. Animals were sacrificed on day 21. B) Representative longitudinal IVIS® images from each treatment group showing a clear reduction in bioluminescent signal in the MSCTRAIL treated group. C) Line graph of longitudinal bioluminescent counts shows a significant difference between treatment with MSCTRAIL compared to either PBS or MSC alone ($p<0.05$, repeated measures ANOVA). Photon count was determined using dedicated regions of interest around the whole body to include both pleural tumour burden and any distant metastatic deposits. D) Box and whiskers plot shows a significant reduction in lung weights in the MSCTRAIL treated group ($p<0.05$, ANOVA with Bonferroni's multiple comparison test).

6.4 Mechanisms of reduction in tumour growth with intravenous MSCTRAIL delivery

Given that intravenous delivery of MSCTRAIL to MPM resulted in a significant reduction in tumour growth but intrapleural delivery did not it was important to determine why there was a difference between these two delivery routes. Broadly speaking tumour growth consists of two main mechanisms; cell growth and cell death and a reduction in tumour growth could therefore be due to a reduction in cell growth or an increase in cell death. TRAIL is known to exert its anti-cancer effect by inducing apoptosis so if the reduction in tumour burden was to be attributed to our therapy an increase in apoptosis would need to be demonstrated with no alteration in cell proliferation. This was addressed using histopathological analysis of sections of tumours dissected at day 21 and performing TUNEL staining to assess apoptosis and BrdU staining to assess cell proliferation.

BrdU analysis demonstrated no significant difference in tumour cell proliferation between intravenously delivered or intrapleurally delivered MSCTRAIL when compared both to each other and to PBS (Figure 6.3A-C and 6.3G). However when quantifying the number of TUNEL positive cells there was a significant increase in the number of cells undergoing apoptosis in the group treated with iv MSCTRAIL ($p<0.01$ ANOVA with Bonferroni multiple comparisons test; Figures 6.3D-F and 6.3H). This confirms that iv MSCTRAIL delivery reduce tumour size by inducing apoptosis which would be entirely consistent with the mechanism of action of TRAIL.

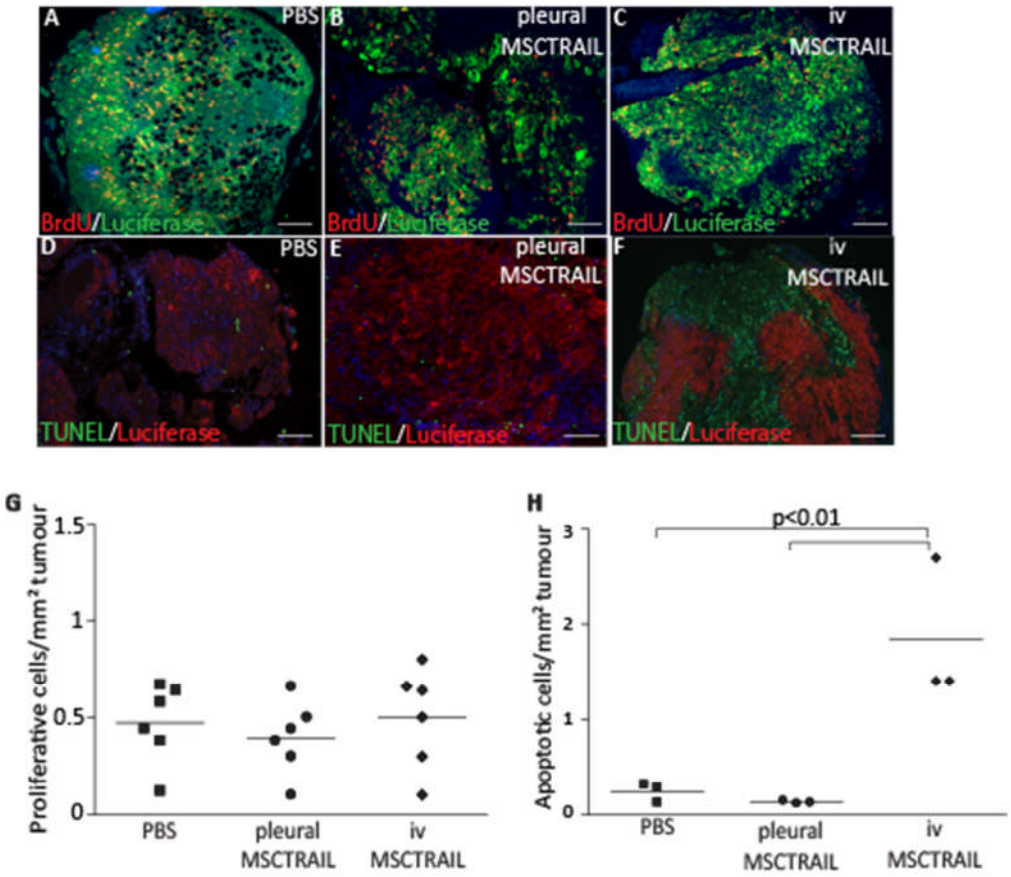

Figure 6.3: MSCTRAIL causes a reduction in tumour growth by inducing apoptosis in MPM cells. MSTO-211HLuc cells were delivered intrapleurally to establish MPM. MSCTRAIL cells were delivered by intravenous injection on days 5, 9, 12, 15 and 18 and lungs and tumours were harvested on day 21. BrdU and TUNEL staining were performed to assess tumour proliferation and apoptosis respectively. Immunofluorescence showing proliferating cells (red) and luciferase positive tumour cells (green) in tumours treated with A) PBS B) intrapleurally delivered MSCTRAIL and C) intravenously delivered MSCTRAIL. D-F) Representative immunofluorescence showing TUNEL positive apoptotic cells (green) within pleural tumours (red) in animals treated with PBS, pleural MSCTRAIL and increased apoptosis in tumours treated with iv MSCTRAIL (magnification 4x, bar 60µm). G) Proliferating cells per tumour area were quantified (Volocity Software) with no significant difference in the number of BrdU positive cells between the treatment groups. H) TUNEL positive cells per tumour area were quantified (Volocity Software) and MSCTRAIL treated animals showed increased levels of apoptosis within tumours compared to all other groups ($p<0.01$, ANOVA with Bonferroni's multiple comparison test).

6.5 Why do intravenously delivered MSCs have a therapeutic effect on MPM tumour burden whilst intrapleurally delivered MSCs do not?

From the previous experiments I have shown that MSCs can home to tumours when delivered both intrapleurally and intravenously but that only MSCTRAIL delivered intravenously has a therapeutic effect on MPM. There could be a number of explanations for this; firstly MSCs may have a different distribution within the tumour with intrapleurally delivered MSCs merely being present around the tumour capsule whilst intravenously delivered MSCs may be delivered within the tumour stroma itself enabling it to exert its therapeutic effect directly within the tumour, secondly MSCs may home to the tumour in greater numbers when delivered intravenously compared to intrapleurally due to cells being delivered directly to the site of tumours rather than relying only on chemokine gradients to move there and finally MSCs may survive longer when delivered intravenously compared to intrapleurally as they are delivered within the systemic circulation where they are healthier compared to their counterparts which need to survive within a pleural cavity. The first possible explanation has been assessed using immunofluorescence from experiments to look at MSC homing (Figure 5.8 H&J) as the DiI stained MSCs are clearly visible within the tumour tissue following both routes of delivery. To address the other two possible explanations further experiments were performed.

6.5.1 Determination of number of MSCs homing to intrapleural tumours and their persistence once delivered

To assess whether similar numbers of MSCs were incorporating within tumours following intrapleural and intravenous delivery $2x10^5$ MSTO-211HLuc were injected intrapleurally and left for 10 days to allow large tumours to develop. $1x10^6$ MSCs stained with DiR were injected either intravenously or intrapleurally. Serial bioluminescent and fluorescent imaging was performed daily and lungs were harvested for histology or tumours were dissected out and digested for flow cytometry. Tumours were successfully established and MSCs were quantified using IVIS (Figure 6.4A). The intensity of the fluorescent signal was determined and demonstrated a significant difference in signal 24 hours post MSC injection ($p=0.0125$; Figure 6.4B). This difference was maintained during the 6 day imaging period. This suggests that MSCs incorporate into tumours in greater numbers when delivered

intravenously compared to intrapleurally. Tumours were digested and flow cytometry was performed using YFP to identify tumour cells and DiI to identify MSCs, which confirmed a greater percentage of MSCs in the tumours following intravenous delivery compared to intrapleural delivery (Figure 6.4 C and 6.4 D).

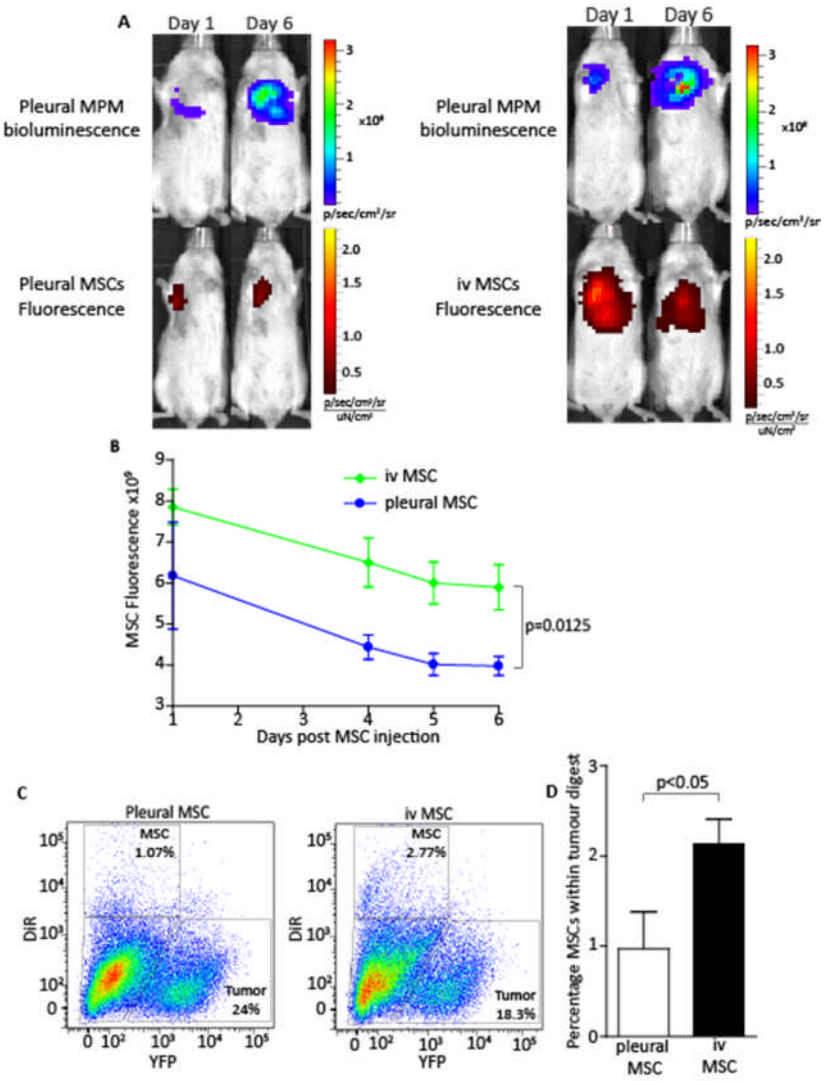

Figure 6.4: Intravenously delivered MSCs are incorporated into tumours in greater numbers than when delivered intrapleurally. A) IVIS images to show established bioluminescent MPM tumours and corresponding fluorescence from DiR labelled MSCs on days 1 and 6 following MSC injection. Intravenously delivered MSCs show a higher fluorescent signal on day 1 and day 6 following injection compared to intrapleurally delivered MSCs. B) Fluorescent signal was quantified and MSCs delivered iv showed a higher signal on day 1 compared to cells delivered ip which persisted until day 6 (p=0.0125). C) Tumours were removed and digested for flow cytometry which revealed a higher percentage of DiR stained MSCs in tumours given iv MSCs than in those given ip MSCs. D) Bar chart to show a significant increase in DiR stained MSCs in tumour digests following iv delivery compared to pleural delivery (p<0.05).

6.6 Combining MSCTRAIL therapy with SAHA – is there a synergistic effect?

From our *in vitro* data I have shown that combining MSCTRAIL therapy with existing chemotherapy agents, such as SAHA, results in a significant increase in cell death and apoptosis when compared to either agent alone (Figure 4.5). Our final aim, therefore, was to determine whether treating MPM with a combination of MSCTRAIL and SAHA resulted in a reduction in tumour growth *in vivo* over and above that seen with MSCTRAIL or SAHA alone. In order to test this hypothesis, intrapleural tumours were established as previously described (section 2.8.4). Treatment started on day 5 and animals were assigned to one of the following treatment groups:

Treatment Group	MSC Therapy	Chemotherapy
PBS Control	Intravenous PBS	Intraperitoneal normal saline
SAHA only	Intravenous PBS	Intraperitoneal SAHA
MSC only	Intravenous MSC	Intraperitoneal normal saline
MSCTRAIL only	Intravenous MSCTRAIL	Intraperitoneal normal saline
MSCTRAIL and SAHA	Intravenous MSCTRAIL	Intraperitoneal SAHA

Table 6.1: Table to show the different treatment groups for the combination chemotherapy with MSCTRAIL *in vivo* experiment.

Animals receiving MSC therapy were given $1x10^6$ MSC or MSCTRAIL delivered intravenously on days 5, 9, 12, 15 and 18 whilst control groups were given PBS. For chemotherapy delivery, animals receiving SAHA were given 20mg/kg SAHA delivered via intraperitoneal injection three times a week, with controls receiving 200 µl of vehicle solution (normal saline/DMSO). All mice received doxycycline administered in the drinking water and animals were imaged using IVIS® twice weekly. On day 21 animals were imaged, then sacrificed and dissected and open imaging was performed to identify tumour deposits. Heart and lungs were removed and weighed and samples were fixed for histological processing.

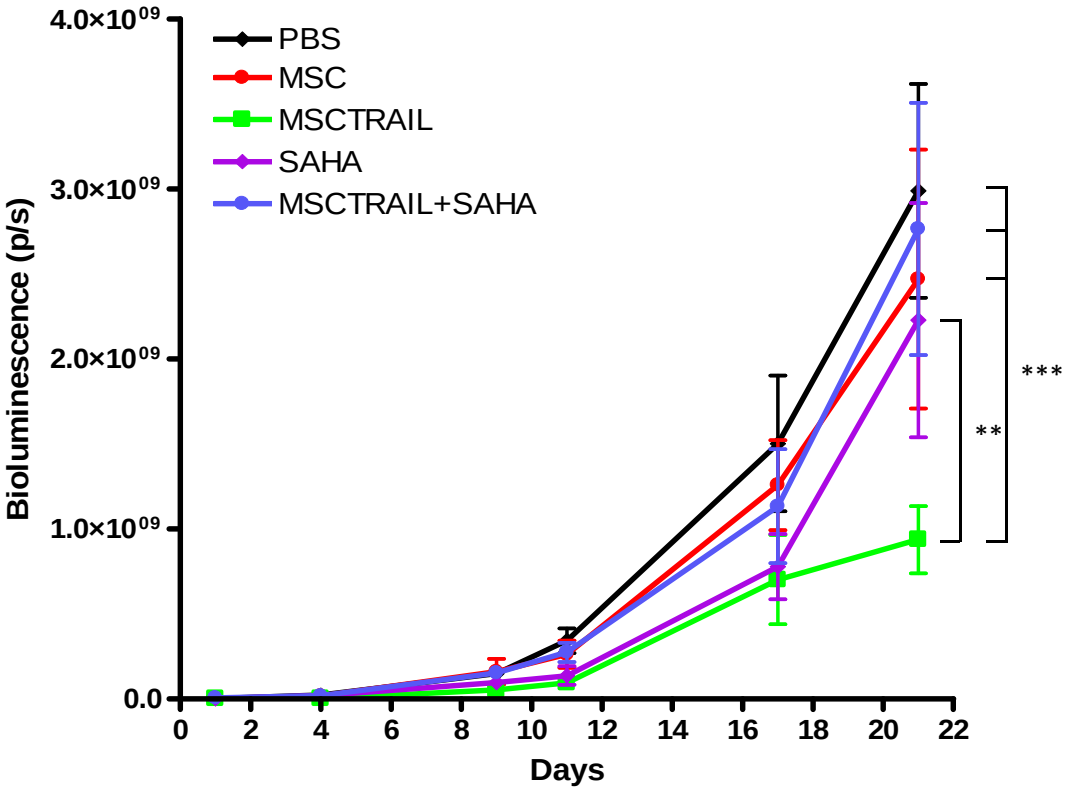

Figure 6.5. Longitudinal bioluminescent signal shows a reduction in tumour burden with iv MSCTRAIL treatment alone but not in combination with chemotherapy. Line graph of longitudinal bioluminescent signal shows a significant reduction in tumour burden in animals treated with MSCTRAIL alone (** p<0.01, ***p<0.001, two-way RM ANOVA with Bonferroni's multiple comparison test; n=7 per group)

Longitudinal bioluminescent imaging showed that treatment with MSCTRAIL resulted in a significant reduction in tumour burden when compared to PBS, MSC and SAHA alone (Figure 6.5) (**p<0.01, ***p<0.001, two-way RM ANOVA with Bonferroni's multiple comparison test). Whilst there was a reduction in bioluminescence in animals treated with SAHA alone compared to treatment with PBS or MSC this did not reach statistical significance. From the *in vitro* results one might have predicted that treatment with MSCTRAIL and SAHA in combination would be more effective than treatment with MSCTRAIL alone and similar in efficacy to SAHA alone. However, our *in vivo* results showed that treatment with MSCTRAIL/SAHA combination was less effective than either of these treatments alone (p<0.001, two-way RM ANOVA with Bonferroni's multiple comparison test). There were a number of possible reasons why this might be:

1. SAHA causes MSC cell death and hence prevents TRAIL delivery
2. The dose of SAHA used was too low to have an effect *in vivo*
3. If SAHA doesn't cause MSC cell death it may alter TRAIL transgene expression

From earlier *in vitro* work I demonstrated that SAHA does not cause a significant increase in death and apoptosis of MSCs (Figure 4.4) so the next step was to determine whether the dose of SAHA used was too low to have a significant effect on tumour burden *in vivo*.

6.6.1 *In vivo* SAHA dose determination

Intrapleural tumours were established as previously described (section 2.8.4) and treatment was started on day 5. Animals were assigned to one of the following treatment groups:

Group	Treatment
A	PBS/DMSO vehicle
B	50 mg/kg
C	100 mg/kg
D	150 mg/kg

Table 6.2: Table to show the different treatment groups for SAHA dose finding

The doses used were chosen to cover a range of doses used in other publications that were shown to be effective in other tumour models. Animals were weighed daily and the

appropriate dose was calculated accordingly, they received 5 injections per week and were imaged twice weekly using IVIS®. Mice were culled on day 21 or when >20% weight loss was recorded.

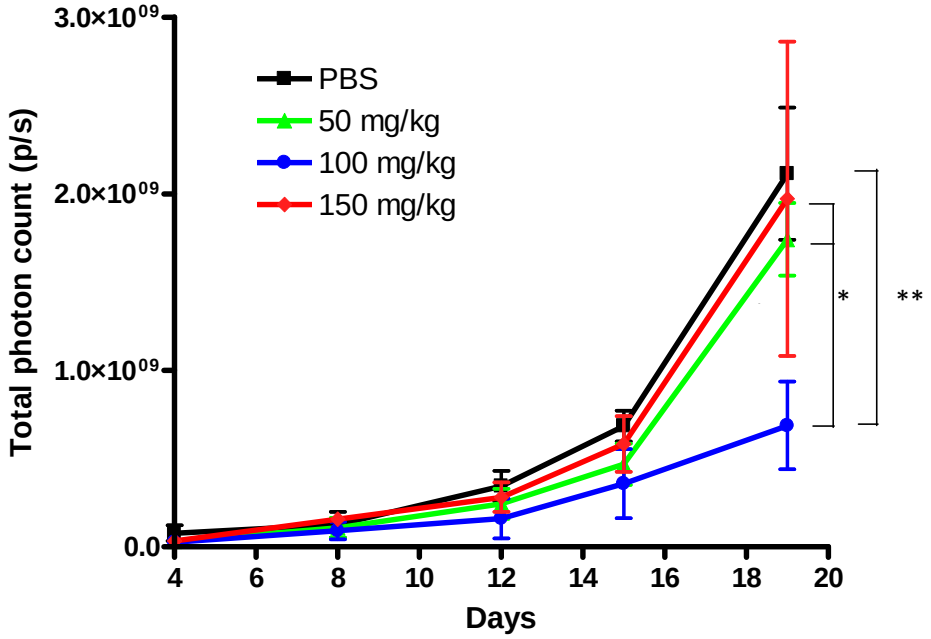

Figure 6.6. Longitudinal bioluminescence showing that treatment with 100 mg/kg SAHA reduces MPM tumour burden. Line graph showing longitudinal bioluminescence over 21 days in animals treated with different doses of SAHA (n=5 per group). Treatment with 100 mg/kg SAHA resulted in a significant reduction in tumour burden whilst other doses were ineffective (* $p<0.05$, ** $p<0.001$, two-way repeated measures ANOVA with Bonferroni's multiple comparison test).

Treatment with 100 mg/kg resulted in a significant reduction in tumour burden compared to either PBS/DMSO control ($p<0.001$) and to treatment with 50 mg/kg and 150 mg/kg ($p<0.05$). It seems unusual that the higher dose of 150 mg/kg had no significant effect on tumour growth but this was likely due to the insolubility of the drug at higher concentrations. SAHA is soluble in organic solvents only such as ethanol or DMSO and administration of 100% DMSO to animals is highly toxic. In order to enable safe drug delivery the SAHA was solubilised in DMSO to make a stock solution and this was then diluted in aqueous solution (PBS) to attain the correct concentration for *in vivo* dosing. In the case of 150 mg/kg solution, when the drug was diluted in PBS it was noted to precipitate out back into crystals and was very difficult to keep in a suspension suitable for injection. It is likely that these animals therefore did not get a dose of 150 mg/kg and may have received a much lower dose that was therapeutically ineffective. These results would suggest that our initial experiment using 20 mg/kg SAHA three times a week was too low a dose to have had a significant effect on tumour growth and future experiments should use a dose of 100 mg/kg delivered 5 times weekly for optimal therapeutic efficacy.

6.7 Discussion

The experiments described in this chapter show that intravenous delivery of MSCTRAIL to a murine model of MPM resulted in a reduction in tumour burden as demonstrated by both a reduction in bioluminescent signal and lung weights. This therapeutic effect was not repeated when MSCTRAIL was delivered intrapleurally despite the fact that MSCs home to tumours when delivered by this route.

6.7.1 Delivery route as a determinant of successful therapy

One of the key components of any therapy is the route of delivery. This can be broadly divided into systemic or topical and the route selected is largely dependent on the distribution of the disease being treated and the mode of action of the therapy. Systemically delivered therapy is largely used for diseases that are multi-site and located in multiple organs enabling treatments to be aimed against all sites of the disease. However, systemic therapeutic administration is dependent on intravenous access and often requires high doses to be delivered in order to achieve therapeutic efficacy to the site of disease. It also has the problem of increased risk of off-target effects as treatment will be delivered to all organs. If disease is located to a single site then topical therapy is a more attractive option as it allows local delivery of therapeutic treatment doses without the need for systemic delivery and reduces the chances of off-target effects. In the case of MPM the greatest burden of disease is within the pleural cavity. The vast majority of patients will require at least one intercostal chest drain to be inserted during either their diagnosis or treatment which allows access directly to the site of the tumour. This local access makes topical treatment of MPM a very appealing option. For this reason our first experiment was designed to assess the efficacy of topical delivery of MSCTRAIL on MPM tumour growth.

As I demonstrated in chapter 5, MSCs are able to home to tumours when delivered intrapleurally, so it was surprising there was no therapeutic effect when MSCTRAIL was delivered via this route. In subsequent experiments we showed that intravenously delivered MSCTRAIL has a good therapeutic effect with a visible reduction in tumour burden

as shown by a reduction in bioluminescent signal when compared with PBS or MSC treatment. For other diseases it has been shown that intrapleurally delivered MSCs localise within the pleural cavity [222] and can be used to reduce the severity of endotoxin-induced acute lung injury [223] in a murine model. Other topical delivery routes have also been assessed in multiple *in vivo* models including intraperitoneal delivery of interferon-β transduced MSCs in an ovarian cancer model [224], direct injection of TSP-1 expressing MSCs to a murine glioma model [225] and intrathecal delivery in a rodent model of spinal cord injury [226].

In addition to the many *in vivo* studies there are a number of clinical trials assessing the therapeutic efficacy of native untransduced MSC delivery in a multitude of diseases. The overwhelming majority of these studies are in patients with either acute or chronic ischaemic heart disease and there are over 100 clinical trials registered looking at safety and efficacy of intracoronary or trans-endocardial delivery of MSCs for both chronic and acute cardiac diseases. There are over 70 early phase clinical trials assessing the use of MSCs in patients suffering from strokes and these use either intravenous or cerebral artery MSC injection as their route of delivery. Although all of these topical delivery routes are safe according to phase I data very few of them show significant efficacy in their phase II arms and the reasons for this are not clear. There are no clinical trials comparing the efficacy of different delivery routes within the same disease and it may be that the clinical efficacy of MSC therapy is affected by delivery route. As with the majority of therapies ensuring the correct dose delivery is essential for treatment efficacy and when it comes to cellular therapy it is likely that the number of cells delivered will directly determine the treatment dose the patient receives. It is possible that intravenous delivery is more effective at delivering cells to their required site of action and it is possible that by increasing the number of cells delivered intrapleurally a therapeutic effect may be achieved. Further experiments would be aimed at increasing the number of MSCTRAIL cells delivered intrapleurally to determine whether the initial lack of therapeutic efficacy can be overcome with an increased dose.

6.7.2 MSC homing and incorporation into tumours

When considering clinical applications the first step for a successfully therapy is to deliver it to the desired target. In the case of MSCTRAIL the initial challenge is to successfully deliver MSCs to the tumour and the second is to ensure that the cells persist within the tumour to allow long term therapeutic gene expression and delivery of an effective dose. In using MSCs as delivery vectors for cellular based gene therapies, it is thought that treatment efficacy is related to the level of MSC accumulation at tumour sites.

Whilst it is well described that MSCs home to tumours most of this evidence is from *in vitro* migration studies and using immunohistochemical techniques to look at cell location in post mortem *in vivo* studies. Our early experiments using dual bioluminescent and fluorescent imaging to track cells demonstrated that MSCs home to tumours following both topical and systemic delivery. The next step was to determine whether there was any effect of delivery route on the number of cells within the tumour or the length of time the cells remained there. Again using dual bioluminescent and fluorescent imaging with both direct and indirect cell labelling techniques I demonstrated that whilst systemic MSC delivery results in higher numbers of cells homing to the tumours, once incorporated within the tumour stroma the MSCs remain there for a similar time regardless of delivery route (Figure 6.4). Whilst there was a slow reduction in fluorescent signal over time it cannot be determined whether this is due to cell death or cell proliferation. It is possible that over time the MSCs die and are cleared from the tumours resulting in a decrease in fluorescent signal but as our fluorescent labelling was performed using a direct staining with a lipophilic tracer it cannot provide any information about cell viability. It is therefore equally possible that the reduction in signal seen is a reflection of increasing cell number as this direct labelling technique is known to be diluted during cell division. What is reassuring is that the route of delivery did not affect the duration of persistence for the MSCs because the signal reduction seen was the same for both groups.

Our study shows that whilst MSC homing occurs regardless of route of delivery the level of MSC accumulation following iv delivery is significantly higher than when delivered ip. It is possible that the increase in apoptosis seen in the iv delivery model is a direct effect of the tumour receiving a greater number of cells and hence a higher dose of TRAIL. But why is it

that MSCs accumulate better with this delivery route? The first step in MSC accumulation within tumours is adhesion to vascular endothelial cells and multiple factors have been suggested to be important for this process including TNFα and NF-κB [227], interleukin 1β and interferon-γ [228] all of which induce VCAM-1 expression on tumour cells. It may be that cells delivered iv have higher accumulation as they are delivered directly to endothelial cells making adhesion more likely. Alternatively ip delivered cells may have lower accumulation as their delivery is not directly to areas of tumour that are well vascularized. These areas are likely to be more hypoxic and MSCs are more likely to die when located within a hypoxic microenvironment [229].

6.7.3 Combination chemotherapy

One of the problems encountered in the management of malignant diseases is the phenomenon of treatment resistance. This can be primary resistance when a cancer type is inherently resistant to a specific therapeutic agent or secondary resistance in which exposure to chemotherapeutics can result in a sub-population of cells developing resistance to the therapy it is exposed to. To try and combat resistance the majority of tumours are treated with multiple agents; MPM being one of these where the recommended first line treatment is cisplatin in combination with pemetrexed [230]. As demonstrated by our results, although all cell lines show an increase in death and apoptosis when treated with MSCTRAIL the levels of cell death are very variable between the cell lines and in the majority of cases show overall low levels of apoptosis (Figure 4.2). This means that a significant number of cells will be inherently resistant to treatment with MSCTRAIL making it unlikely to be a curative therapy. However, it has been shown that by targeting both the extrinsic apoptotic pathway with a compound such as TRAIL and the intrinsic apoptotic pathway using chemotherapy or radiation a synergistic effect occurs resulting in significantly greater apoptosis than by targeting either arm individually [231]. Agents such as etoposide, rapamycin and anisomycin have been shown to act at the level of the mitochondria increasing crosstalk between the two sides of the apoptotic pathway [232, 233] whilst agents such as SAHA have been shown to increase MPM apoptosis by targeting FLIP and caspase 8 [93].

From our *in vitro* co-culture experiments assessing the combination of SAHA and MSCTRAIL I demonstrated that in the most sensitive cell line MSTO-211H that the combination of MSCTRAIL and SAHA was as effective but no more so than either SAHA or MSCTRAIL alone. The *in vivo* results however demonstrated a significant reduction in tumour burden when using MSCTRAIL alone compared to either SAHA alone or MSCTRAIL and SAHA in combination which does not correlate with the *in vitro* data. I sought to determine why there was a difference in results and evidence from the *in vitro* experiments suggests that SAHA does not kill the MSCs and so MSCTRAIL delivery should be effective. I then performed a dose finding experiment in an *in vivo* model and showed that the dosage used in the combination experiment was probably too low to achieve a significant effect and for future experiments the higher dose of 100 mg/kg SAHA 5 times a week would be the appropriate dosing schedule.

One of the limitations of this study was the use of a 'TRAIL sensitive' cell line where you might expect to gain only small advantages in combination therapy over single agent therapy and what would be more significant is trying to overcome resistance in a 'TRAIL resistant' cell line such as H28. One of the major problems with the use of the xenograft model is that whilst it allows us to assess the effect of human MSCTRAIL on human MPM in order to establish this disease model an immunodeficient mouse has to be used. One of the problems with human MPM cell lines is that not all of them are tumorigenic in mice and H28 has previously shown to be a non-tumorigenic cell line [217]. This meant that I was not able to expand the data on H28 and combination chemotherapy by performing *in vivo* studies however it would be interesting to see if an alternative murine model could be established to demonstrate this. Future work could include either trying to establish a xenograft model of H28 in a more immunosuppressed mouse such as the NOD/SCID/GAMMA (NSG) or by using a syngeneic model of mesothelioma. If this route were to be taken then to prevent immune rejection of the human MSCs, murine MSCs would have to be used as the therapeutic vectors and the *in vitro* data would have to be revalidated as it is known that murine cells have only one TRAIL receptor rather than five and so the response to MSCTRAIL may be different.

6.8 Summary

- Systemically administered MSCTRAIL causes a reduction in tumour burden as demonstrated by a reduction in bioluminescence and lung weights whilst topically delivered therapy is not effective
- Systemically administered MSCTRAIL reduces tumour growth by increasing cancer cell apoptosis but does not affect tumour proliferation
- Both systemically and topically delivered MSCs home to intrapleural tumours but when delivered systemically they engraft in higher numbers than when delivered topically
- It is possible that the lack of therapeutic efficacy seen with topically delivered MSCTRAIL could be due to lower levels of cell engraftment resulting in a sub-therapeutic dose of TRAIL at the site of the tumour
- Combination therapy with MSCTRAIL and SAHA does not improve tumour cell death when compared to either therapy alone although this could be due to a sub-therapeutic dose of SAHA being used

Chapter 7

Summary and Future Directions

7 Summary

The hypothesis for this thesis was that human bone marrow-derived mesenchymal stem cells could be used as therapeutic vectors to deliver TRAIL directly to the site of tumours and cause tumour cell death in a murine model of malignant pleural mesothelioma and that combining MSCTRAIL with chemotherapy agents would provide synergistic benefit in reducing tumour growth. I have shown that MSCs can be successfully transduced with a lentiviral vector carrying the TRAIL transgene whose expression is controlled by doxycycline and that MSCTRAIL induces apoptosis and cell death in all MPM cell lines tested. I have demonstrated using dual bioluminescent and fluorescent imaging that MSCs home to tumours when delivered either systemically or topically but that only systemically delivered MSCTRAIL results in a reduction in tumour burden in a murine model of MPM. Whilst the precise mechanism by which this occurs is unknown it is possibly due to a higher number of MSCs located within the tumours following systemic delivery. Combining MSCTRAIL with chemotherapy results in increased apoptosis and cell death *in vitro* but this was not demonstrated *in vivo*. The results of these experiments in combination with other work performed within the laboratory have resulted in the initiation of the pathway to gain regulatory approval and future funding applications with the aim of running a phase I/II clinical trial.

7.1 MSCs as delivery vectors for combined gene and cellular therapy

Despite the clear potential of this therapy there are still many unanswered questions that need to be addressed in further laboratory work. The optimal timing of delivery and number of cells required to have a therapeutic effect need to be established. Early delivery of a larger number of MSCs have shown a greater therapeutic effect in a cerebral ischaemia model [234] [235] and there is also known to be a plateau at which increasing cell numbers has no additional benefit [236]. However, these studies have used a model of cerebral ischaemia which has an identifiable onset unlike tumour development which is largely unnoticed until the tumour mass is large enough to produce symptoms by which time the disease is often metastatic, and it uses untransduced MSCs as the therapy rather than using

them as a vector to deliver a therapy. When taking a combined cellular and gene therapy forward into a clinical trial not only does the timing of cell delivery in a well-established disease need to be determined, the number of cells required to deliver a therapeutic dose must also be addressed. The timing of cell delivery is likely to be dependent on the length of time MSCs reside within the targeted tumour, whether they proliferate and the duration of transgene expression. These questions have been difficult to answer in pre-clinical studies as most evidence for MSC homing and engrafting have been dependent on immunohistochemical analysis of post mortem murine tissues and are unable to provide information on the longitudinal behaviour of the cells *in vivo* or on their proliferative capacity [104]. The only work assessing the long term engraftment of MSCs in human subjects has also been from post-mortem studies in patients who have had intravenously delivered MSCs to treat graft vs host disease (GVHD). In these cases all organs were assessed at post-mortem for the presence of MSC donor DNA and in the vast majority of cases this was found only at low levels within 50 days of MSC delivery [237]. This thesis is the first to describe the use of dual bioluminescent and fluorescent imaging to track MSCs longitudinally and one of the main limitations in our study was the use of the lipophilic fluorescent tracer to monitor MSCs. This family of tracers provide no information on cell viability and the signal will deteriorate over time regardless of cell viability and activity. Initial attempts were made to directly label the MSCs with a lentiviral vector containing the fluorophore mCherry but this was toxic resulting in a significant impairment of cell proliferation and profound changes in morphology. Future work should address the duration of MSC engraftment and the maintenance of transgene expression within the targeted tumours.

When delivering TRAIL using MSCs as cellular vectors, one of the aims is to deliver the therapy directly to the site where its action is required whilst keeping systemic levels low. Although this is beneficial when aiming to reduce off-target and systemic toxicity it also means that determining the dose of treatment being delivered is extremely difficult as the agent cannot be monitored systemically. This remains an important consideration to

address when planning clinical trials and it is likely that both cell number and frequency of delivery will need to be determined in early phase trials.

Our data also suggests that route of delivery is also of critical importance in therapeutic efficacy and this may be related to the homing efficiency of the MSCs being dependent on delivery route. Further work should be directed at determining the key mediators of MSC homing and whether these can be exploited to improve homing and therefore therapeutic efficacy. In the case of MPM it would also be useful to determine whether increasing the number of cells delivered topically would result in a therapeutic effect, in which case the use of topical treatment would again be feasible. Whilst mesothelioma is classically considered a locally advanced disease there is increasing evidence that it is a metastatic disease with post-mortem series revealing extra-pleural deposits in >80% of patients [238] suggesting that there might be a role for using both routes of delivery to treat a single disease.

7.2 TRAIL resistance and combination chemotherapy

As demonstrated by the data within this thesis despite all MPM cell lines showing increased cell death and apoptosis on treatment with MSCTRAIL the percentage of cell death was highly variable between cell lines with the most sensitive line showing 58% cell death whilst the least sensitive showed as little as ~7% cell death. This suggests that MSCTRAIL as a single agent therapy is unlikely to be successful for all patients with MPM as such low levels of cell death will probably not translate to any improvement in clinical outcome. There is data from *in vitro* studies on mesothelioma looking at combining agents that target both the extrinsic and intrinsic apoptotic pathways to improve levels of apoptosis [78, 233] but there are no studies combing MSCTRAIL with chemotherapeutics. My *in vitro* data showed that combining MSCTRAIL with SAHA resulted in increased cell death in the cell line with high TRAIL sensitivity but more importantly I showed a significant increase in the line with low TRAIL sensitivity. Initial *in vivo* studies were performed using the MSTO-211H cell line as this is previously reported to be tumorigenic *in vivo* whilst H28 is not but there was no significant reduction in tumour burden compared to controls. Whilst it is possible this was

due to a sub-therapeutic dose of SAHA being used rather than simply repeating the initial experiment with a higher dose of SAHA it would be more interesting therapeutically to show successful treatment in a tumour with low TRAIL sensitivity. For this reason future work should be directed at developing a tumour model using a cell line with low TRAIL sensitivity and determining the effect of MSCTRAIL both alone and in combination with SAHA and other chemotherapeutic agents such as cisplatin and pemetrexed. In pilot work carried out as part of this project H28 cells have been successfully transduced with luciferase-YFP lentivirus and delivered intrapleurally to NOD/SCID/GAMMA mice which are considered more immunosuppressed than NOD/SCID animals. Early imaging shows that tumours can be established with $2x10^6$ cells and the kinetics of tumour growth will be determined over 30-60 days to determine the optimal delivery time for MSCTRAIL.

7.3 Clinical translation

The ultimate aim for the work presented in this thesis is to allow its translation into the clinic. Combined cellular and gene therapy is a novel treatment approach that as yet is not well established in clinical trials. Cell therapy using unmodified MSCs have been widely used in early phase clinical trials in the treatment of a number of diseases, mostly cardiovascular and haematological diseases or those with a significant inflammatory component such as inflammatory bowel disease with a good safety profile. However therapeutic efficacy is often limited. There is also increasing use of gene therapies particularly for the treatment of rare metabolic conditions that require correction of a single gene and although there were initial concerns over the safety of using lentiviral vectors in gene therapy the newer vectors in clinical trials are safer. Although there is growth in each of these fields individually there are very few clinical trials using combined gene and cell therapy and none using modified MSCS to treat cancer.

Based on work from this thesis in combination with work previously performed in the laboratory I am currently preparing to apply for regulatory approval for MSCTRAIL and grant funding to allow a phase I/II clinical trial to be undertaken to determine the safety and efficacy of MSCTRAIL in metastatic lung cancer. Whilst much of the data in the thesis will

provide valuable information for these applications there are still many unanswered questions that will need to be addressed either before or during any clinical trial.

7.4 Final conclusion

The data presented in this thesis has demonstrated that MSCs can be successfully used as cellular vectors to deliver a gene therapy for malignant pleural mesothelioma and provide promise for future pre-clinical studies, in particular to overcome some of the issues regarding low TRAIL sensitivity and ultimately lead to translation into a clinical trial.

Appendix 1: ECOG Performance Status

Grade	ECOG
0	Fully active, able to carry on all pre-disease performance without restriction
1	Restricted in physically strenuous activity but ambulatory and able to carry out work of a light or sedentary nature
2	Ambulatory and capable of all selfcare but unable to carry out any work activities. Up and about more than 50% of waking hours
3	Capable of only limited selfcare, confined to bed or chair more than 50% of waking hours
4	Totally confined to bed or chair. Completely disabled, unable to carry out any selfcare

Chapter 8

References

8 REFERENCES

1. Wagner, J.C., C.A. Sleggs, and P. Marchand, *Diffuse pleural mesothelioma and asbestos exposure in the North Western Cape Province.* Br J Ind Med, 1960. **17**: p. 260-71.
2. Goodman, J.E., M.A. Nascarella, and P.A. Valberg, *Ionizing radiation: a risk factor for mesothelioma.* Cancer causes & control : CCC, 2009. **20**(8): p. 1237-54.
3. Cristaudo, A., et al., *SV40 enhances the risk of malignant mesothelioma among people exposed to asbestos: a molecular epidemiologic case-control study.* Cancer research, 2005. **65**(8): p. 3049-52.
4. Manfredi, J.J., et al., *Evidence against a role for SV40 in human mesothelioma.* Cancer research, 2005. **65**(7): p. 2602-9.
5. Hammond, E.C., I.J. Selikoff, and H. Seidman, *Asbestos exposure, cigarette smoking and death rates.* Ann N Y Acad Sci, 1979. **330**: p. 473-90.
6. in *www.hse.gov.uk/statistics/causdis/mesothelioma/scale.html*.
7. Hodgson, J.T., et al., *The expected burden of mesothelioma mortality in Great Britain from 2002 to 2050.* Br J Cancer, 2005. **92**(3): p. 587-93.
8. Husain, A.N., et al., *Guidelines for Pathologic Diagnosis of Malignant Mesothelioma: 2012 Update of the Consensus Statement from the International Mesothelioma Interest Group.* Archives of pathology & laboratory medicine, 2012.
9. Ray, M. and H.L. Kindler, *Malignant pleural mesothelioma: an update on biomarkers and treatment.* Chest, 2009. **136**(3): p. 888-96.
10. Wittekind CH, G.F., Hutter RVP et al, ed. *Illustrated Guide to the TMN Classification of Malignant Tumours*. 5th ed. TNM Atlas2004, Springer: Berlin. 169-176.
11. Rusch, V.W., *A proposed new international TNM staging system for malignant pleural mesothelioma from the International Mesothelioma Interest Group.* Lung Cancer, 1996. **14**(1): p. 1-12.
12. Steele, J.P., *Prognostic factors for mesothelioma.* Hematology/oncology clinics of North America, 2005. **19**(6): p. 1041-52, vi.
13. Herndon, J.E., et al., *Factors predictive of survival among 337 patients with mesothelioma treated between 1984 and 1994 by the Cancer and Leukemia Group B.* Chest, 1998. **113**(3): p. 723-31.
14. Curran, D., et al., *Prognostic factors in patients with pleural mesothelioma: the European Organization for Research and Treatment of Cancer experience.* Journal of clinical oncology : official journal of the American Society of Clinical Oncology, 1998. **16**(1): p. 145-52.
15. Vogelzang, N.J., et al., *Phase III study of pemetrexed in combination with cisplatin versus cisplatin alone in patients with malignant pleural mesothelioma.* Journal of Clinical Oncology : Official Journal of the American Society of Clinical Oncology, 2003. **21**(14): p. 2636-44.
16. Treasure, T., et al., *The MARS trial: mesothelioma and radical surgery.* Interactive Cardiovascular and Thoracic Surgery, 2006. **5**(1): p. 58-9.
17. Sugarbaker, D.J., et al., *Resection margins, extrapleural nodal status, and cell type determine postoperative long-term survival in trimodality therapy of malignant pleural mesothelioma: results in 183 patients.* J Thorac Cardiovasc Surg, 1999. **117**(1): p. 54-63; discussion 63-5.
18. Flores, R.M., et al., *Extrapleural pneumonectomy versus pleurectomy/decortication in the surgical management of malignant pleural mesothelioma: results in 663 patients.* J Thorac Cardiovasc Surg, 2008. **135**(3): p. 620-6, 626 e1-3.
19. Treasure, T., et al., *Extra-pleural pneumonectomy versus no extra-pleural pneumonectomy for patients with malignant pleural mesothelioma: clinical outcomes of the Mesothelioma and Radical Surgery (MARS) randomised feasibility study.* The lancet oncology, 2011. **12**(8): p. 763-72.

20. Vogelzang, N.J., et al., *Phase III study of pemetrexed in combination with cisplatin versus cisplatin alone in patients with malignant pleural mesothelioma.* J Clin Oncol, 2003. **21**(14): p. 2636-44.
21. Ceresoli, G.L., et al., *Phase II study of pemetrexed plus carboplatin in malignant pleural mesothelioma.* J Clin Oncol, 2006. **24**(9): p. 1443-8.
22. Kindler, H.L., *Systemic treatments for mesothelioma: standard and novel.* Curr Treat Options Oncol, 2008. **9**(2-3): p. 171-9.
23. Muers, M.F., et al., *Active symptom control with or without chemotherapy in the treatment of patients with malignant pleural mesothelioma (MS01): a multicentre randomised trial.* Lancet, 2008. **371**(9625): p. 1685-94.
24. Razak, A.R., K.J. Chatten, and A.N. Hughes, *Retreatment with pemetrexed-based chemotherapy in malignant pleural mesothelioma (MPM): a second line treatment option.* Lung Cancer, 2008. **60**(2): p. 294-7.
25. Xanthopoulos, A., et al., *Gemcitabine combined with oxaliplatin in pretreated patients with malignant pleural mesothelioma: an observational study.* J Occup Med Toxicol, 2008. **3**: p. 34.
26. Zucali, P.A., et al., *Gemcitabine and vinorelbine in pemetrexed-pretreated patients with malignant pleural mesothelioma.* Cancer, 2008. **112**(7): p. 1555-61.
27. Sorensen, J.B., et al., *Pemetrexed as second-line treatment in malignant pleural mesothelioma after platinum-based first-line treatment.* Journal of thoracic oncology : official publication of the International Association for the Study of Lung Cancer, 2007. **2**(2): p. 147-52.
28. Jassem, J., et al., *Phase III trial of pemetrexed plus best supportive care compared with best supportive care in previously treated patients with advanced malignant pleural mesothelioma.* J Clin Oncol, 2008. **26**(10): p. 1698-704.
29. Ramalingam, S.S. and C.P. Belani, *Recent advances in the treatment of malignant pleural mesothelioma.* Journal of thoracic oncology : official publication of the International Association for the Study of Lung Cancer, 2008. **3**(9): p. 1056-64.
30. Rusch, V.W., et al., *A phase II trial of surgical resection and adjuvant high-dose hemithoracic radiation for malignant pleural mesothelioma.* The Journal of thoracic and cardiovascular surgery, 2001. **122**(4): p. 788-95.
31. Allen, A.M., et al., *Fatal pneumonitis associated with intensity-modulated radiation therapy for mesothelioma.* International journal of radiation oncology, biology, physics, 2006. **65**(3): p. 640-5.
32. Davies, H.E., A.W. Musk, and Y.C. Lee, *Prophylactic radiotherapy for pleural puncture sites in mesothelioma: the controversy continues.* Current opinion in pulmonary medicine, 2008. **14**(4): p. 326-30.
33. Kindler, H.L., et al., *Multicenter, double-blind, placebo-controlled, randomized phase II trial of gemcitabine/cisplatin plus bevacizumab or placebo in patients with malignant mesothelioma.* Journal of clinical oncology : official journal of the American Society of Clinical Oncology, 2012. **30**(20): p. 2509-15.
34. Zalcman, G., et al., *IFCT-GFPC-0701 MAPS trial, a multicenter randomized phase III trial of pemetrexed-cisplatin with or without bevacizumab in patients with malignant pleural mesothelioma (MPM).* Journal of Clinical Oncology, 2012. **30**(15).
35. Garland, L.L., et al., *Phase II study of cediranib in patients with malignant pleural mesothelioma: SWOG S0509.* Journal of thoracic oncology : official publication of the International Association for the Study of Lung Cancer, 2011. **6**(11): p. 1938-45.
36. Rossoni G, G.V., Vigano MG, *NGR-hTNF as second-line treatment in malignant pleural mesothelioma (MPM).* ASCO Meeting Abstracts, 2012. **30**: p. 7076.

37. Hassan, R., Jahan, TM, Kindler, HL et al, *Amatuximab, a chimeric monoclonal antibody to mesothelin, in combination with pemetrexed and cisplatin in patients with unresectable pleural mesothelioma: results of a multicenter phase II clinical trial.* ASCO Meeting Abstracts, 2012. **30**: p. 7030.
38. Hassan, R., Sharon, E, Schuler, B et al, *Antitumor activity of SS1P with pemetrexed and cisplatin for front-line treatment of pleural mesothelioma and utility of serum mesothelin as a marker of tumor response.* ASCO Meeting Abstracts, 2011. **29**: p. 7026.
39. Filiberti, R., et al., *Serum PDGF-AB in pleural mesothelioma.* Tumour biology : the journal of the International Society for Oncodevelopmental Biology and Medicine, 2005. **26**(5): p. 221-6.
40. Motadi, L.R., et al., *Molecular genetics and mechanisms of apoptosis in carcinomas of the lung and pleura: therapeutic targets.* International immunopharmacology, 2007. **7**(14): p. 1934-47.
41. Levine, A.J., *p53, the cellular gatekeeper for growth and division.* Cell, 1997. **88**(3): p. 323-31.
42. Ashkenazi, A., et al., *Safety and antitumor activity of recombinant soluble Apo2 ligand.* J Clin Invest, 1999. **104**(2): p. 155-62.
43. Fransen, L., et al., *Molecular cloning of mouse tumour necrosis factor cDNA and its eukaryotic expression.* Nucleic acids research, 1985. **13**(12): p. 4417-29.
44. Kriegler, M., et al., *A novel form of TNF/cachectin is a cell surface cytotoxic transmembrane protein: ramifications for the complex physiology of TNF.* Cell, 1988. **53**(1): p. 45-53.
45. Wiley, S.R., et al., *Identification and characterization of a new member of the TNF family that induces apoptosis.* Immunity, 1995. **3**(6): p. 673-82.
46. Falschlehner, C., et al., *TRAIL signalling: decisions between life and death.* Int J Biochem Cell Biol, 2007. **39**(7-8): p. 1462-75.
47. Emery, J.G., et al., *Osteoprotegerin is a receptor for the cytotoxic ligand TRAIL.* J Biol Chem, 1998. **273**(23): p. 14363-7.
48. Degli-Esposti, M.A., et al., *The novel receptor TRAIL-R4 induces NF-kappaB and protects against TRAIL-mediated apoptosis, yet retains an incomplete death domain.* Immunity, 1997. **7**(6): p. 813-20.
49. Degli-Esposti, M.A., et al., *Cloning and characterization of TRAIL-R3, a novel member of the emerging TRAIL receptor family.* J Exp Med, 1997. **186**(7): p. 1165-70.
50. Kimberley, F.C. and G.R. Screaton, *Following a TRAIL: update on a ligand and its five receptors.* Cell Res, 2004. **14**(5): p. 359-72.
51. Meng, R.D., et al., *The TRAIL decoy receptor TRUNDD (DcR2, TRAIL-R4) is induced by adenovirus-p53 overexpression and can delay TRAIL-, p53-, and KILLER/DR5-dependent colon cancer apoptosis.* Mol Ther, 2000. **1**(2): p. 130-44.
52. Griffith, T.S., et al., *Functional analysis of TRAIL receptors using monoclonal antibodies.* J Immunol, 1999. **162**(5): p. 2597-605.
53. MacFarlane, M., et al., *Chronic lymphocytic leukemic cells exhibit apoptotic signaling via TRAIL-R1.* Cell Death Differ, 2005. **12**(7): p. 773-82.
54. Wagner, K.W., et al., *Death-receptor O-glycosylation controls tumor-cell sensitivity to the proapoptotic ligand Apo2L/TRAIL.* Nat Med, 2007. **13**(9): p. 1070-7.
55. Song, J.H., et al., *Lipid rafts and nonrafts mediate tumor necrosis factor related apoptosis-inducing ligand induced apoptotic and nonapoptotic signals in non small cell lung carcinoma cells.* Cancer Res, 2007. **67**(14): p. 6946-55.
56. Wu, X.X., et al., *Enhancement of TRAIL/Apo2L-mediated apoptosis by adriamycin through inducing DR4 and DR5 in renal cell carcinoma cells.* Int J Cancer, 2003. **104**(4): p. 409-17.
57. Nimmanapalli, R., et al., *Pretreatment with paclitaxel enhances apo-2 ligand/tumor necrosis factor-related apoptosis-inducing ligand-induced apoptosis of prostate cancer cells by inducing death receptors 4 and 5 protein levels.* Cancer Res, 2001. **61**(2): p. 759-63.

58. Varfolomeev, E., et al., *Molecular determinants of kinase pathway activation by Apo2 ligand/tumor necrosis factor-related apoptosis-inducing ligand.* J Biol Chem, 2005. **280**(49): p. 40599-608.
59. Ehrhardt, H., et al., *TRAIL induced survival and proliferation in cancer cells resistant towards TRAIL-induced apoptosis mediated by NF-kappaB.* Oncogene, 2003. **22**(25): p. 3842-52.
60. Takeda, K., et al., *Critical role for tumor necrosis factor-related apoptosis-inducing ligand in immune surveillance against tumor development.* J Exp Med, 2002. **195**(2): p. 161-9.
61. Cretney, E., et al., *Increased susceptibility to tumor initiation and metastasis in TNF-related apoptosis-inducing ligand-deficient mice.* J Immunol, 2002. **168**(3): p. 1356-61.
62. Smyth, M.J., et al., *Nature's TRAIL--on a path to cancer immunotherapy.* Immunity, 2003. **18**(1): p. 1-6.
63. Motoki, K., et al., *Enhanced apoptosis and tumor regression induced by a direct agonist antibody to tumor necrosis factor-related apoptosis-inducing ligand receptor 2.* Clin Cancer Res, 2005. **11**(8): p. 3126-35.
64. Pukac, L., et al., *HGS-ETR1, a fully human TRAIL-receptor 1 monoclonal antibody, induces cell death in multiple tumour types in vitro and in vivo.* Br J Cancer, 2005. **92**(8): p. 1430-41.
65. Lin, T., et al., *Targeted expression of green fluorescent protein/tumor necrosis factor-related apoptosis-inducing ligand fusion protein from human telomerase reverse transcriptase promoter elicits antitumor activity without toxic effects on primary human hepatocytes.* Cancer Res, 2002. **62**(13): p. 3620-5.
66. Kagawa, S., et al., *Antitumor activity and bystander effects of the tumor necrosis factor-related apoptosis-inducing ligand (TRAIL) gene.* Cancer Res, 2001. **61**(8): p. 3330-8.
67. Yee L, F.M., Dimick K, Calvert S, Robins C, Ing J et al. , *Phase IB safety and pharmacokinetic study of recombinant humna Apo2L/TRAIL in combination with rituximab in patients with low-grade non-Hodgkin lymphoma.* Journal of Clinical Oncology ASCO Annual Meeting Proceedings Part 1, 2007. **25**(18s): p. 8078.
68. Herbst, R.S., et al., *Phase I dose-escalation study of recombinant human Apo2L/TRAIL, a dual proapoptotic receptor agonist, in patients with advanced cancer.* J Clin Oncol, 2010. **28**(17): p. 2839-46.
69. Hotte, S.J., et al., *A phase 1 study of mapatumumab (fully human monoclonal antibody to TRAIL-R1) in patients with advanced solid malignancies.* Clin Cancer Res, 2008. **14**(11): p. 3450-5.
70. Mom, C.H., et al., *Mapatumumab, a fully human agonistic monoclonal antibody that targets TRAIL-R1, in combination with gemcitabine and cisplatin: a phase I study.* Clin Cancer Res, 2009. **15**(17): p. 5584-90.
71. Plummer, R., et al., *Phase 1 and pharmacokinetic study of lexatumumab in patients with advanced cancers.* Clin Cancer Res, 2007. **13**(20): p. 6187-94.
72. Shankar, S., T.R. Singh, and R.K. Srivastava, *Ionizing radiation enhances the therapeutic potential of TRAIL in prostate cancer in vitro and in vivo: Intracellular mechanisms.* Prostate, 2004. **61**(1): p. 35-49.
73. Shankar, S., X. Chen, and R.K. Srivastava, *Effects of sequential treatments with chemotherapeutic drugs followed by TRAIL on prostate cancer in vitro and in vivo.* Prostate, 2005. **62**(2): p. 165-86.
74. Singh, T.R., S. Shankar, and R.K. Srivastava, *HDAC inhibitors enhance the apoptosis-inducing potential of TRAIL in breast carcinoma.* Oncogene, 2005. **24**(29): p. 4609-23.
75. Dumitru, C.A., et al., *Doxorubicin enhances TRAIL-induced cell death via ceramide-enriched membrane platforms.* Apoptosis, 2007. **12**(8): p. 1533-41.
76. El-Zawahry, A., J. McKillop, and C. Voelkel-Johnson, *Doxorubicin increases the effectiveness of Apo2L/TRAIL for tumor growth inhibition of prostate cancer xenografts.* BMC Cancer, 2005. **5**: p. 2.

77. Vivo, C., W. Liu, and V.C. Broaddus, *c-Jun N-terminal kinase contributes to apoptotic synergy induced by tumor necrosis factor-related apoptosis-inducing ligand plus DNA damage in chemoresistant, p53 inactive mesothelioma cells.* J Biol Chem, 2003. **278**(28): p. 25461-7.
78. Broaddus, V.C., et al., *Bid mediates apoptotic synergy between tumor necrosis factor-related apoptosis-inducing ligand (TRAIL) and DNA damage.* J Biol Chem, 2005. **280**(13): p. 12486-93.
79. Liu, W., et al., *Tumor necrosis factor-related apoptosis-inducing ligand and chemotherapy cooperate to induce apoptosis in mesothelioma cell lines.* Am J Respir Cell Mol Biol, 2001. **25**(1): p. 111-8.
80. Haag, C., et al., *Identification of c-FLIP(L) and c-FLIP(S) as critical regulators of death receptor-induced apoptosis in pancreatic cancer cells.* Gut, 2011. **60**(2): p. 225-37.
81. Kock, N., et al., *Tumor therapy mediated by lentiviral expression of shBcl-2 and S-TRAIL.* Neoplasia, 2007. **9**(5): p. 435-42.
82. Li, L., et al., *A small molecule Smac mimic potentiates TRAIL- and TNFalpha-mediated cell death.* Science, 2004. **305**(5689): p. 1471-4.
83. Khanbolooki, S., et al., *Nuclear factor-kappaB maintains TRAIL resistance in human pancreatic cancer cells.* Mol Cancer Ther, 2006. **5**(9): p. 2251-60.
84. Martelli, A.M., et al., *A new selective AKT pharmacological inhibitor reduces resistance to chemotherapeutic drugs, TRAIL, all-trans-retinoic acid, and ionizing radiation of human leukemia cells.* Leukemia, 2003. **17**(9): p. 1794-805.
85. Krueger, A., et al., *Cellular FLICE-inhibitory protein splice variants inhibit different steps of caspase-8 activation at the CD95 death-inducing signaling complex.* J Biol Chem, 2001. **276**(23): p. 20633-40.
86. Kataoka, T., et al., *The caspase-8 inhibitor FLIP promotes activation of NF-kappaB and Erk signaling pathways.* Curr Biol, 2000. **10**(11): p. 640-8.
87. Safa, A.R. and K.E. Pollok, *Targeting the Anti-Apoptotic Protein c-FLIP for Cancer Therapy.* Cancers (Basel), 2011. **3**(2): p. 1639-1671.
88. Mezzanzanica, D., et al., *CD95-mediated apoptosis is impaired at receptor level by cellular FLICE-inhibitory protein (long form) in wild-type p53 human ovarian carcinoma.* Clin Cancer Res, 2004. **10**(15): p. 5202-14.
89. Rogers, K.M., et al., *Cellular FLICE-inhibitory protein regulates chemotherapy-induced apoptosis in breast cancer cells.* Mol Cancer Ther, 2007. **6**(5): p. 1544-51.
90. Zhang, X., et al., *Persistent c-FLIP(L) expression is necessary and sufficient to maintain resistance to tumor necrosis factor-related apoptosis-inducing ligand-mediated apoptosis in prostate cancer.* Cancer Res, 2004. **64**(19): p. 7086-91.
91. Wilson, T.R., et al., *c-FLIP: a key regulator of colorectal cancer cell death.* Cancer Res, 2007. **67**(12): p. 5754-62.
92. Rippo, M.R., et al., *FLIP overexpression inhibits death receptor-induced apoptosis in malignant mesothelial cells.* Oncogene, 2004. **23**(47): p. 7753-60.
93. Hurwitz, J.L., et al., *Vorinostat/SAHA-induced apoptosis in malignant mesothelioma is FLIP/caspase 8-dependent and HR23B-independent.* European journal of cancer, 2012. **48**(7): p. 1096-107.
94. Bolden, J.E., M.J. Peart, and R.W. Johnstone, *Anticancer activities of histone deacetylase inhibitors.* Nature reviews. Drug discovery, 2006. **5**(9): p. 769-84.
95. Watanabe, K., K. Okamoto, and S. Yonehara, *Sensitization of osteosarcoma cells to death receptor-mediated apoptosis by HDAC inhibitors through downregulation of cellular FLIP.* Cell death and differentiation, 2005. **12**(1): p. 10-8.
96. Frew, A.J., et al., *Combination therapy of established cancer using a histone deacetylase inhibitor and a TRAIL receptor agonist.* Proceedings of the National Academy of Sciences of the United States of America, 2008. **105**(32): p. 11317-22.

97. Nakata, S., et al., *Histone deacetylase inhibitors upregulate death receptor 5/TRAIL-R2 and sensitize apoptosis induced by TRAIL/APO2-L in human malignant tumor cells.* Oncogene, 2004. **23**(37): p. 6261-71.
98. Insinga, A., et al., *Inhibitors of histone deacetylases induce tumor-selective apoptosis through activation of the death receptor pathway.* Nat Med, 2005. **11**(1): p. 71-6.
99. Imai, T., et al., *FR901228 induces tumor regression associated with induction of Fas ligand and activation of Fas signaling in human osteosarcoma cells.* Oncogene, 2003. **22**(58): p. 9231-42.
100. Schuchmann, M., et al., *Histone deacetylase inhibition by valproic acid down-regulates c-FLIP/CASH and sensitizes hepatoma cells towards CD95- and TRAIL receptor-mediated apoptosis and chemotherapy.* Oncol Rep, 2006. **15**(1): p. 227-30.
101. Kelley, R.F., et al., *Receptor-selective mutants of apoptosis-inducing ligand 2/tumor necrosis factor-related apoptosis-inducing ligand reveal a greater contribution of death receptor (DR) 5 than DR4 to apoptosis signaling.* J Biol Chem, 2005. **280**(3): p. 2205-12.
102. MacFarlane, M., et al., *TRAIL receptor-selective mutants signal to apoptosis via TRAIL-R1 in primary lymphoid malignancies.* Cancer Res, 2005. **65**(24): p. 11265-70.
103. Johnstone, R.W., A.J. Frew, and M.J. Smyth, *The TRAIL apoptotic pathway in cancer onset, progression and therapy.* Nat Rev Cancer, 2008. **8**(10): p. 782-98.
104. Loebinger, M.R., et al., *Mesenchymal stem cell delivery of TRAIL can eliminate metastatic cancer.* Cancer Res, 2009. **69**(10): p. 4134-42.
105. Sasportas, L.S., et al., *Assessment of therapeutic efficacy and fate of engineered human mesenchymal stem cells for cancer therapy.* Proc Natl Acad Sci U S A, 2009. **106**(12): p. 4822-7.
106. Orkin, S.H. and S.J. Morrison, *Stem-cell competition.* Nature, 2002. **418**(6893): p. 25-7.
107. Bonnet, D., *Biology of human bone marrow stem cells.* Clin Exp Med, 2003. **3**(3): p. 140-9.
108. Reagan, M.R. and D.L. Kaplan, *Concise review: Mesenchymal stem cell tumor-homing: detection methods in disease model systems.* Stem Cells, 2011. **29**(6): p. 920-7.
109. Krause, D.S., et al., *Multi-organ, multi-lineage engraftment by a single bone marrow-derived stem cell.* Cell, 2001. **105**(3): p. 369-77.
110. Ortiz, L.A., et al., *Mesenchymal stem cell engraftment in lung is enhanced in response to bleomycin exposure and ameliorates its fibrotic effects.* Proc Natl Acad Sci U S A, 2003. **100**(14): p. 8407-11.
111. Rojas, M., et al., *Bone marrow-derived mesenchymal stem cells in repair of the injured lung.* Am J Respir Cell Mol Biol, 2005. **33**(2): p. 145-52.
112. Direkze, N.C., et al., *Multiple organ engraftment by bone-marrow-derived myofibroblasts and fibroblasts in bone-marrow-transplanted mice.* Stem Cells, 2003. **21**(5): p. 514-20.
113. Ishii, G., et al., *In vivo characterization of bone marrow-derived fibroblasts recruited into fibrotic lesions.* Stem Cells, 2005. **23**(5): p. 699-706.
114. Hashimoto, N., et al., *Bone marrow-derived progenitor cells in pulmonary fibrosis.* J Clin Invest, 2004. **113**(2): p. 243-52.
115. Desmouliere, A., C. Guyot, and G. Gabbiani, *The stroma reaction myofibroblast: a key player in the control of tumor cell behavior.* Int J Dev Biol, 2004. **48**(5-6): p. 509-17.
116. Bhowmick, N.A., E.G. Neilson, and H.L. Moses, *Stromal fibroblasts in cancer initiation and progression.* Nature, 2004. **432**(7015): p. 332-7.
117. Orimo, A., et al., *Stromal fibroblasts present in invasive human breast carcinomas promote tumor growth and angiogenesis through elevated SDF-1/CXCL12 secretion.* Cell, 2005. **121**(3): p. 335-48.
118. Barth, P.J., et al., *CD34+ fibrocytes in neoplastic and inflammatory pancreatic lesions.* Virchows Arch, 2002. **440**(2): p. 128-33.

119. Barth, P.J., et al., *CD34+ fibrocytes in invasive ductal carcinoma, ductal carcinoma in situ, and benign breast lesions.* Virchows Arch, 2002. **440**(3): p. 298-303.
120. Hasebe, T., et al., *Proliferative activity of intratumoral fibroblasts is closely correlated with lymph node and distant organ metastases of invasive ductal carcinoma of the breast.* Am J Pathol, 2000. **156**(5): p. 1701-10.
121. Ohuchida, K., et al., *Radiation to stromal fibroblasts increases invasiveness of pancreatic cancer cells through tumor-stromal interactions.* Cancer Res, 2004. **64**(9): p. 3215-22.
122. Ishii, G., et al., *Bone-marrow-derived myofibroblasts contribute to the cancer-induced stromal reaction.* Biochem Biophys Res Commun, 2003. **309**(1): p. 232-40.
123. Direkze, N.C., et al., *Bone marrow contribution to tumor-associated myofibroblasts and fibroblasts.* Cancer Res, 2004. **64**(23): p. 8492-5.
124. Sangai, T., et al., *Effect of differences in cancer cells and tumor growth sites on recruiting bone marrow-derived endothelial cells and myofibroblasts in cancer-induced stroma.* Int J Cancer, 2005. **115**(6): p. 885-92.
125. Direkze, N.C., et al., *Bone marrow-derived stromal cells express lineage-related messenger RNA species.* Cancer Res, 2006. **66**(3): p. 1265-9.
126. Anderson, S.A., et al., *Noninvasive MR imaging of magnetically labeled stem cells to directly identify neovasculature in a glioma model.* Blood, 2005. **105**(1): p. 420-5.
127. Ferrari, N., et al., *Bone marrow-derived, endothelial progenitor-like cells as angiogenesis-selective gene-targeting vectors.* Gene Ther, 2003. **10**(8): p. 647-56.
128. Dwenger, A., et al., *Transplanted bone marrow cells preferentially home to the vessels of in situ generated murine tumors rather than of normal organs.* Stem Cells, 2004. **22**(1): p. 86-92.
129. Nakamizo, A., et al., *Human bone marrow-derived mesenchymal stem cells in the treatment of gliomas.* Cancer Res, 2005. **65**(8): p. 3307-18.
130. Menon, L.G., et al., *Differential gene expression associated with migration of mesenchymal stem cells to conditioned medium from tumor cells or bone marrow cells.* Stem Cells, 2007. **25**(2): p. 520-8.
131. Xin, H., et al., *Targeted delivery of CX3CL1 to multiple lung tumors by mesenchymal stem cells.* Stem Cells, 2007. **25**(7): p. 1618-26.
132. Khakoo, A.Y., et al., *Human mesenchymal stem cells exert potent antitumorigenic effects in a model of Kaposi's sarcoma.* J Exp Med, 2006. **203**(5): p. 1235-47.
133. Studeny, M., et al., *Mesenchymal stem cells: potential precursors for tumor stroma and targeted-delivery vehicles for anticancer agents.* J Natl Cancer Inst, 2004. **96**(21): p. 1593-603.
134. Devine, S.M., et al., *Mesenchymal stem cells distribute to a wide range of tissues following systemic infusion into nonhuman primates.* Blood, 2003. **101**(8): p. 2999-3001.
135. Gao, J., et al., *The dynamic in vivo distribution of bone marrow-derived mesenchymal stem cells after infusion.* Cells, tissues, organs, 2001. **169**(1): p. 12-20.
136. Gerdin, B. and R. Hallgren, *Dynamic role of hyaluronan (HYA) in connective tissue activation and inflammation.* Journal of internal medicine, 1997. **242**(1): p. 49-55.
137. Chute, J.P., *Stem cell homing.* Curr Opin Hematol, 2006. **13**(6): p. 399-406.
138. Phillips, R.J., et al., *Circulating fibrocytes traffic to the lungs in response to CXCL12 and mediate fibrosis.* J Clin Invest, 2004. **114**(3): p. 438-46.
139. Xu, J., et al., *Role of the SDF-1/CXCR4 axis in the pathogenesis of lung injury and fibrosis.* Am J Respir Cell Mol Biol, 2007. **37**(3): p. 291-9.
140. Dwyer, R.M., et al., *Monocyte chemotactic protein-1 secreted by primary breast tumors stimulates migration of mesenchymal stem cells.* Clinical cancer research : an official journal of the American Association for Cancer Research, 2007. **13**(17): p. 5020-7.

141. Coffelt, S.B., et al., *The pro-inflammatory peptide LL-37 promotes ovarian tumor progression through recruitment of multipotent mesenchymal stromal cells.* Proceedings of the National Academy of Sciences of the United States of America, 2009. **106**(10): p. 3806-11.
142. Ponte, A.L., et al., *The in vitro migration capacity of human bone marrow mesenchymal stem cells: comparison of chemokine and growth factor chemotactic activities.* Stem Cells, 2007. **25**(7): p. 1737-45.
143. Ringe, J., et al., *Towards in situ tissue repair: human mesenchymal stem cells express chemokine receptors CXCR1, CXCR2 and CCR2, and migrate upon stimulation with CXCL8 but not CCL2.* J Cell Biochem, 2007. **101**(1): p. 135-46.
144. Honczarenko, M., et al., *Human bone marrow stromal cells express a distinct set of biologically functional chemokine receptors.* Stem Cells, 2006. **24**(4): p. 1030-41.
145. Chamberlain, G., et al., *Concise review: mesenchymal stem cells: their phenotype, differentiation capacity, immunological features, and potential for homing.* Stem Cells, 2007. **25**(11): p. 2739-49.
146. Ozaki, Y., et al., *Comprehensive analysis of chemotactic factors for bone marrow mesenchymal stem cells.* Stem Cells Dev, 2007. **16**(1): p. 119-29.
147. Javazon, E.H., K.J. Beggs, and A.W. Flake, *Mesenchymal stem cells: paradoxes of passaging.* Exp Hematol, 2004. **32**(5): p. 414-25.
148. Studeny, M., et al., *Bone marrow-derived mesenchymal stem cells as vehicles for interferon-beta delivery into tumors.* Cancer Res, 2002. **62**(13): p. 3603-8.
149. Chen, X.C., et al., *Prophylaxis against carcinogenesis in three kinds of unestablished tumor models via IL12-gene-engineered MSCs.* Carcinogenesis, 2006. **27**(12): p. 2434-41.
150. Chen, X., et al., *A tumor-selective biotherapy with prolonged impact on established metastases based on cytokine gene-engineered MSCs.* Mol Ther, 2008. **16**(4): p. 749-56.
151. Li, X., et al., *In vitro effect of adenovirus-mediated human Gamma Interferon gene transfer into human mesenchymal stem cells for chronic myelogenous leukemia.* Hematol Oncol, 2006. **24**(3): p. 151-8.
152. Mei, S.H., et al., *Prevention of LPS-induced acute lung injury in mice by mesenchymal stem cells overexpressing angiopoietin 1.* PLoS Med, 2007. **4**(9): p. e269.
153. Kanki-Horimoto, S., et al., *Implantation of mesenchymal stem cells overexpressing endothelial nitric oxide synthase improves right ventricular impairments caused by pulmonary hypertension.* Circulation, 2006. **114**(1 Suppl): p. I181-5.
154. Matsumoto, R., et al., *Vascular endothelial growth factor-expressing mesenchymal stem cell transplantation for the treatment of acute myocardial infarction.* Arterioscler Thromb Vasc Biol, 2005. **25**(6): p. 1168-73.
155. Glennie, S., et al., *Bone marrow mesenchymal stem cells induce division arrest anergy of activated T cells.* Blood, 2005. **105**(7): p. 2821-7.
156. Corcione, A., et al., *Human mesenchymal stem cells modulate B-cell functions.* Blood, 2006. **107**(1): p. 367-72.
157. Ramasamy, R., et al., *Mesenchymal stem cells inhibit dendritic cell differentiation and function by preventing entry into the cell cycle.* Transplantation, 2007. **83**(1): p. 71-6.
158. Wolf, D. and A.M. Wolf, *Mesenchymal stem cells as cellular immunosuppressants.* Lancet, 2008. **371**(9624): p. 1553-4.
159. Sato, K., et al., *Nitric oxide plays a critical role in suppression of T-cell proliferation by mesenchymal stem cells.* Blood, 2007. **109**(1): p. 228-34.
160. Le Blanc, K., et al., *Mesenchymal stem cells for treatment of steroid-resistant, severe, acute graft-versus-host disease: a phase II study.* Lancet, 2008. **371**(9624): p. 1579-86.
161. Weiss, D.J., *Stem cells and cell therapies for cystic fibrosis and other lung diseases.* Pulm Pharmacol Ther, 2008. **21**(4): p. 588-94.
162. http://www.osiris.com/prod_pulmonary.php.

163. Abdel-Latif, A., et al., *Adult bone marrow-derived cells for cardiac repair: a systematic review and meta-analysis.* Arch Intern Med, 2007. **167**(10): p. 989-97.
164. Lipinski, M.J., et al., *Impact of intracoronary cell therapy on left ventricular function in the setting of acute myocardial infarction: a collaborative systematic review and meta-analysis of controlled clinical trials.* J Am Coll Cardiol, 2007. **50**(18): p. 1761-7.
165. Bartsch, T., et al., *Transplantation of autologous mononuclear bone marrow stem cells in patients with peripheral arterial disease (the TAM-PAD study).* Clin Res Cardiol, 2007. **96**(12): p. 891-9.
166. Parekkadan, B., et al., *Mesenchymal stem cell-derived molecules reverse fulminant hepatic failure.* PLoS One, 2007. **2**(9): p. e941.
167. Li, Y., et al., *Human marrow stromal cell therapy for stroke in rat: neurotrophins and functional recovery.* Neurology, 2002. **59**(4): p. 514-23.
168. Togel, F., et al., *Vasculotropic, paracrine actions of infused mesenchymal stem cells are important to the recovery from acute kidney injury.* Am J Physiol Renal Physiol, 2007. **292**(5): p. F1626-35.
169. Patel, S.A., et al., *Mesenchymal stem cells protect breast cancer cells through regulatory T cells: role of mesenchymal stem cell-derived TGF-beta.* Journal of immunology, 2010. **184**(10): p. 5885-94.
170. Djouad, F., et al., *Immunosuppressive effect of mesenchymal stem cells favors tumor growth in allogeneic animals.* Blood, 2003. **102**(10): p. 3837-44.
171. Hung, S.C., et al., *Angiogenic effects of human multipotent stromal cell conditioned medium activate the PI3K-Akt pathway in hypoxic endothelial cells to inhibit apoptosis, increase survival, and stimulate angiogenesis.* Stem Cells, 2007. **25**(9): p. 2363-70.
172. Mishra, P.J., et al., *Carcinoma-associated fibroblast-like differentiation of human mesenchymal stem cells.* Cancer research, 2008. **68**(11): p. 4331-9.
173. Dawson, M.R., et al., *Direct evidence for lineage-dependent effects of bone marrow stromal cells on tumor progression.* American journal of cancer research, 2011. **1**(2): p. 144-54.
174. Karnoub, A.E. and R.A. Weinberg, *Chemokine networks and breast cancer metastasis.* Breast Dis, 2006. **26**: p. 75-85.
175. Sasser, A.K., et al., *Human bone marrow stromal cells enhance breast cancer cell growth rates in a cell line-dependent manner when evaluated in 3D tumor environments.* Cancer Lett, 2007. **254**(2): p. 255-64.
176. Lu, Y.R., et al., *The growth inhibitory effect of mesenchymal stem cells on tumor cells in vitro and in vivo.* Cancer Biol Ther, 2008. **7**(2): p. 245-51.
177. Nakamura, K., et al., *Antitumor effect of genetically engineered mesenchymal stem cells in a rat glioma model.* Gene Ther, 2004. **11**(14): p. 1155-64.
178. Sun, B., et al., *Therapeutic potential of mesenchymal stromal cells in a mouse breast cancer metastasis model.* Cytotherapy, 2009. **11**(3): p. 289-98, 1 p following 298.
179. Maestroni, G.J., E. Hertens, and P. Galli, *Factor(s) from nonmacrophage bone marrow stromal cells inhibit Lewis lung carcinoma and B16 melanoma growth in mice.* Cell Mol Life Sci, 1999. **55**(4): p. 663-7.
180. Reagan, M.R., et al., *Stem Cell Implants for Cancer Therapy: TRAIL-Expressing Mesenchymal Stem Cells Target Cancer Cells In Situ.* Journal of breast cancer, 2012. **15**(3): p. 273-82.
181. Rubio, D., et al., *Spontaneous human adult stem cell transformation.* Cancer Res, 2005. **65**(8): p. 3035-9.
182. Tolar, J., et al., *Sarcoma derived from cultured mesenchymal stem cells.* Stem Cells, 2007. **25**(2): p. 371-9.
183. Aguilar, S., et al., *Murine but not human mesenchymal stem cells generate osteosarcoma-like lesions in the lung.* Stem Cells, 2007. **25**(6): p. 1586-94.

184. Houghton, J., et al., *Gastric cancer originating from bone marrow-derived cells.* Science, 2004. **306**(5701): p. 1568-71.
185. Bernardo, M.E., et al., *Human bone marrow derived mesenchymal stem cells do not undergo transformation after long-term in vitro culture and do not exhibit telomere maintenance mechanisms.* Cancer Res, 2007. **67**(19): p. 9142-9.
186. Horwitz, E.M., et al., *Isolated allogeneic bone marrow-derived mesenchymal cells engraft and stimulate growth in children with osteogenesis imperfecta: Implications for cell therapy of bone.* Proc Natl Acad Sci U S A, 2002. **99**(13): p. 8932-7.
187. Iyer, S.S., C. Co, and M. Rojas, *Mesenchymal stem cells and inflammatory lung diseases.* Panminerva Med, 2009. **51**(1): p. 5-16.
188. De Wever, O. and M. Mareel, *Role of tissue stroma in cancer cell invasion.* J Pathol, 2003. **200**(4): p. 429-47.
189. Bhowmick, N.A., et al., *TGF-beta signaling in fibroblasts modulates the oncogenic potential of adjacent epithelia.* Science, 2004. **303**(5659): p. 848-51.
190. Wait, S.D., et al., *Somatic mutations in VHL germline deletion kindred correlate with mild phenotype.* Ann Neurol, 2004. **55**(2): p. 236-40.
191. Brown, K. and N.A. Bhowmick, *Linking TGF-beta-mediated Cdc25A inhibition and cytoskeletal regulation through RhoA/p160(ROCK) signaling.* Cell Cycle, 2004. **3**(4): p. 408-10.
192. Marshall, E., *Gene therapy death prompts review of adenovirus vector.* Science, 1999. **286**(5448): p. 2244-5.
193. Bastide, C., et al., *A Nod Scid mouse model to study human prostate cancer.* Prostate Cancer Prostatic Dis, 2002. **5**(4): p. 311-5.
194. Baratti, D., et al., *Cytoreductive surgery with selective versus complete parietal peritonectomy followed by hyperthermic intraperitoneal chemotherapy in patients with diffuse malignant peritoneal mesothelioma: a controlled study.* Ann Surg Oncol, 2012. **19**(5): p. 1416-24.
195. Hacein-Bey-Abina, S., G. de Saint Basile, and M. Cavazzana-Calvo, *Gene therapy of X-linked severe combined immunodeficiency.* Methods Mol Biol, 2003. **215**: p. 247-59.
196. Hacein-Bey-Abina, S., et al., *LMO2-associated clonal T cell proliferation in two patients after gene therapy for SCID-X1.* Science, 2003. **302**(5644): p. 415-9.
197. Levine, B.L., et al., *Gene transfer in humans using a conditionally replicating lentiviral vector.* Proceedings of the National Academy of Sciences of the United States of America, 2006. **103**(46): p. 17372-7.
198. Cartier, N., et al., *Hematopoietic stem cell gene therapy with a lentiviral vector in X-linked adrenoleukodystrophy.* Science, 2009. **326**(5954): p. 818-23.
199. Cavazzana-Calvo, M., et al., *Transfusion independence and HMGA2 activation after gene therapy of human beta-thalassaemia.* Nature, 2010. **467**(7313): p. 318-22.
200. Demaison, C., et al., *High-level transduction and gene expression in hematopoietic repopulating cells using a human immunodeficiency [correction of imunodeficiency] virus type 1-based lentiviral vector containing an internal spleen focus forming virus promoter.* Human gene therapy, 2002. **13**(7): p. 803-13.
201. Wiseman, J.W., et al., *A comparison of linear and branched polyethylenimine (PEI) with DCChol/DOPE liposomes for gene delivery to epithelial cells in vitro and in vivo.* Gene therapy, 2003. **10**(19): p. 1654-62.
202. Belyanskaya, L.L., et al., *Human agonistic TRAIL receptor antibodies Mapatumumab and Lexatumumab induce apoptosis in malignant mesothelioma and act synergistically with cisplatin.* Mol Cancer, 2007. **6**: p. 66.
203. Liu, W., et al., *Tumor necrosis factor-related apoptosis-inducing ligand and chemotherapy cooperate to induce apoptosis in mesothelioma cell lines.* American journal of respiratory cell and molecular biology, 2001. **25**(1): p. 111-8.

204. Selikoff, I.J. and E.C. Hammond, *Asbestos and smoking.* JAMA, 1979. **242**(5): p. 458-9.
205. Suriano, G., et al., *The intracellular E-cadherin germline mutation V832 M lacks the ability to mediate cell-cell adhesion and to suppress invasion.* Oncogene, 2003. **22**(36): p. 5716-9.
206. Nguyen, H.T., M. Geens, and C. Spits, *Genetic and epigenetic instability in human pluripotent stem cells.* Human reproduction update, 2013. **19**(2): p. 187-205.
207. Cabrera, C.M., et al., *Identity tests: determination of cell line cross-contamination.* Cytotechnology, 2006. **51**(2): p. 45-50.
208. Drexler, H.G., R.A. MacLeod, and W.G. Dirks, *Cross-contamination: HS-Sultan is not a myeloma but a Burkitt lymphoma cell line.* Blood, 2001. **98**(12): p. 3495-6.
209. Gonzalvez, F. and A. Ashkenazi, *New insights into apoptosis signaling by Apo2L/TRAIL.* Oncogene, 2010. **29**(34): p. 4752-65.
210. Rubins, J.B., et al., *Inhibition of mesothelioma cell growth in vitro by doxycycline.* The Journal of laboratory and clinical medicine, 2001. **138**(2): p. 101-6.
211. Fife, R.S. and G.W. Sledge, Jr., *Effects of doxycycline on in vitro growth, migration, and gelatinase activity of breast carcinoma cells.* The Journal of laboratory and clinical medicine, 1995. **125**(3): p. 407-11.
212. Duivenvoorden, W.C., H.W. Hirte, and G. Singh, *Use of tetracycline as an inhibitor of matrix metalloproteinase activity secreted by human bone-metastasizing cancer cells.* Invasion & metastasis, 1997. **17**(6): p. 312-22.
213. Bettany, J.T. and R.G. Wolowacz, *Tetracycline derivatives induce apoptosis selectively in cultured monocytes and macrophages but not in mesenchymal cells.* Advances in dental research, 1998. **12**(2): p. 136-43.
214. Fife, R.S., et al., *Inhibition of proliferation and induction of apoptosis by doxycycline in cultured human osteosarcoma cells.* The Journal of laboratory and clinical medicine, 1997. **130**(5): p. 530-4.
215. Wu, J., et al., *Mitochondria and calpains mediate caspase-dependent apoptosis induced by doxycycline in HeLa cells.* Cellular and molecular life sciences : CMLS, 2006. **63**(7-8): p. 949-57.
216. Nici, L., B. Monfils, and P. Calabresi, *The effects of taurolidine, a novel antineoplastic agent, on human malignant mesothelioma.* Clin Cancer Res, 2004. **10**(22): p. 7655-61.
217. Veldwijk, M.R., et al., *Characterization of human mesothelioma cell lines as tumor models for suicide gene therapy.* Onkologie, 2008. **31**(3): p. 91-6.
218. Suzuki, Y., et al., *Inhibition of Met/HGF receptor and angiogenesis by NK4 leads to suppression of tumor growth and migration in malignant pleural mesothelioma.* Int J Cancer, 2010. **127**(8): p. 1948-57.
219. Kircher, M.F., S.S. Gambhir, and J. Grimm, *Noninvasive cell-tracking methods.* Nature reviews. Clinical oncology, 2011. **8**(11): p. 677-88.
220. Ruster, B., et al., *Mesenchymal stem cells display coordinated rolling and adhesion behavior on endothelial cells.* Blood, 2006. **108**(12): p. 3938-44.
221. Sackstein, R., et al., *Ex vivo glycan engineering of CD44 programs human multipotent mesenchymal stromal cell trafficking to bone.* Nature medicine, 2008. **14**(2): p. 181-7.
222. Qin, Z.H., et al., *Intrapleural delivery of mesenchymal stem cells: a novel potential treatment for pleural diseases.* Acta pharmacologica Sinica, 2011. **32**(5): p. 581-90.
223. Qin, Z.H., et al., *Intrapleural delivery of MSCs attenuates acute lung injury by paracrine/endocrine mechanism.* Journal of cellular and molecular medicine, 2012. **16**(11): p. 2745-53.
224. Dembinski, J.L., et al., *Tumor stroma engraftment of gene-modified mesenchymal stem cells as anti-tumor therapy against ovarian cancer.* Cytotherapy, 2013. **15**(1): p. 20-32.
225. van Eekelen, M., et al., *Human stem cells expressing novel TSP-1 variant have anti-angiogenic effect on brain tumors.* Oncogene, 2010. **29**(22): p. 3185-95.

226. Lim, J.Y., et al., *Therapeutic effects of human umbilical cord blood-derived mesenchymal stem cells after intrathecal administration by lumbar puncture in a rat model of cerebral ischemia.* Stem cell research & therapy, 2011. **2**(5): p. 38.
227. Uchibori, R., et al., *NF-kappaB Activity Regulates Mesenchymal Stem Cell Accumulation at Tumor Sites.* Cancer Research, 2013. **73**(1): p. 364-72.
228. Hosokawa, Y., et al., *Cytokines differentially regulate ICAM-1 and VCAM-1 expression on human gingival fibroblasts.* Clinical and Experimental Immunology, 2006. **144**(3): p. 494-502.
229. Copland, I.B., et al., *Improved autograft survival of mesenchymal stromal cells by plasminogen activator inhibitor 1 inhibition.* Stem Cells, 2009. **27**(2): p. 467-77.
230. http://publications.nice.org.uk/pemetrexed-for-the-treatment-of-malignant-pleural-mesothelioma-ta135.
231. Broaddus, V.C., et al., *Bid mediates apoptotic synergy between tumor necrosis factor-related apoptosis-inducing ligand (TRAIL) and DNA damage.* The Journal of biological chemistry, 2005. **280**(13): p. 12486-93.
232. Abayasiriwardana, K.S., et al., *Malignant mesothelioma cells are rapidly sensitized to TRAIL-induced apoptosis by low-dose anisomycin via Bim.* Molecular cancer therapeutics, 2007. **6**(10): p. 2766-76.
233. Barbone, D., et al., *Mammalian target of rapamycin contributes to the acquired apoptotic resistance of human mesothelioma multicellular spheroids.* The Journal of biological chemistry, 2008. **283**(19): p. 13021-30.
234. Chen, J., et al., *Therapeutic benefit of intravenous administration of bone marrow stromal cells after cerebral ischemia in rats.* Stroke; a journal of cerebral circulation, 2001. **32**(4): p. 1005-11.
235. Omori, Y., et al., *Optimization of a therapeutic protocol for intravenous injection of human mesenchymal stem cells after cerebral ischemia in adult rats.* Brain research, 2008. **1236**: p. 30-8.
236. Wu, J., et al., *Intravenously administered bone marrow cells migrate to damaged brain tissue and improve neural function in ischemic rats.* Cell transplantation, 2008. **16**(10): p. 993-1005.
237. von Bahr, L., et al., *Analysis of tissues following mesenchymal stromal cell therapy in humans indicates limited long-term engraftment and no ectopic tissue formation.* Stem Cells, 2012. **30**(7): p. 1575-8.
238. Finn, R.S., et al., *Postmortem findings of malignant pleural mesothelioma: a two-center study of 318 patients.* Chest, 2012. **142**(5): p. 1267-73.